The Sveconorwegian orogeny

Accepted version on October 21, 2020

The Sveconorwegian orogeny

Bernard Bingen [1], Giulio Viola [2], Charlotte Möller [3], Jacqueline Vander Auwera [4], Antonin Laurent [5], Keewook Yi [6]

1 Corresponding author, Geological Survey of Norway, 7491 Trondheim, Norway; bernard.bingen@ngu.no; ORCID; 0000-0002-4901-2016

2 Department of Biological, Geological and Environmental Sciences, BiGeA, University of Bologna, 40126 Bologna, Italy; giulio.viola3@unibo.it

3 Department of Geology, Lund University, Sölvegatan 12, SE-223 62 Lund, Sweden; charlotte.moller@geol.lu.se

4 Department of Geology, University of Liège, 4000 Liège, Belgium; jvdauwera@uliege.be

5 Université de Lyon, UJM-Saint-Etienne, CNRS, UCA, IRD, LMV UMR 6524, F-42023 Saint-Etienne, France; antonin.laurent@univ-st-etienne.fr

6 Korea Basic Science Institute, 363-883 Chungbuk, South Korea; kyi@kbsi.re.kr

GRAPHICAL ABSTRACT

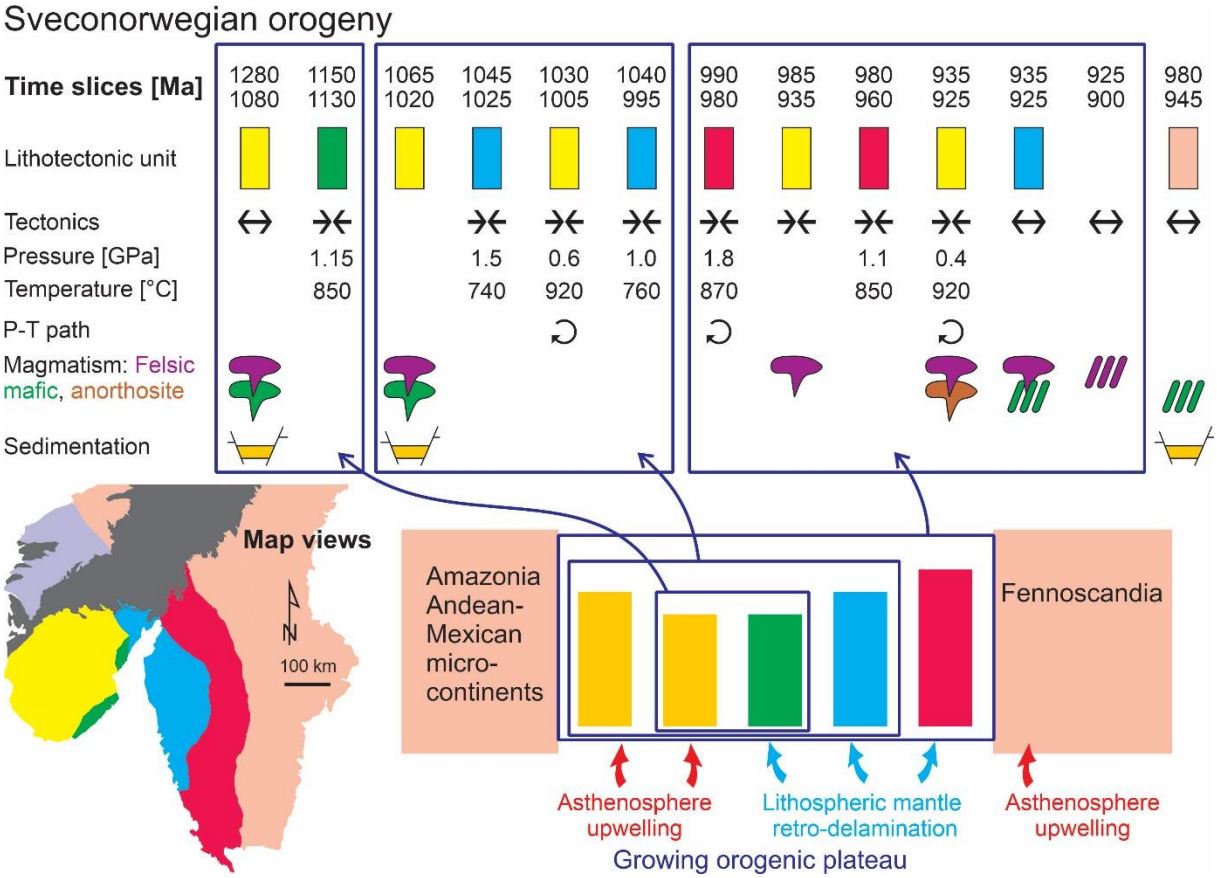

ABSTRACT

This article reviews the geology of the Sveconorwegian orogen in south Scandinavia and existing tectonic models for the Mesoproterozoic to Neoproterozoic Sveconorwegian orogeny. It proposes an updated geodynamic scenario of large, hot, long-duration continental collision starting at c. 1065 Ma between proto-Baltica and another plate, presumably Amazonia, in a Rodinia-forming context. An orogenic plateau formed at 1280 Ma as a back-arc Cordillera-style plateau, and then grew further stepwise after 1065 Ma, as a collisional Tibetan-style plateau. Voluminous mantle- and crustal-derived Sveconorwegian magmatism took place in the hinterland in the west of the orogen, mainly: (i) bimodal magmatism at 1280–1145 Ma, overlapping with extensional intramontane basin sedimentation, (ii) the calc-alkaline Sirdal magmatic belt at 1065–1020 Ma, (iii) the hydrous ferroan hornblende-biotite granite (HBG) suite at 985–925 Ma and (iv) the anhydrous ferroan massif-type anorthosite-mangerite-charnockite (AMC) suite at 935–915 Ma. High-alumina orthopyroxene megacrysts

in anorthosite imply mafic underplating at 1040 Ma and remelting of the underplates at 930 Ma. Overlapping with magmatism, protracted low-pressure, granulite-facies metamorphism reached twice ultra-high temperature conditions, of 0.6 GPa-920 °C at 1030–1005 Ma and 0.4 GPa-920 °C at 930 Ma. These features imply shallow asthenosphere under the crust. Towards the foreland in the east, metamorphism shows increasing high-pressure signature eastwards with time, with peak P-T values of 1.15 GPa-850 °C at 1150–1120 Ma in the Bamble-Kongsberg lithotectonic units, 1.5 GPa-740 °C at c. 1050 Ma in the Idefjorden lithotectonic unit, and 1.8 GPa-870 °C at c. 990 Ma in the Eastern Segment under eclogite-facies conditions. These are attributed to retreating delamination of the dense sub-continental lithospheric mantle and growth of the orogenic plateau towards the foreland. After c. 930 Ma, convergence came to a halt, the orogenic plateau collapsed, and 16 km of overburden was removed by extension and erosion.

Keywords: Sveconorwegian, Mesoproterozoic, Rodinia, continental collision, orogenic plateau - lithospheric mantle delamination

Highlights:

- Review of the geology of the Sveconorwegian orogen in south Scandinavia.
- Review of geodynamic models for the Mesoproterozoic to Neoproterozoic Sveconorwegian orogeny.
- Model of large, hot, long-duration continental collision for the Sveconorwegian orogeny.
- Orogenic plateau construction is associated with retreating delamination of the continental lithospheric mantle.
- Protracted shallow asthenosphere lead to crustal melting and ultra-high temperature granulite-facies metamorphism.

- Massif-type anorthosite-mangerite-charnockite plutonism resulted from remelting of mafic underplates at 1.1 GPa under high heat flow conditions.
- The Sveconorwegian orogeny contributed to assembly of Rodinia supercontinent

1 Introduction

Late-Mesoproterozoic orogenic belts are interpreted as products of the closure of oceanic realms and the collision between continents to form supercontinent Rodinia at the end of the Mesoproterozoic (Hoffman, 1991; Li et al., 2008). The Rodinia paradigm is robust, and supported by a peak in the abundance of late Mesoproterozoic detrital zircons (Hawkesworth et al., 2009). This notwithstanding, paleogeographic models for Rodinia configuration and plate tectonic models for Rodinia assembly remain in essence ill-defined (Torsvik, 2003). Proto-Baltica (Proterozoic Baltica = East European Craton, here after called Baltica) is a core piece of Rodinia in almost all models (Fig. 1) (Li et al., 2008; Merdith et al., 2017), and the Sveconorwegian orogen at the western margin of Baltica provides key geological evidence for the assembly of Rodinia (Bingen et al., 2008a; Bingen et al., 2008c; Bogdanova et al., 2008; Cawood and Pisarevsky, 2017; Cawood et al., 2010; Falkum and Petersen, 1980; Gee et al., 2015; Gower et al., 2008; Hartz and Torsvik, 2002; He et al., 2018; Ibanez-Mejia et al., 2011; Lorenz et al., 2012; Pisarevsky et al., 2014; Roberts, 2013; Roberts and Slagstad, 2015; Slagstad et al., 2019; Slagstad et al., 2020; Slagstad et al., 2018; Slagstad et al., 2017; Stephens and Wahlgren, 2020b; Torsvik et al., 1996; Weber et al., 2010).

The Sveconorwegian orogen is well exposed and accessible in its type area in southwest Scandinavia (south Norway and southwest Sweden). It represents therefore an excellent natural laboratory to study Precambrian geodynamics (Bingen and Viola, 2018; Laurent et al., 2018a; Möller and Andersson, 2018; Slagstad et al., 2018; Stephens and Wahlgren, 2020b; Vander Auwera et al., 2011; Viola and Henderson, 2010).

The body of geological data on the Sveconorwegian orogen has been steadily growing over the last 20 years, leading to contrasting conceptual models. This article reviews the existing structural, metamorphic, magmatic, geochronological and isotopic record across the entire Sveconorwegian orogen, and discusses the orogenic models that have been proposed in the literature. In fact, there is a lively debate in the literature on whether the Sveconorwegian orogeny was a collisional or a non-collisional (Andean) orogeny (Bingen et al., 2008a; Möller and Andersson, 2018; Slagstad et al., 2020; Slagstad et al., 2017; Slagstad et al., 2013; Stephens and Wahlgren, 2020b). We address this debate and conclude proposing an updated model of large, hot, and long-duration continent-continent collision for the Sveconorwegian orogeny at the margin of Baltica / Fennoscandia. This model involves the stepwise propagation of an orogenic plateau towards the foreland and hinterland of the orogen, associated with retreating delamination of the continental lithospheric mantle. It takes into account a number of key features of the orogeny, including the zoning of metamorphism, the distribution of magmatism and the genesis of massif-type anorthosites.

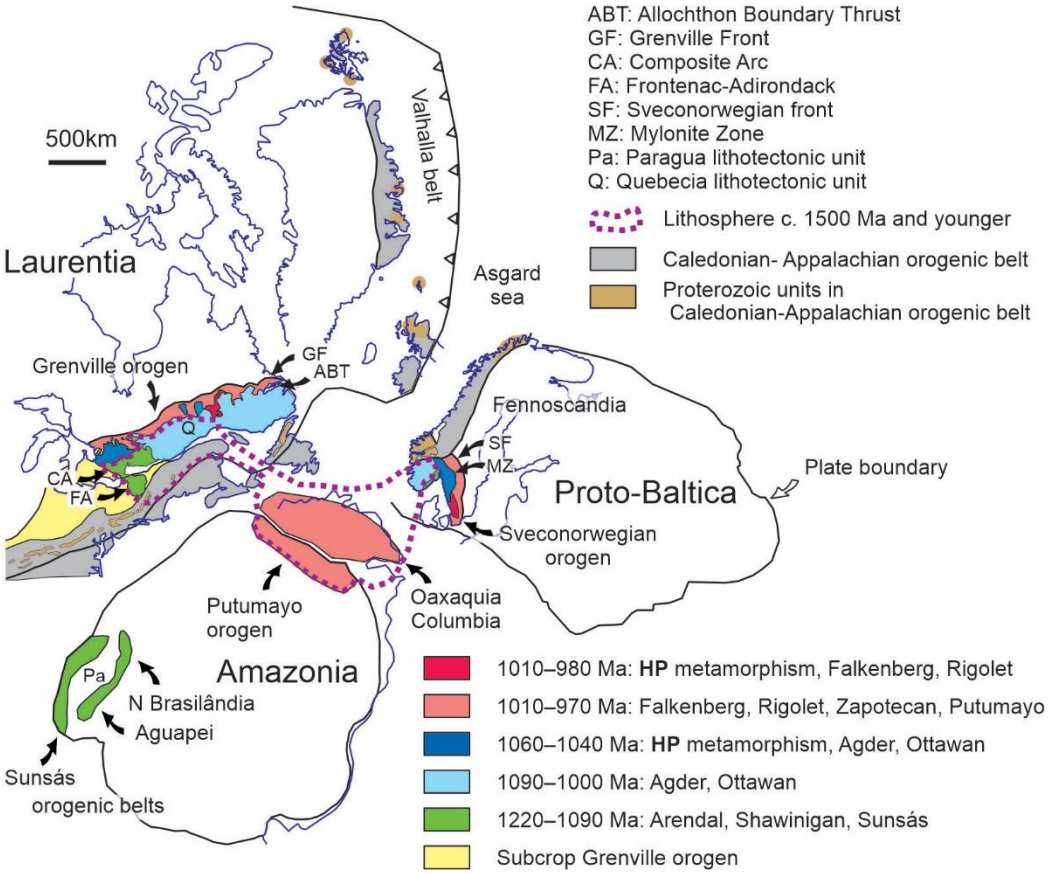

Figure 1. Archetypal paleogeographic reconstruction of proto-Baltica (Baltica), Laurentia and Amazonia in their Rodinia framework at the Mesoproterozoic-Neoproterozoic boundary (Cawood and Pisarevsky, 2017; Hoffman, 1991; Li et al., 2008). The first order architecture of the Meso- to Neoproterozoic orogenic belts is shown, with emphasis on the geochronology of metamorphism (Hynes and Rivers, 2010; Ibanez-Mejia et al., 2011; Rivers, 2008; Tohver et al., 2005). The high-pressure (HP) metamorphic belts are shown separately. The names of the main tectonometamorphic phases in the different orogens are listed in the legend, with Arendal, Agder, Falkenberg for the Sveconorwegian orogen, Shawinigan, Ottawan, Rigolet for the Grenville orogen, Putumayo for the Putumayo orogenic belt, Zapotecan for the Oaxaquia lithotectonic unit, and Sunsás for the Sunsás, Aguapei and N Brasilândia belts.

Table 1. Chart of geological events in the Sveconorwegian orogen.

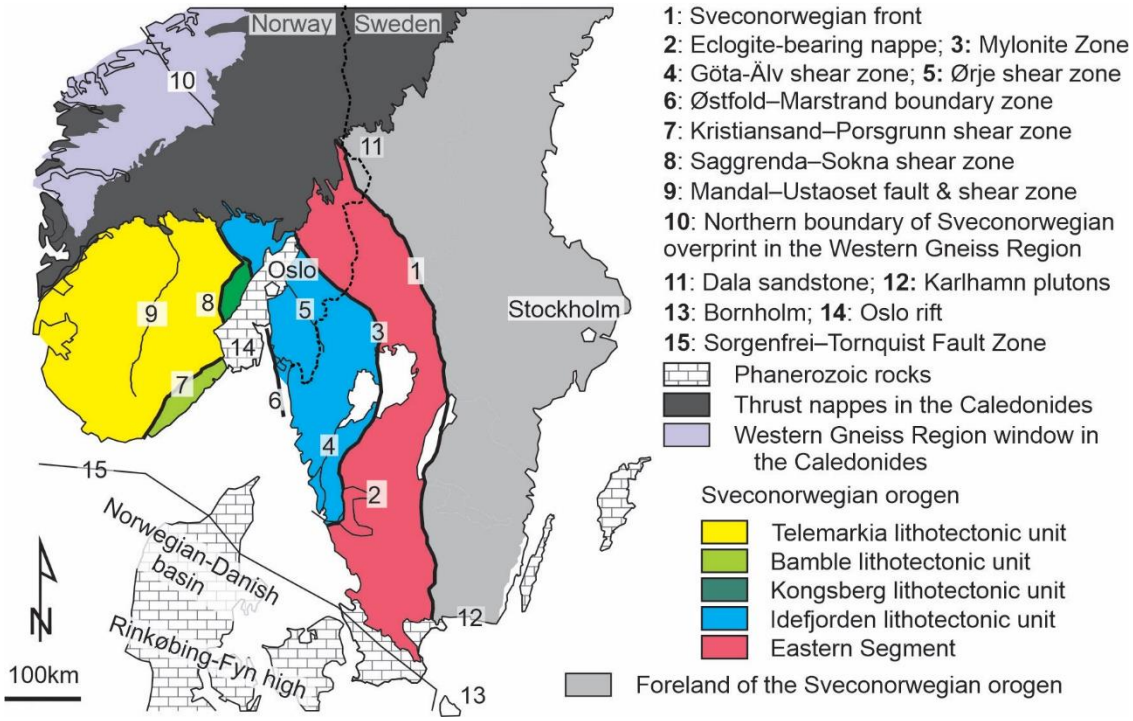

Figure 2. Sketch map of the Sveconorwegian orogen, with nomenclature of lithotectonic units and main shear and fault zones.

---

2 Context

2.1 The Sveconorwegian orogen and Sveconorwegian orogeny

The Sveconorwegian orogen is located along the southwestern margin of Fennoscandia, which is the northern part of proto-Baltica (Fig. 1; Fig. 2; Table 1) (Bogdanova et al., 2008; Koistinen et al., 2001; Stephens et al., 2020). The Sveconorwegian orogen consists of Paleoproterozoic to Mesoproterozoic continental lithosphere reworked during the Sveconorwegian orogeny at the transition between the Mesoproterozoic and the Neoproterozoic (Stenian to Tonian). This lithosphere was generated during the Svecokarelian (1910–1750 Ma), post-Svecokarelian (1710–1660 Ma), Gothian (1660–1520 Ma), Telemarkian (1520–1480 Ma) and Hallandian (1465–1380 Ma) accretionary orogenies.

The exposed Sveconorwegian orogen is presently c. 550 km wide and has a general N–S structural grain (Fig. 2) (Berthelsen, 1980; Demaiffe and Michot, 1985; Falkum, 1985; Falkum and Petersen, 1980). In the east, it is separated from the Paleoproterozoic foreland by the nearly 700 km long Sveconorwegian front (Möller and Andersson, 2018; Möller et al., 2015; Stephens and Wahlgren, 2020a; Wahlgren et al., 1994).

In the north, the Sveconorwegian orogen was reworked during the Caledonian orogeny (Fig. 2). Precambrian rocks with a Meso- to Neoproterozoic overprint are observed in the Western Gneiss Region, the largest basement window in the Caledonides (Røhr et al., 2013; Tucker et al., 1990) and are also found in Caledonian thrust nappes of the Lower and Middle Allochthons of the Caledonides (Augland et al., 2014; Corfu, 2019; Lundmark and Corfu, 2008; Roffeis and Corfu, 2014; Wiest et al., 2018). In the south, the Sveconorwegian basement is overlain by Phanerozoic sedimentary rocks and affected by Carboniferous-Permian and younger faulting and rifting along the WNW–ESE trending Sorgenfrei-Tornquist Fault Zone and NNE–SSW trending Oslo rift (Fig. 2) (Bergerat et al., 2007; Erlström, 2020; Larsen et al., 2008; Torgersen et al., 2015). As inferred from geophysical data and a few deep wells in Denmark, a Sveconorwegian basement probably underlies the Norwegian-Danish Basin (Ringkøbing-Fyn high), reaching the southern boundary of the Baltica plate (Trans-European Suture Zone and Elbe line) (Lassen and Thybo, 2012; Olesen et al., 2004; Olivarius et al., 2015; Thybo, 2001).

The Sveconorwegian orogen can be conceptually subdivided into five, orogen-parallel lithotectonic units (INSPIRE_Directive, 2007), called, from east to west, the Eastern Segment, and the Idefjorden, Kongsberg, Bamble, and Telemarkia lithotectonic units (also referred to as units in short in the following text) (Fig. 2) (Bingen et al., 2008c). These lithotectonic units are separated by major Sveconorwegian shear zones and are characterized by distinct geological histories.

153 The first high-grade metamorphism attributed to the Sveconorwegian orogeny dates back
154 to between 1150 and 1120 Ma and is recorded in the Bamble and Kongsberg lithotectonic
155 units. It is referred to as the Arendal phase in Bingen et al. (2008a; 2008c). As elaborated
156 further below, this early-Sveconorwegian event can be interpreted as the outcome of a
157 geodynamic evolution starting after the Hallandian orogeny, i.e. after c. 1340 Ma, and
158 hereafter referred to as the pre-Sveconorwegian. The main Sveconorwegian orogeny started at
159 c. 1065 Ma, and can be summarized by three orogenic phases (Bingen et al., 2008a; Bingen et
160 al., 2008c): the Agder phase (1065–1000 Ma), the Falkenberg phase (1000–970 Ma) and the
161 Dalane phase (970–900 Ma). As more geological data become available, however, these three
162 phases are becoming increasingly difficult to discriminate in time and they are not used
163 systematically in the following text. Intrusion of pegmatite fields and lamprophyre dykes
164 sealed the orogeny at c. 915–900 Ma (Müller et al., 2015; Müller et al., 2017; Wahlgren et al.,
165 2015).

166 ### *2.2 Rodinia assembly*

167 Several paleogeographic and tectonic models have been proposed for the configuration and
168 assembly of supercontinent Rodinia at the end of the Mesoproterozoic (Hoffman, 1991; Li et
169 al., 2008; Merdith et al., 2017; Torsvik, 2003). Classical models (Fig. 1), integrating
170 paleomagnetic data and geological information from the Proterozoic to the Phanerozoic,
171 suggest that Rodinia formed by the reassembly of continents previously assembled into
172 supercontinent Nuna (Columbia) during the Paleo- and Mesoproterozoic (Evans and Mitchell,
173 2011; Johansson, 2009; Pisarevsky et al., 2014; Rogers and Santosh, 2002; Zhang et al.,
174 2012). These models locate Laurentia in the centre of Rodinia, with Baltica to the east and
175 Amazonia south of Laurentia, respectively (Fig. 1) (Cawood and Pisarevsky, 2017; Dalziel,
176 1997; Gong et al., 2018; Hoffman, 1991; Li et al., 2008; Merdith et al., 2017; Torsvik et al.,

1996). Alternative Baltica–Laurentia reconstructions are proposed by Torsvik (2003), Lorenz et al. (2012) and Slagstad et al. (2019).

It is beyond the scope of this paper to review Rodinia assembly models. In the following text and in several figures, updated geological, geochronological and isotopic data from the Sveconorwegian orogen are compared with data from the Grenville orogen of Laurentia, the Putumayo and Sunsás orogens of Amazonia and Mesoproterozoic lithotectonic units in the Andes (Garzón, Las Minas inliers) and Mexico (Oaxaquia). The goal is to show that it is realistic to consider the Sveconorwegian orogen as part of a large orogenic zone between Laurentia, Amazonia and Baltica (Fig. 1). The comparative analysis offers a broader perspective for the Sveconorwegian orogeny in a Rodinia context.

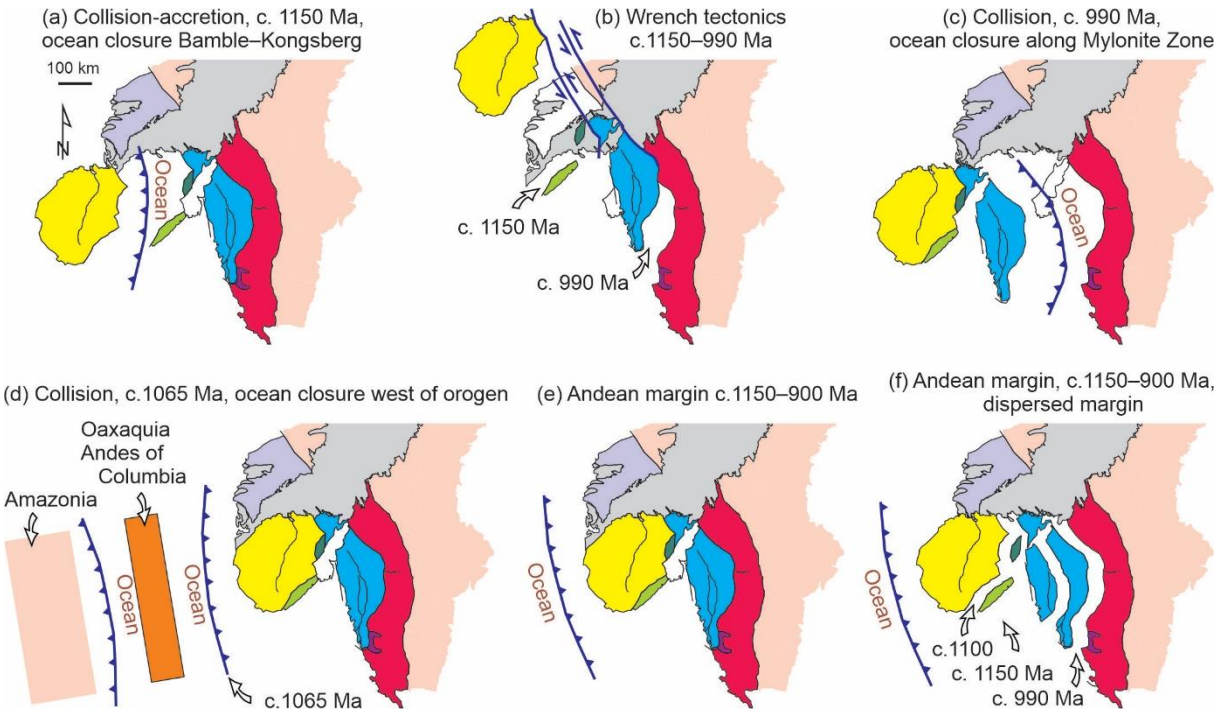

Figure 3. Conceptual tectonic models, in map view, for the Sveconorwegian orogeny, reviewed in this paper. Same colour coding as in Fig. 2. (a) Early-Sveconorwegian accretion of the Telemarkia lithotectonic unit, with suturing along the Bamble-Kongsberg lithotectonic units (Bingen et al., 2005). (b) Wrench tectonics involving large-strike-slip displacements

between the five lithotectonic units of the orogen, all endemic to Fennoscandia (Lamminen and Köykkä, 2010; Stephens and Wahlgren, 2020b). (c) Collision at c. 990 Ma between Baltica (Fennoscandia) and a continent comprising the four western lithotectonic units of the orogen (Möller and Andersson, 2018; Petersson et al., 2015b). (d) Collision at c. 1065 Ma between Baltica (Fennoscandia) and another continental plate (Amazonia) with closure of oceanic basins to the west of the exposed orogen (Bogdanova et al., 2008; Cawood and Pisarevsky, 2017; Ibanez-Mejia et al., 2011). (e, f) non-collisional (Andean) models, with orogeny controlled by a subduction system outboard of Fennoscandia during the entire duration of orogeny from c. 1150 to 900 Ma. (e) The margin was either well assembled before the orogeny (Falkum and Petersen, 1980; Slagstad et al., 2013) or (f) dispersed and re-assembled during the orogeny (Slagstad et al., 2020).

2.3 A diversity of orogenic models

Many large-scale tectonic models have been proposed to explain the Sveconorwegian orogenic evolution. In Fig. 3, six possible conceptual end-member models are sketched in map view. They range from collisional (Himalaya-Tibet type) to non-collisional (Andean type), and some involve accretion of exotic lithotectonic units to Fennoscandia. In Fig. 3 a, the early-Sveconorwegian closure of an ocean between the Telemarkia and Idefjorden lithotectonic units resulted in the formation of the Bamble-Kongsberg lithotectonic units at c. 1150–1120 Ma, and accretion of an exotic Telemarkia lithotectonic unit (Bingen et al., 2005). In Fig. 3 b, the five lithotectonic units are all endemic to Fennoscandia. Only large-scale movements between them are considered, steered by large scale wrench tectonics, which is controlled by strike-slip shearing along the main Sveconorwegian shear zones (Bingen et al., 2005; Lamminen and Köykkä, 2010; Stephens and Wahlgren, 2020b). In Fig. 3 c, closure of an oceanic basin at c. 990 Ma between the Eastern Segment and the Idefjorden lithotectonic

218 unit along the Mylonite Zone, resulted in collision between Baltica (Fennoscandia) and a
219 continent composed of the four western lithotectonic units of the orogen ('Sveconorwegia')
220 (Möller and Andersson, 2018; Petersson et al., 2015b). In Fig. 3 d, an (Himalaya-Tibet type)
221 collision at and after c. 1065 Ma between Baltica (Fennoscandia) and one (or several)
222 continental plate(s) (possibly Amazonia, Laurentia, and intervening terranes exposed in
223 Mexico and the Andes of Colombia) involved closure of oceanic basins to the west of the
224 exposed orogen (Bingen et al., 2008c; Bogdanova et al., 2008; Cawood and Pisarevsky, 2017;
225 Ibanez-Mejia et al., 2011; Stephens and Wahlgren, 2020b; Weber et al., 2010). In Fig. 3 e and
226 f, non-collisional (Andean type) models feature an eastward subduction of an oceanic plate
227 below the western margin of Baltica (Fennoscandia) during the entire Sveconorwegian
228 orogeny, from 1150 to 900 Ma, in the absence of a final collision. The lithotectonic units in
229 the orogen either were assembled already before the Sveconorwegian orogeny (Fig. 3 e)
230 (Falkum and Petersen, 1980; Slagstad et al., 2013) or, alternatively, they were dispersed
231 during the pre-Sveconorwegian time interval (1280–1150 Ma) and then re-assembled during
232 the Sveconorwegian orogeny after 1150 Ma (Fig. 3 f) (Slagstad et al., 2020). These six
233 models are not mutually exclusive because terrane assembly (Fig. 3 a, c) can be anticipated
234 before a collision (Fig. 3 d) or during a protracted subduction history (Fig. 3 e, f), and because
235 deformation partitioning (Fig. 3 b) can take place before, during and after a collision or during
236 protracted subduction. Arguments supporting or dismissing aspects of each of these orogenic
237 models are discussed in more detail below.

238 ### *2.4 Secular evolution of the Earth, mantle delamination and orogenic plateau*

239 Estimates of heat flow and heat production through Earth history suggest that the
240 asthenosphere was c. 100°C hotter in the Mesoproterozoic than at present (Gerya, 2014;
241 Herzberg et al., 2010; Johnson et al., 2013; Korenaga, 2008; Sizova et al., 2014). A hotter
242 asthenosphere implies a weaker rheology of lithospheric plates. The tectonic consequences of

a hotter asthenosphere on the dynamics of orogeny are multiple and include, but are not limited to, ductile thick-skinned deformation, lower topography, more proximal sedimentation, shallower slab breakoff, widespread partial melting in the lower to middle crust, widespread syn-orogenic magmatism, ultrahigh temperature granulite-facies metamorphism (above 900°C), decoupling between crust and lithospheric mantle, and remelting of basaltic underplates to produce anorthosite plutons (Brown, 2006, 2013; Gerya, 2014; Rey and Houseman, 2006; Sizova et al., 2014; Vander Auwera et al., 2011; Vanderhaeghe, 2012). These consequences can be evaluated qualitatively in the Proterozoic geological record (Cagnard et al., 2011; Chardon et al., 2009). However, they are difficult to assess and quantify individually (Sizova et al., 2014).

There is wide consensus that after the Archean, plate tectonics has imposed dominant horizontal movements to orogenies. However, an evaluation of the composition and temperature of the lithosphere through Earth history suggests that, after the Archean, the sub-continental lithospheric mantle was, on average, denser than the asthenosphere (Griffin et al., 2009; Poudjom Djomani et al., 2001). The sub-continental lithospheric mantle was therefore gravitationally unstable in the Proterozoic, like in the Phanerozoic, and prone to delamination and foundering (subduction) (Bird, 1979; Chen et al., 2017; Krystopowicz and Currie, 2013). Delamination of the lithospheric mantle is compensated by upwelling of asthenosphere. The parameters and geometry of delamination in convergent orogens were explored numerically by Li et al. (2016). Delamination is promoted by the density contrast between the lithospheric mantle and the asthenosphere, rheological weakness of the lower crust and the lithospheric mantle, convergence rate, and eclogitization of the lower crust.

The Sveconorwegian orogeny is characterized by widespread crustal partial melting, low-pressure–ultrahigh-temperature metamorphism and massif-type anorthosite plutonism, typical of hot orogens. Orogenic models for the Sveconorwegian orogeny should integrate the

evolution of the mantle (and not only the crust). They require consideration of vertical movements of the lithospheric mantle and the asthenosphere in addition to horizontal movements of the lithospheric plates.

Orogenic plateaus are a hallmark of large and hot convergent orogens (Beaumont et al., 2006; Godin et al., 2006; Jamieson and Beaumont, 2013; Li et al., 2016; Rey et al., 2001; Royden et al., 2008; Vanderhaeghe, 2012). An orogenic plateau consists of elevated and thickened crust spreading by gravitational forces, above a lithospheric mantle thinned by delamination. Temperature in the crust is regulated by self-heating and basal heating from the mantle. The crust of a plateau is characterized by a little viscous low- to middle-crust, weakened by partial melting, called infrastructure, overlain by a brittle upper crust, called superstructure or orogenic lid (Jamieson and Beaumont, 2013; Rey et al., 2001; Vanderhaeghe, 2012). In the infrastructure, metamorphism typically carries a high-temperature signature, overprinting pre-plateau metamorphic signatures (for example early high-pressure metamorphism) (Godin et al., 2006). Due to the difference in viscosity, the infrastructure and superstructure are structurally decoupled. The infrastructure can flow under the superstructure (channel flow), leading to a situation where the superstructure is in extension, while the infrastructure is in compression. An orogenic plateau can be anticipated to grow with time if convergence is maintained (Li et al., 2016; Royden et al., 2008).

The Sveconorwegian orogen consists of a patchwork of high-grade gneiss complexes and low-grade rocks (Fig. 4). In this paper, these are interpreted as the remnants of the infrastructure and superstructure of an orogenic plateau, respectively.

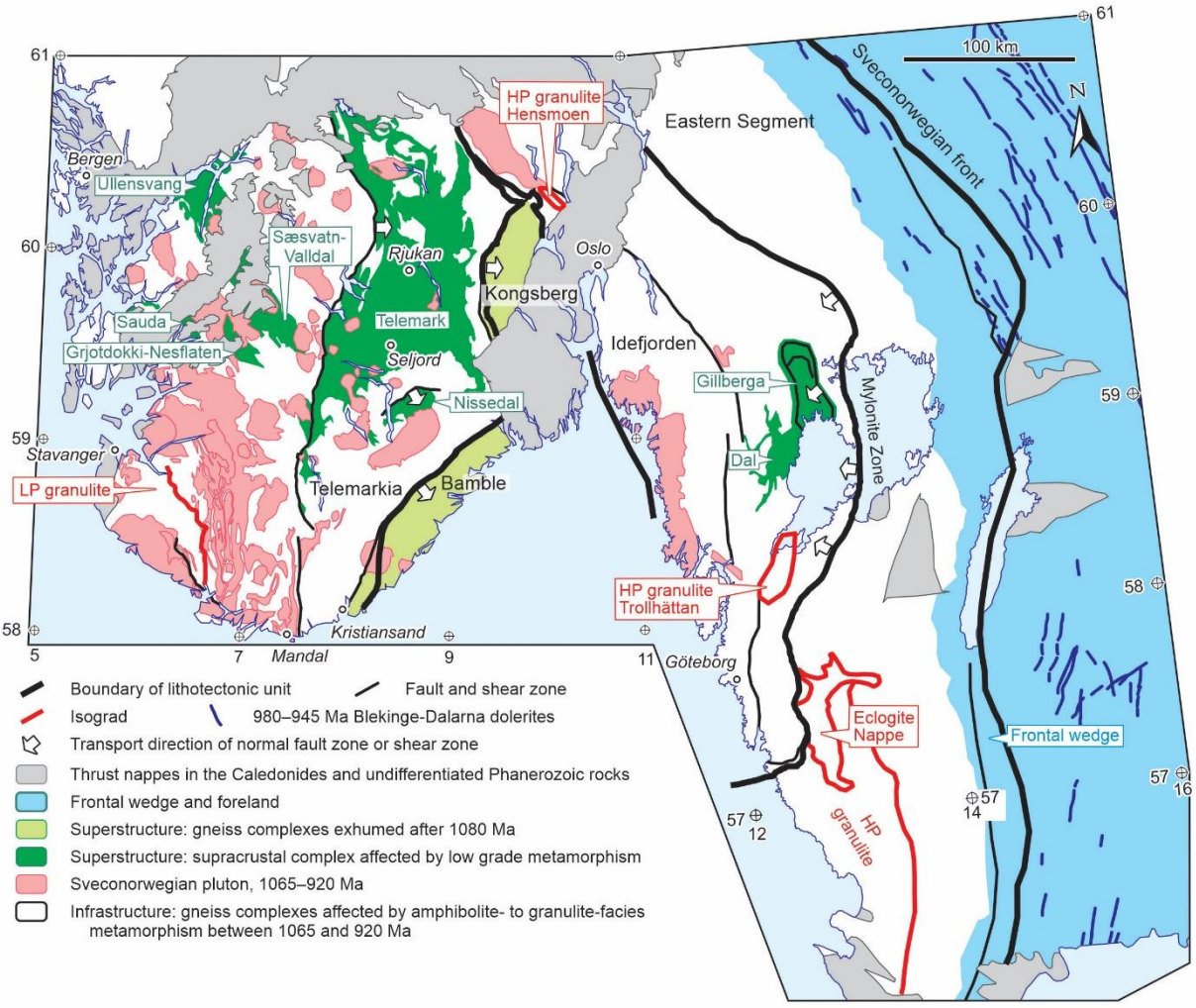

Figure 4. Sketch map of the Sveconorwegian orogen, showing the extent of the infrastructure and superstructure (orogenic lid) of the orogen during the main Sveconorwegian orogeny (1065–920 Ma) and Sveconorwegian plutons (1065–920 Ma).

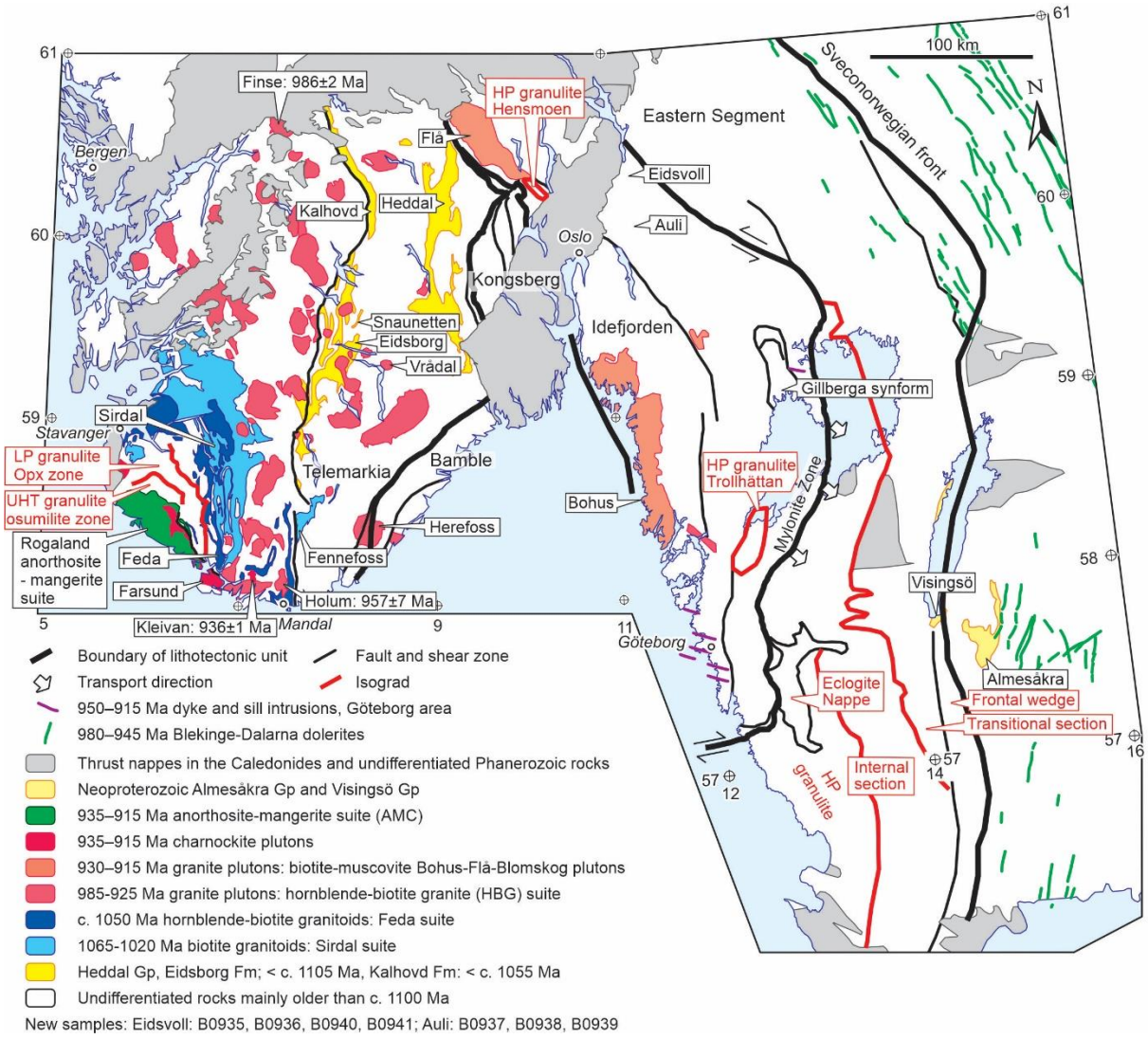

Figure 5. Sketch map of the Sveconorwegian orogen, with emphasis on Sveconorwegian events younger than c. 1100 Ma. Localities of samples in Auli and Eidsvoll analysed in this study are shown. Age intervals in the legend rounded in 5 Ma intervals.

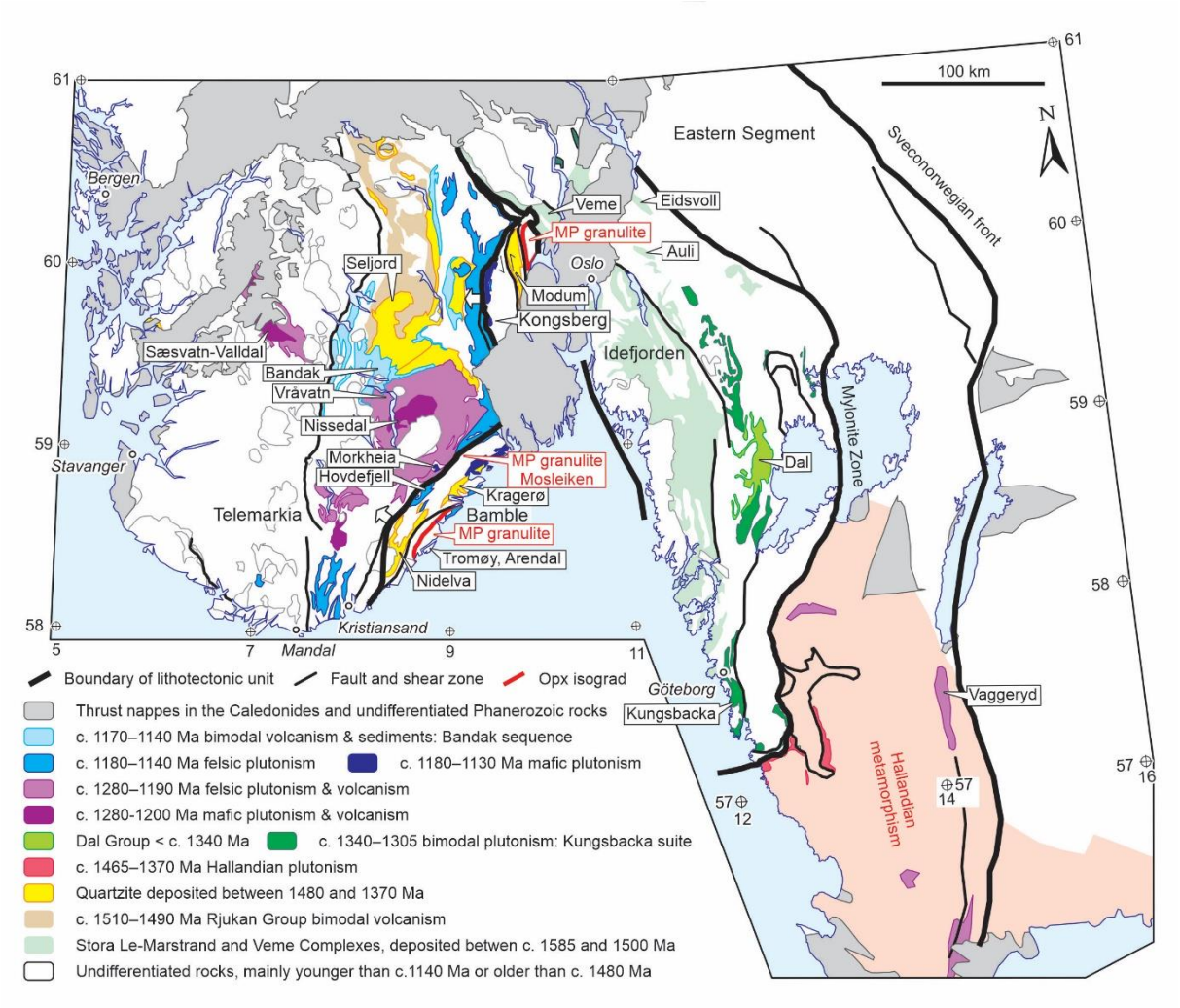

Figure 6. Sketch map of the Sveconorwegian orogen, with emphasis on pre- and early-Sveconorwegian events and rocks.

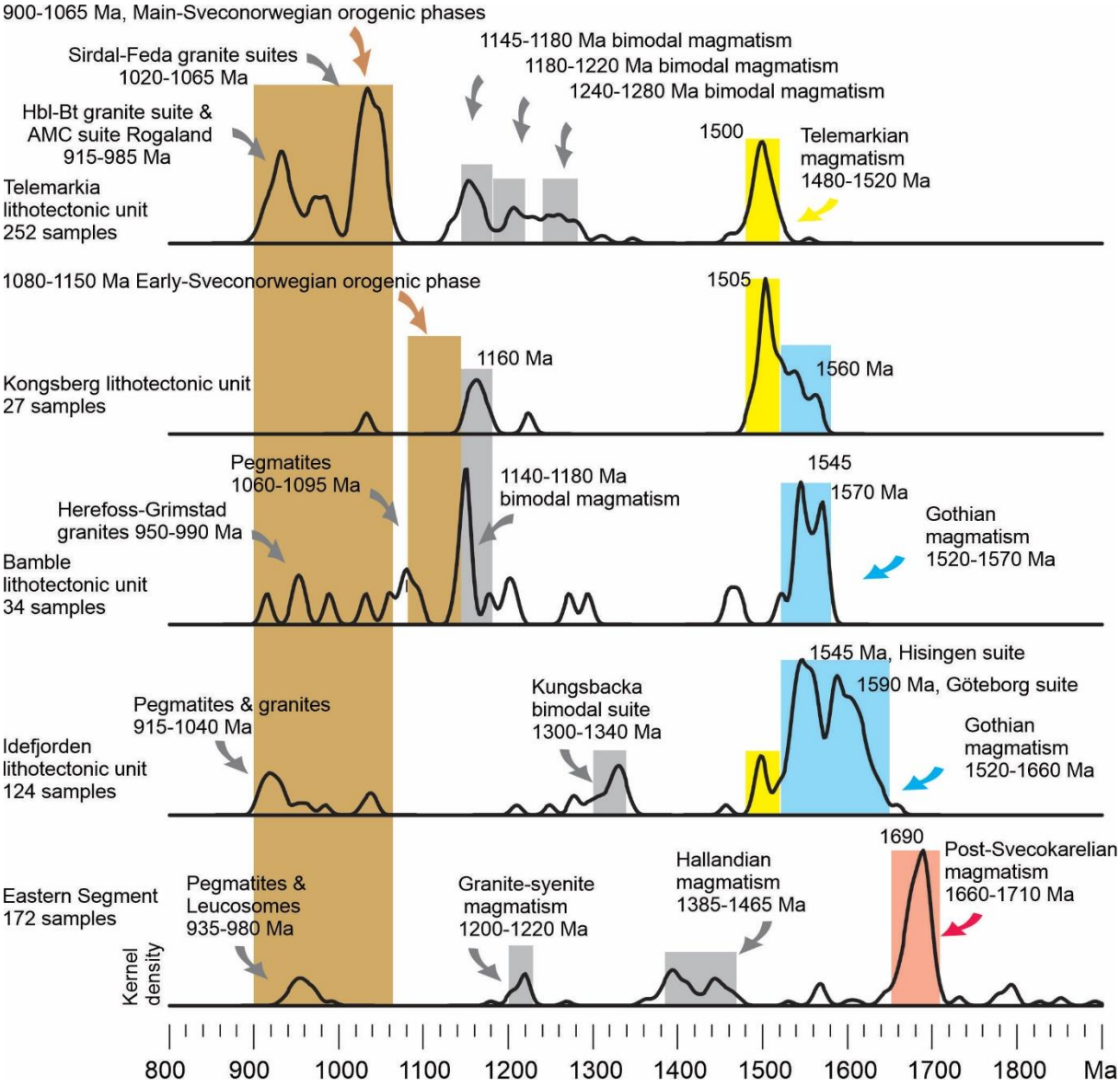

Figure 7. Kernel density estimators summarizing the geochronology of magmatic rocks in the five lithotectonic units of the Sveconorwegian orogen, on a compilation of published data. The plots are generated with "DensityPlotter" (Vermeesch, 2012) (each published age is entered as one value, with a bandwidth of 6 Ma; the height of the five curves is identical and normalized to the one of the largest peak). The compilation is provided in the supplementary material, with referencing.

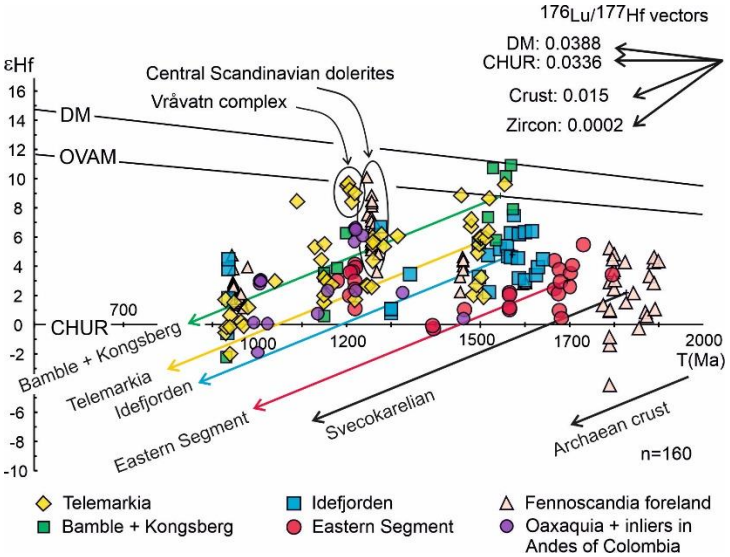

Figure 8. Hafnium isotopic composition of magmatic rocks in the Sveconorwegian orogen and Fennoscandia foreland, expressed as ε_{Hf} (initial value) as a function of intrusion age. Interpretations of the distribution of data are discussed in the text. The five lithotectonic units are shown with distinct colours and summarized by an evolution vector. The Oaxaquia lithotectonic unit (Mexico) and the inliers in the Andes of Colombia are shown for comparison. Each symbol represents the average value for one sample, of the isotopic composition of several analyses of zircon or baddeleyite or of one whole-rock analysis (only a few samples), at the recommended time of intrusion (zircon or baddeleyite U–Pb age). Total of 220 samples. Sources of data: Sveconorwegian orogen and foreland: Andersen et al. (2009; 2002b; 2007), Lamminen et al. (2011) , Pedersen et al. (2009), Petersson et al. (2015a; 2015b), Roberts et al. (2013); Söderlund et al. (2005); Oaxaquia and inliers in the Andes of Colombia: Ibanez-Mejia et al. (2015), Weber et al. (2010); DM: depleted mantle (Griffin et al., 2000); OVAM: oceanic volcanic arc mantle (Dhuime et al., 2011); CHUR: chondritic reservoir (Bouvier et al., 2008). The top right inset shows the $^{176}Lu/^{177}Hf$ ratio and evolution vectors of isotopic reservoirs and typical zircon.

---

3 Geology of the Sveconorwegian orogen

The geology of the Sveconorwegian orogen is reviewed below from east to west, using the nomenclature summarized in Table 1 and the maps of Fig. 2, Fig. 4, Fig. 5 and Fig. 6. A compilation of the geochronology of magmatic rocks is provided in Fig. 7, and a compilation of Lu–Hf isotopic data in Fig. 8.

3.1 Fennoscandian foreland

The Fennoscandian foreland of the Sveconorwegian orogen (Fig. 2) comprises mainly metamorphosed Paleoproterozoic magmatic rocks (plutonic and volcanic rocks) and siliciclastic sedimentary rocks, dating back to between c. 1960 Ma and 1740 Ma (Bergman et al., 2008; Korja et al., 2006; Lahtinen et al., 2009; Stephens, 2020). These rocks were assembled during the accretionary Svecokarelian orogeny. They were unconformably overlain and crosscut by post-Svecokarelian volcanic and plutonic complexes formed between c. 1710 and 1680 Ma (Appelquist et al., 2011; Brander et al., 2012; Högdahl et al., 2004; Ripa and Stephens, 2020a). These rocks are attributed in the literature to the Phase 2 of the Transcandinavian Igneous Belt and are little deformed to undeformed. They are interpreted to have formed in a supra-subduction geodynamic setting after the Svecokarelian orogeny. Younger Mesoproterozoic magmatic rocks intruded this basement, including granite plutons (1530–1220 Ma ; Andersson et al., 2002b; Brander and Söderlund, 2009; Cecys and Benn, 2007; Johansson et al., 2016), dolerites (c. 1460 Ma; Söderlund et al., 2005), and the so-called Central Scandinavian dolerites (1271 ± 1 to 1246 ± 2 Ma; Brander et al., 2011; Ripa and Stephens, 2020c; Söderlund et al., 2006).

The c. 1 km thick unconformable Jotnian sandstone was deposited in a gentle continental sag basin between c. 1580 Ma and 1270 Ma and it is not deformed (Lundmark and Lamminen, 2016; Ripa and Stephens, 2020b). The southernmost part of the Fennoscandian foreland was reworked during the Hallandian orogenic event between 1465 and 1385 Ma

(Fig. 6) (Bogdanova et al., 2008; Brander and Söderlund, 2009; Ulmius et al., 2015; Wahlgren and Stephens, 2020).

Sveconorwegian-related brittle deformation reached far into the Fennoscandian foreland (Andréasson and Rodhe, 1994; Elminen et al., 2018; Mattila and Viola, 2014; Saintot et al., 2011; Viola et al., 2009; Viola et al., 2013). The Blekinge-Dalarna dolerites form a weakly arcuate N-S trending dyke swarm parallel to the Sveconorwegian front (Fig. 4; Fig. 5). They intruded between 978 ± 2 and 946 ± 1 Ma, in the easternmost part of the Sveconorwegian orogen and its foreland (Gong et al., 2018; Ripa and Stephens, 2020d; Söderlund et al., 2005). The c. 1200 m thick, sandstone dominated, Almesåkra Group represents possible remnants of a Sveconorwegian fold-and-thrust belt, to the east of the Sveconorwegian front (Fig. 5) (Ripa and Stephens, 2020d; Rodhe, 1987). Locally preserved peperitic contacts between the Blekinge-Dalarna dolerites and these sediments suggest that the sandstone was unconsolidated during intrusion of the dolerites and therefore that the two rock types are broadly coeval.

The Neoproterozoic, c. 1400 m thick, microfossil-bearing, Visingsö Group is exposed along the Sveconorwegian front in Sweden (Fig. 5). Its deposition is bracketed between 886 ± 9 Ma (detrital zircon U–Pb data) and c. 740 Ma (biostratigraphy). It can be considered as the infill of a post-Sveconorwegian, fault-controlled basin (Loron and Moczydłowska, 2018; Moczydłowska et al., 2018; Pulsipher and Dehler, 2019; Wickström and Stephens, 2020).

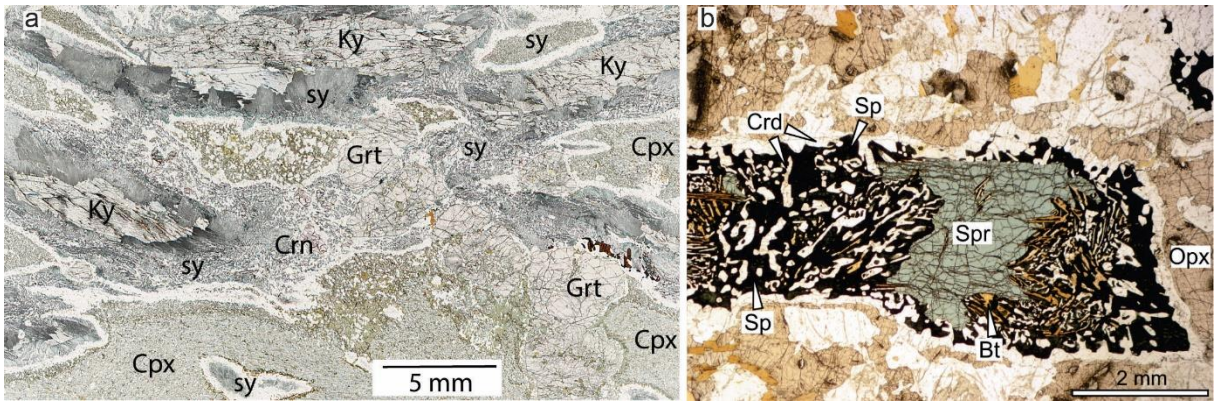

Figure 9. Microphotographs of thin sections showing the contrast between high-pressure (eclogite-facies) and ultrahigh temperature (granulite-facies) metamorphism, east and west of the Sveconorwegian orogen, respectively, at c. 1000 Ma. (a) Kyanite-bearing (retro)eclogite from the eclogite-bearing nappe in the Eastern Segment (Möller and Andersson, 2018). The thin section shows a partly preserved peak eclogite-facies assemblage of garnet (Grt) + omphacite (Cpx) + kyanite (Ky) + amphibole + rutile (1.8 GPa - 870°C - 988 ± 6 Ma) breaking down into a symplectitic (sy) assemblage during isothermal decompression. Symplectites (sy) include a sapphirine + corundum + anorthite reaction rim around kyanite, an orthopyroxene + plagioclase + amphibole reaction rim around clinopyroxene, and plagioclase expulsion symplectite in former omphacite (Cpx). Garnet preserves a prograde (pre-eclogite-facies) zoning, and the rock shows evidence for a hairpin P-T path (Tual et al., 2017). (b) Sapphirine + orthopyroxene granulite from the Ivesdal locality, in the ultra-high temperature (UHT) zone of Rogaland, in the Telemarkia lithotectonic unit (Laurent et al., 2018b). The thin section shows the peak assemblage of sapphirine (Spr) mantled by orthopyroxene (Opx) (0.6 GPa - 920°C - 1029 ± 9 to 1006 ± 8 Ma) breaking down into an assemblage of cordierite (Crd) + hercynite (Sp) with additional biotite (Bt) (4.5 GPa – 900°C) giving evidence for a clockwise P-T path.

3.2 Eastern Segment

394 *3.2.1 Svecokarelian and post-Svecokarelian evolution*

395 The Eastern Segment is a 60 to 120 km wide, N–S trending lithotectonic unit mainly
396 consisting of granitic to quartz-monzonitic orthogneiss (Fig. 2) (Berthelsen, 1980; Möller and
397 Andersson, 2018; Stephens and Wahlgren, 2020a). The protoliths formed between c. 1900
398 and 1660 Ma, with a strong frequency maximum of crystallization ages between 1710 and
399 1660 Ma (Fig. 7). They have an alkali-calcic geochemical composition and are characterized
400 by a mildly positive ε_{Hf} and ε_{Nd} isotopic signature (average ε_{Hf} = + 3.0 at 1700 Ma; Fig. 8)
401 (Appelquist et al., 2011; Appelquist et al., 2008; Brander et al., 2012; Gorbatschev and
402 Bogdanova, 2006; Petersson et al., 2015a; Söderlund et al., 1999; Söderlund et al., 2002;
403 Stephens and Wahlgren, 2020a). They represent the western continuation of the
404 Paleoproterozoic crust exposed in the foreland of the Sveconorwegian orogen, especially the
405 post-Svecokarelian, 1710–1680 Ma, magmatic rocks exposed just east of the Sveconorwegian
406 front (Petersson et al., 2015a; Ripa and Stephens, 2020a; Stephens and Wahlgren, 2020a).
407 They were presumably formed in the same geodynamic setting along the same active
408 continental margin.

409 *3.2.2 Hallandian and pre-Sveconorwegian evolution*

410 After an event of mafic magmatism around 1565 Ma (Beckman et al., 2017; Söderlund et al.,
411 2004; Söderlund et al., 2005), the southern part of the Eastern Segment and the
412 Sveconorwegian foreland were together affected by the Hallandian orogeny (Fig. 6; Fig. 7).
413 The Hallandian orogeny involved low-pressure amphibolite- to granulite-facies
414 metamorphism, migmatitization and deformation between c. 1465 and 1385 Ma (Brander et
415 al., 2012; Möller et al., 2007; Piñán-Llamas et al., 2015; Söderlund et al., 2002; Ulmius et al.,
416 2015), and was accompanied by magmatism during the same time interval (Fig. 7) (Åhäll et
417 al., 1997; Andersson et al., 1999; Brander and Söderlund, 2009; Cecys et al., 2002;
418 Christoffel et al., 1999; Möller et al., 2015; Ulmius et al., 2015). The final stage of Hallandian

magmatism includes a suite of charnockite-mangerite, granite and anorthosite plutons formed between c. 1400 and 1380 Ma (Åhäll et al., 1997; Christoffel et al., 1999; Harlov et al., 2013; Möller et al., 2015). The Hallandian orogeny may have involved subduction along the southern margin of Baltica and may record a change in the configuration of subduction zones around Baltica, from E-dipping before 1480 Ma to N-dipping after 1465 Ma (Pisarevsky et al., 2014; Roberts and Slagstad, 2015; Stephens and Wahlgren, 2020b; Ulmius et al., 2015).

Post-Hallandian bimodal plutonism took place between 1225 and 1180 Ma, including dolerites (Protogine zone dolerites) and syenitic to granitic plutons (e.g. the Vaggeryd syenite; Fig. 6) (Larsson and Söderlund, 2005; Petersson et al., 2015a; Söderlund and Ask, 2006; Söderlund et al., 2005). These rocks are characterized by a supra-chondritic (radiogenic) ε_{Hf} isotopic signature ($+1.2 < \varepsilon_{Hf} < + 6.6$) implying an influx of depleted mantle derived magmas along the Sveconorwegian front (Fig. 8) (Petersson et al., 2015a; Söderlund et al., 2005).

3.2.3 Sveconorwegian orogeny

The Sveconorwegian metamorphic grade in the Eastern Segment increases towards the WSW (Fig. 5) (Johansson et al., 1991; Möller and Andersson, 2018; Möller et al., 2015; Piñán-Llamas et al., 2015). Four zones of distinct metamorphic and structural reworking can be defined from east to west: (i) a frontal wedge, (ii) a transitional section, (iii) an internal section and (iv) an eclogite-bearing ductile nappe (Möller and Andersson, 2018; Möller et al., 2015).

The frontal wedge (i) is a zone of non-penetrative Sveconorwegian deformation forming a steep or fan-shaped structure in cross section that narrows and steepens towards the south (Möller and Andersson, 2018; Stephens and Wahlgren, 2020a; Wahlgren et al., 1994). The zone comprises a network of thin (<100 m), N–S trending, steeply dipping, greenschist- to amphibolite-facies ductile shear zones with mainly western-block-up kinematics (Andréasson and Dallmeyer, 1995; Brander et al., 2012; Gorbatschev and Bogdanova, 2006; Söderlund et

444 al., 2004; Wahlgren et al., 1994). The frontal wedge is bound in the east by the
445 Sveconorwegian front, which in the north is a system of discontinuous west dipping shear
446 zones with reverse top-to-east sense of shear (Wahlgren et al., 1994). In the northernmost part
447 of the Eastern Segment in Norway, the frontal wedge is poorly documented.

448 The transitional section (ii) exhibits a near-penetrative amphibolite-facies overprint, with
449 little evidence for partial melting (Beckman et al., 2017; Möller and Andersson, 2018;
450 Söderlund et al., 1999). The internal section (iii) is characterized by upper-amphibolite-facies
451 conditions increasing westwards to high-pressure granulite-facies conditions (1.1 GPa -
452 850°C; Fig. 5). This metamorphic evolution caused widespread migmatitization, transposition
453 leading to mafic and felsic gneissic layering (banding), dynamic recrystallization of original
454 magmatic textures, as well as reworking of previous Hallandian structures, where present
455 (Andersson et al., 1999; Connelly et al., 1996; Hansen et al., 2015; Möller et al., 2015; Möller
456 et al., 2007; Piñán-Llamas et al., 2015). The regional aeromagnetic map (Geological Survey
457 of Sweden) unveils prominent, regional scale fold interference patterns, with E-W trending
458 and gently-plunging fold axes and trains of N–S trending folds (Möller et al., 2007; Stephens
459 and Wahlgren, 2020a; Viola et al., 2011). Several generations of folds can be recognised (F1
460 to F4), including km-scale asymmetric to recumbent folds and late upright folds (Möller and
461 Andersson, 2018; Möller et al., 2015 ; Piñán-Llamas et al., 2015; Tual et al., 2015). These
462 different generations record continued deformation under high-grade metamorphic conditions.

463 The eclogite-bearing ductile nappe (iv) is hosted in the innermost section of the Eastern
464 Segment as an E-vergent ductile nappe, folded into a c. 50 x 75 km large recumbent fold (Fig.
465 5) (Möller et al., 2015; Tual et al., 2015). It is well defined on the regional aeromagnetic map
466 and bordered (on the southern and eastern flanks) by a sheet of c. 1380 Ma granite (Fig. 6).
467 The ductile nappe hosts retro-eclogite bodies up to 2 km in length (Möller, 1998, 1999;
468 Möller and Andersson, 2018; Möller et al., 2015; Tual et al., 2015). The retro-eclogite bodies

469 are layered mafic rocks, including two characteristic varieties, a Mg-Al-rich kyanite-bearing
470 variety and a Fe-Ti-rich variety. Retro-eclogites preserve prograde growth zoning of garnet
471 and show widespread retrogression of omphacite and kyanite into granulite-facies
472 symplectites (clinopyroxene + plagioclase, orthopyroxene + plagioclase, and anorthite +
473 sapphirine + corundum) (Fig. 9 a). They constrain a narrow (hairpin) clockwise pressure-
474 temperature path at high temperature. Eclogite-facies peak conditions of 1.65–1.9 GPa and
475 850–900°C were followed by near-isothermal decompression (Tual et al., 2017). Eclogite
476 boudins are hosted in strongly deformed, partly migmatitic, gneisses characterized by a
477 pervasive foliation, E–W stretching lineation, and S- to E-vergent folds (Möller et al., 2015;
478 Tual et al., 2015). Two post-eclogite-facies deformation phases (D1-D2) are described as
479 successively documenting an early stage of exhumation and east-directed transport of the
480 ductile nappe, lubricated by partial melts.

481 A zircon U–Pb age determination from an eclogite sample defines a maximum age for
482 eclogite-facies metamorphism of 988 ± 6 Ma (Möller et al., 2015). Zircon in felsic and mafic
483 gneiss, migmatite and syn-kinematic granite in the entire Eastern Segment, including the
484 eclogite-bearing nappe, yields a consistent age interval between 978 ± 7 and 961 ± 6 Ma for
485 amphibolite- to granulite-facies metamorphism, deformation and partial melting (Andersson
486 et al., 2002a; Beckman et al., 2017; Hansen et al., 2015; Möller et al., 2015; Möller et al.,
487 2007; Piñán-Llamas et al., 2015; Söderlund et al., 2002). Cross-cutting pegmatite dykes
488 intruded between 961 ± 13 and 934 ± 6 Ma (Andersson et al., 1999; Möller et al., 2007;
489 Möller and Söderlund, 1997; Söderlund et al., 2008b; Söderlund et al., 2002). Titanite U–Pb
490 ages range from c. 976 ± 4 to 923 ± 3 Ma, with the oldest age recorded in the northern part of
491 the transitional section and the youngest ages in the internal section (Connelly et al., 1996;
492 Johansson et al., 2001; Söderlund et al., 1999; Wang et al., 1998). Hornblende and biotite
493 $^{40}Ar/^{39}Ar$ plateau ages in the internal section are interpreted to date regional cooling between

c. 530 and 330°C between c. 901 ± 2 and 893 ± 3 Ma (Ulmius et al., 2018). Biotite and muscovite $^{40}Ar/^{39}Ar$ plateau ages collected in the frontal wedge range from 930 ± 6 to 882 ± 2 Ma (Andréasson and Dallmeyer, 1995; Page et al., 1996a; Ulmius et al., 2018). The youngest ages are recorded in the southernmost exposed section of the orogen. These ages either record discrete events of (re)crystallization or cooling after deformation by shear zones at the front of the orogen (Andréasson and Dallmeyer, 1995; Page et al., 1996a; Ulmius et al., 2018).

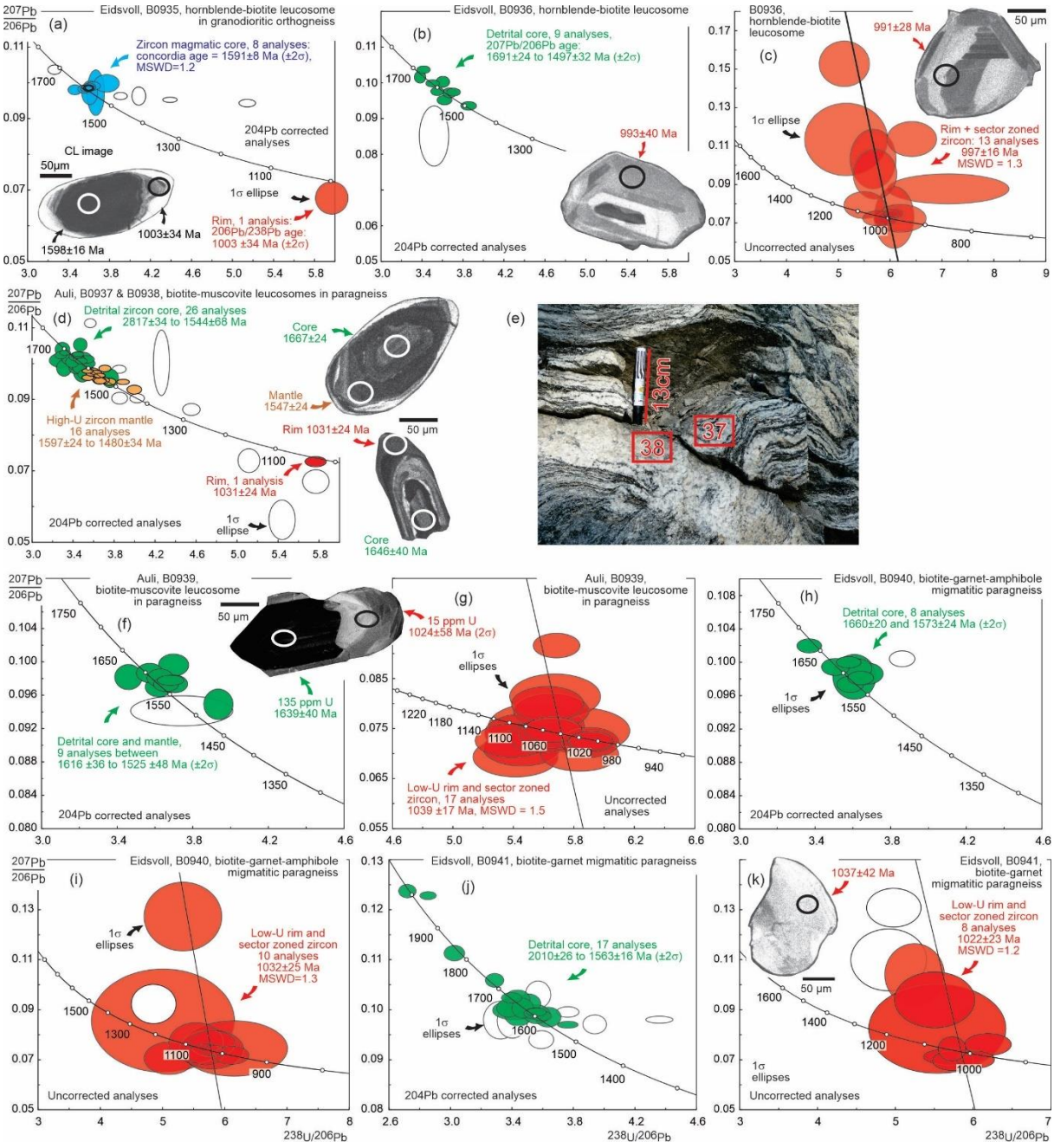

Figure 10. New geochronological data of migmatitic gneisses in the Eidsvoll-Auli area, Idefjorden lithotectonic unit (Fig. 5). (a–k) Tera-Wasserburg concordia diagrams with zircon SIMS U–Pb analyses and a selection of CL images of zircon with position of analyses. Blue ellipses for magmatic zircon cores, green ellipses for detrital zircon cores, and red ellipses for low-U sector zoned zircon and zircon rims attributed to migmatitization. One sigma error ellipses. (e) Photo of outcrop where two samples represent two generations of leucosomes, with B0938 crosscutting B0937. Interpretation: migmatites from the five studied localities are characterized by abundant, interconnected leucosomes (stromatic texture) parallel to the gneissic foliation. Zircon contains an inherited core (magmatic or detrital), a CL-dark mantle and a CL-bright rim. Analyses of the mantle overlap with those of the core and define a significant spread in each sample. The spread of apparent ages can be interpreted to represent partial recrystallization of the core during partial melting. Newly formed CL-bright rims or large crystals with oscillatory to weakly sector zoning reflect crystallization of zircon related to migmatitization (Harley et al., 2007; Kelsey et al., 2008; Rubatto et al., 2009) between 1039 ± 17 and 997 ± 16 Ma (a, c, g, i, k). In this c. 40 Myr time interval, the biotite-muscovite and biotite-garnet leucosomes range from 1039 ± 17 to 1022 ± 23 Ma (d, g, i, k), while the hornblende-biotite-bearing leucosomes are marginally to significantly younger with ages of 1003 ± 34 and 997 ± 16 Ma (a, c). This difference suggests that muscovite and biotite dehydration melting took place before amphibole dehydration melting, in what can be interpreted as reflecting increasing temperature or isothermal decompression.

Table 2. Summary of sampling and zircon U-Pb data for migmatitic gneisses, Eidsvoll-Auli area, Idefjorden lithotectonic unit.

3.3 Idefjorden lithotectonic unit

The Idefjorden lithotectonic unit is a c. 140 km wide unit exposed west of the Eastern Segment on either side of the Permian Oslo Rift (Fig. 2, Fig. 5) (Åhäll and Connelly, 2008; Åhäll and Gower, 1997; Bergström et al., 2020; Bingen et al., 2001; Park et al., 1991; Viola et al., 2011). It is bounded in the east by the 450 km long, west dipping, Mylonite Zone.

3.3.1 Gothian and pre-Sveconorwegian evolution

The Idefjorden lithotectonic unit is made up of plutonic and volcanic rocks formed during the Gothian accretionary orogeny mainly between 1660 and 1520 Ma and associated with metasedimentary rocks (Fig. 7) (Åhäll and Connelly, 2008; Åhäll and Larson, 2000; Ahlin et al., 2006; Andersen et al., 2004a; Bergström et al., 2020; Bingen et al., 2005; Brewer et al., 1998; Graversen and Pedersen, 1999). From east to west, three complexes (called formations or belts in the literature) are described as younging towards the west (Åhäll and Connelly, 2008; Brewer et al., 1998): (i) the 1660–1640 Ma metavolcanic Horred Complex, (ii) the 1630–1590 Ma metavolcanic and metasedimentary Åmål Complex associated with the Göteborg granite suite, and (iii) the 1590–1520 Ma metasedimentary and metavolcanic Stora Le-Marstrand Complex, associated with the 1580–1520 Ma plutonic Hisingen Suite. The Stora Le-Marstrand Complex, exposed east of the Oslo Rift, correlates with the Veme Complex west of the Oslo Rift (Fig. 6) (Bingen et al., 2001). The Stora Le-Marstrand and Veme complexes comprise several metasedimentary successions (Åhäll and Connelly, 2008), consisting of thick packages of turbiditic psammite and greywacke metamorphosed under amphibolite-facies conditions (Bingen et al., 2001). Sedimentation started before c. 1585 Ma (metagreywacke xenoliths in a 1584 ± 7 Ma granite pluton) and continued to after c. 1500 Ma (detrital zircon geochronology in 12 samples) (Åhäll and Connelly, 2008; Åhäll et al., 1998; Andersen et al., 2004a; Bingen et al., 2001; Bingen and Viola, 2018). The paragneisses analysed in this study just east of the Oslo Rift (Eidsvoll and Auli; Fig. 5; Fig. 6; Fig. 10) are attributed to the Stora Le-Marstrand Complex.

552 The c. 1660–1520 Ma (Gothian) magmatic suites (Fig. 7) are characterized by low- to
553 medium-K calc-alkaline geochemical compositions, with supra-chondritic Hf and Nd isotopic
554 signature (average ε_{Hf} = + 4.8 in the Idefjorden lithotectonic unit at 1570 Ma; Fig. 8),
555 reflecting continental and oceanic volcanic arc magmatism (Andersen et al., 2004a; Andersen
556 et al., 2002b; Bergström et al., 2020; Brewer et al., 1998; Petersson et al., 2015b). Metabasalts
557 interlayered in the Stora Le-Marstrand rocks are tholeiitic and interpreted as oceanic back-arc
558 magmatism (Brewer et al., 1998).
559 The c. 1660–1520 Ma rocks were assembled during the Gothian accretionary orogenic
560 event (Åhäll and Connelly, 2008; Andersen et al., 2004a; Petersson et al., 2015b; Roberts and
561 Slagstad, 2015). Convincing evidence for Gothian regional deformation and metamorphism
562 includes crosscutting relationships (folded xenoliths in a 1584 ± 7 Ma pluton) and U–Pb
563 geochronological data in zircon and monazite ranging from 1546 ± 5 to 1539 ± 8 Ma from a
564 few localities in the Veme and Stora Le-Marstrand complexes (Åhäll and Connelly, 1998,
565 2008; Bingen et al., 2008b; Bingen and Viola, 2018; Connelly and Åhäll, 1996).
566 The 1660–1520 Ma rocks are intruded by the 1457 ± 6 Ma, N–S trending Orust tholeiitic
567 dolerite dykes (Åhäll and Connelly, 1998), and the 1340–1305 Ma bimodal Kungsbacka suite
568 (Fig. 6) (Austin Hegardt et al., 2007). The Dal Group (or Dalsland Group) is a c. 2 km thick
569 succession of low-grade clastic sedimentary rocks and tholeiitic basalt, exposed in a syncline
570 structure, overlying (and therefore younger than) the Kungsbacka suite (Fig. 6) (Brewer et al.,
571 2002). The Dal Group is poorly characterized. However, it may provide critical evidence for
572 the tectonic evolution of the Idefjorden lithotectonic unit before the Sveconorwegian orogeny
573 (Brewer et al., 2002) and therefore would warrant new investigations.
574 *3.3.2 Sveconorwegian orogeny*
575 In the Idefjorden lithotectonic unit, the Sveconorwegian deformation is associated with a N–S
576 to NW–SE structural grain and has variable strain intensity. Several shear zones, including the

prominent Ørje and Göta Älv shear zones (Fig. 2), are parallel to this structural grain (Bergström et al., 2020; Park et al., 1991; Viola et al., 2011; Wahlgren et al., 2015). Metamorphism ranges from greenschist- to granulite-facies. The low-grade rocks are exposed in syncline structures (Fig. 4). For example, between the Göta Älv shear zone and the Mylonite Zone, the Gillberga syncline hosts the Glaskogen low-grade complex, bounded by low-angle shear zones (Lindh et al., 1998), and the Åmal volcanic rocks (1614 ± 7 Ma), known for good preservation of primary volcanic structures (Lundqvist and Skiöld, 1993). In the amphibolite-facies gneiss complexes east and west of the Göta-Älv shear zone, garnet amphibolites provide pressure-temperatures estimates of 0.9 to 1.2 GPa – 730 to 790 °C (3 samples; Austin Hegardt, 2010). High-pressure garnet–clinopyroxene-bearing granulite-facies assemblages are reported from metadolerite dykes hosted in amphibolite-facies gneisses from several localities east of the Göta-Älv shear zone (Trollhättan, Fig. 5) (Söderlund et al., 2008a). Geothermobarometry coupled with zircon U–Pb data and mineral isochron data from two dykes indicate conditions of c. 1.5 GPa – 740 °C at 1046 ± 6 Ma and c. 1.0 GPa – 700 °C at 1026 ± 5 Ma (Söderlund et al., 2008a). In the Veme Complex, west of the Oslo rift in Norway, a kyanite-garnet-rutile paragneiss hosting clinopyroxene-garnet-plagioclase-rutile mafic boudins also records high-pressure granulite-facies conditions, with pressure-temperature estimates of 1.2 GPa – 780 °C (Hensmoen, Fig. 5) (Bingen et al., 2008b). Monazite in the kyanite-rutile-gneiss records peak metamorphism at 1052 ± 4 Ma (Bingen et al., 2008b).

East of the Oslo rift in Norway, amphibolite-facies metamorphism is associated with a foliation dipping unimodally to the NE and with folds verging to the W to SW (Viola et al., 2011). The timing of this metamorphism is provided by the new U–Pb data from zircon rims in migmatitic samples (Eidsvoll–Auli area, Fig. 5, Fig. 10, Table 2). The dates range from 1039 ± 17 to 997 ± 16 Ma, in seven samples affected by both muscovite- biotite- and

amphibole-dehydration melting. The dates are interpreted to record crystallization of the leucosomes. This interval overlaps with published zircon and titanite U–Pb data and a Sm-Nd mineral isochron interpreted to record high-grade metamorphism between 1043 ± 11 Ma and 1024 ± 9 (7 samples ; Åhäll et al., 1998; Austin Hegardt, 2010; Austin Hegardt et al., 2007; Bingen et al., 2008b), and also with intrusion of rare-mineral pegmatites between 1041 ± 2 and 984 ± 6 Ma (Romer and Smeds, 1996).

Several mafic to felsic magmatic intrusions, with a consistent WNW–ESE trend and dated between 951 ± 7 and 915 ± 1 Ma, crosscut the regional amphibolite-facies ductile fabric in the coastal area of Sweden (Årebäck et al., 2008; Hellström et al., 2004; Scherstén et al., 2000; Wahlgren et al., 2015). These include a lamprophyre dyke (915 ± 1 Ma) (Wahlgren et al., 2015) and the small Hakefjorden norite-anorthosite complex (916 ± 11 Ma), carrying evidence for extensive fractional crystallization (Årebäck and Stigh, 2000). The Flå and Bohus biotite-muscovite granite plutons intruded between 932 ± 8 and 922 ± 3 Ma, as large tabular bodies, in pressure conditions of c. 0.4 GPa (Fig. 5) (Eliasson et al., 2003; Eliasson and Schöberg, 1991; Lamminen et al., 2011). A final batch of rare-mineral pegmatite formed between 909 ± 1 and 906 ± 6 Ma (Müller et al., 2017).

3.3.3 The Mylonite Zone

The Mylonite Zone is a generally west dipping shear zone juxtaposing the Eastern Segment and Idefjorden lithotectonic unit. It is several km thick, continuous for some 450 km and characterized by a widespread greenschist- to upper amphibolite-facies mylonitic fabric (Fig. 2, Fig. 5) (Andersson et al., 2002a; Bergström et al., 2020; Möller et al., 2015; Park et al., 1991; Stephens et al., 1996; Viola and Henderson, 2010; Viola et al., 2011). It possibly roots in the mantle (EUGENO-S-working-group, 1988).

The Mylonite Zone is interpreted as a Sveconorwegian mid-crustal thrust zone placing the Idefjorden lithotectonic unit on top of the Eastern Segment, with an overall southeastward

transport direction oblique to the orogen (Stephens et al., 1996; Viola and Henderson, 2010; Viola et al., 2011). Shear zones inside the Idefjorden lithotectonic unit, including the Ørje and Göta Älv shear zones (Fig. 2) are similarly interpreted as transpressional thrust zones (Park et al., 1991; Viola et al., 2011; Wahlgren et al., 2015).

In the north (in Norway), the Mylonite Zone trends NW–SE and has a steep attitude with sinistral strike-slip kinematics. This segment has been interpreted as the sinistral lateral ramp to the thrust frontal ramp farther to the southeast. The frontal ramp dips gently to moderately to the west and bears a NW plunging stretching lineation associated with dominant top-to-southeast reverse displacement. In the southernmost part, the shear zone turns quite abruptly E–W, dipping gently to the north, and accommodating a dominant component of dextral strike-slip shearing. This part is interpreted as a dextral lateral ramp of the thrust zone (Viola and Henderson, 2010; Viola et al., 2011). The importance of the southernmost dextral lateral ramp is downplayed by Bergström et al. (2020), who interpret the Mylonite Zone, as a whole, as a sinistral transpressional thrust zone. Zircon U–Pb data in the Mylonite Zone and close hanging wall and footwall record amphibolite-facies migmatitization and associated ductile deformation between 980 ± 13 and 969 ± 13 Ma (Andersson et al., 2002a).

The Mylonite Zone was reactivated in extension with top-to-the-west kinematics along a network of localized shear zones, contributing to exhumation of the Eastern Segment in the footwall (Viola and Henderson, 2010; Viola et al., 2011). Muscovite and biotite $^{40}Ar/^{39}Ar$ data suggest that this deformation took place between 923 ± 4 and 861 ± 5 Ma (Viola et al., 2011).

3.4 Kongsberg and Bamble lithotectonic units

The Bamble and Kongsberg lithotectonic units are two narrow c. 25 km wide units situated in the center of the exposed Sveconorwegian orogen (Fig. 2). Kongsberg trends N–S while Bamble trends NE–SW. These two lithotectonic units share a number of features, including

652 evidence for early-Sveconorwegian metamorphism (1150-1120 Ma) (Bingen et al., 2008b;
653 Bingen and Viola, 2018; Engvik et al., 2016; Knudsen et al., 1997; Nijland et al., 2014;
654 Starmer, 1985; Viola et al., 2016).

655 *3.4.1 Gothian–Telemarkian evolution*

656 Two main lithological complexes are present in the Bamble and Kongsberg lithotectonic
657 units, (i) an orthogneiss complex, referred to as Kongsberg Complex in Kongsberg and
658 Bamble Complex in Bamble, and (ii) a quartzite-dominated metasedimentary complex, called
659 Modum Complex in Kongsberg and Nidelva and Kragerø Complexes in Bamble (Fig. 6). (i)
660 The orthogneiss complex consists of penetratively deformed orthogneisses with composition
661 ranging from dioritic to tonalitic, to granitic, and more competent gabbro plutons (Holleia and
662 Blengsvatn ; Bingen and Viola, 2018; Nijland et al., 2000). The orthogneisses are interlayered
663 with comparatively heterogeneous layered gneisses (referred to as banded gneiss in the field),
664 commonly migmatitic, and generally fine-grained. The layered gneisses derive probably from
665 both volcanic and sedimentary protoliths. Thin sulfide-rich or graphite-rich schistose layers
666 are common (falhbands) (Broekmans et al., 1994; Gammon, 1966). The protoliths of the
667 orthogneisses range in age from 1575 ± 44 to 1460 ± 21 Ma, with two frequency maxima
668 around 1545 and 1505 Ma (Fig. 7) (Andersen et al., 2004a; Bingen and Viola, 2018; Engvik
669 et al., 2016). The orthogneisses have tholeiitic to low-K calc-alkaline geochemical signature,
670 typical of volcanic arc magmatism (Andersen et al., 2004a). Their Hf isotopic signature is
671 very radiogenic, with an average ε_{Hf} = + 8.8 (+7 < ε_{Hf} < +11), approaching the depleted
672 mantle reservoir at 1550 Ma (Fig. 8) (Andersen et al., 2002b). (ii) The metasedimentary
673 complexes (Fig. 6) consist of coarse quartzite, interlayered with mica schist, sillimanite gneiss
674 and sulfide-rich schist (Morton, 1971; Nijland et al., 2014; Nijland et al., 1993). They host
675 metasomatic rocks such as orthoamphibole-cordierite gneiss, talc schist, albitite, scapolitite
676 and dolomite, generally located at the interface with gabbro bodies (Dahlgren et al., 1993;

Engvik et al., 2014; Munz, 1990; Munz et al., 1994). Deposition of the sedimentary protoliths took place after 1467 ± 33 Ma (detrital zircon U–Pb data in quartzite samples), implying that they represent part of a cover to the orthogneiss basement (Åhäll et al., 1998; Bingen et al., 2001).

3.4.2 Pre- to early-Sveconorwegian plutonism

The orthogneiss and quartzite-rich metasedimentary complexes are intruded by variably sized, gabbroic plutons. These plutons are commonly zoned, with (sub)ophitic picritic gabbro in the core and garnet amphibolite along the margin (Munz and Morvik, 1991). Two such gabbro plutons have been dated by the Sm-Nd method at 1224 ± 15 and 1207 ± 14 Ma (Morud and Vestre Dale gabbro, not represented in Fig. 7 ; deHaas et al., 2002b; Munz and Morvik, 1991), and two have been dated with the U–Pb method at 1164 ± 12 and 1149 ± 7 Ma (Vinoren and Ringsjø; Bingen and Viola, 2018; Engvik et al., 2011). Felsic intrusive rocks are quite common. They include thin gneissic units ranging in age from 1178 ± 9 to 1149 ± 8 Ma (Andersen et al., 2004b; Bingen and Viola, 2018; Engvik et al., 2016), and also, in Bamble, larger plutons ranging in age from 1152 ± 11 to 1140 ± 13 Ma (Gjeving, Ubergsmoen, Hovdefjell-Vegårshei plutons, Fig. 6) (Bingen and Viola, 2018). These metaplutons are characterized by a weakly foliated magmatic charnockite facies in the centre and a garnet-bearing augen gneiss facies at the margin (Touret, 1971a, b), and therefore place a maximum age bracket for the high-grade deformation and metamorphism in Bamble.

3.4.3 Sveconorwegian orogeny

The Sveconorwegian overprint in the Bamble and Kongsberg lithotectonic units is typified by a steep to subvertical foliation, isoclinal and highly transposed folds and a penetrative tectonic layering (Bingen and Viola, 2018; Slagstad et al., 2020; Starmer, 1985, 1991). These features are interpreted as evidence for roughly orthogonal, syn-metamorphic shortening, oriented E–W for Kongsberg and NW–SE for Bamble (Bingen and Viola, 2018). A steep stretching

lineation on the steep foliation planes suggests a component of near-vertical stretching. Inside the Kongsberg lithotectonic unit, the N–S trending Hokksund-Solumsmo shear zone (Starmer, 1985) is characterized by a component of sinistral strike-slip shearing that overprinted and thus postdates the orthogonal shortening (Scheiber et al., 2015).

Metamorphic grade increases across strike, northeastwards in Kongsberg and southeastwards in Bamble. In Kongsberg, it increases from epidote-amphibolite facies to upper amphibolite-facies conditions, with local occurrences of granulite-facies rocks towards the northeast (Fig. 6). In Bamble, the grade increases from amphibolite-facies to granulite-facies conditions towards the southeast, i.e. towards the coast (Tromøy and Hisøy islands; Fig. 6) (Clough and Field, 1980; Harlov, 2000; Knudsen, 1996; Nijland et al., 2014; Nijland and Maijer, 1993; Touret, 1971a). However, patches of granulite facies rocks are scattered throughout the amphibolite-facies domain of Bamble (Mosleiken granulite; Fig. 6), underscoring the importance of fluid activity on mineral parageneses (Engvik et al., 2016; Nijland et al., 1998). The granulite-facies rocks record peak pressure-temperature values of 1.15 GPa and 850 °C, followed by hydration and decompression to 0.8 GPa – 740 °C (Engvik et al., 2016).

Zircon and monazite U–Pb data constrain the peak of amphibolite- and granulite-facies metamorphism between 1147 ±12 and 1122 ± 8 Ma in both the Bamble and Kongsberg lithotectonic units (Bingen et al., 2008b; Bingen and Viola, 2018; Cosca et al., 1998; Engvik et al., 2016; Knudsen et al., 1997). In coastal Bamble, the granulite-facies Tromøy complex (Fig. 6) consists of low-K calc-alkaline enderbitic gneisses depleted in large ion-lithophile elements (LILE) (Cooper and Field, 1977; Field et al., 1980; Knudsen and Andersen, 1999). Zircon U–Pb data demonstrate that the protoliths formed between 1575 ± 44 and 1544 ± 14 Ma while the granulite facies overprint took place between 1147 ± 12 and 1132 ± 6 Ma (Bingen and Viola, 2018). These data show that the volcanic arc magmatism belongs to the

727 Gothian orogenic cycle, while the granulite-facies metamorphism is early-Sveconorwegian in
728 age (Andersen et al., 2004a; Bingen et al., 2008c; Field et al., 1985).
729 Titanite U–Pb dates and a trail of monazite dates in gneisses range from 1107 ± 9 to 1091
730 ± 2 Ma (Bingen et al., 2008b; Cosca et al., 1998; deHaas et al., 2002a) while hornblende
731 $^{40}Ar/^{39}Ar$ plateau ages range from 1099 ± 3 to 1079 ± 5 Ma (Cosca et al., 1998; Cosca and
732 O'Nions, 1994). These dates are related to regional cooling and exhumation. Monazite, titanite
733 and rutile in albitite record at least two phases of fluid-rock interaction below 550 °C
734 (metasomatism), between 1104 ± 5 and 1078 ± 3 Ma (Engvik et al., 2017; Engvik et al., 2011;
735 Munz et al., 1994), while gadolinite-columbite data in pegmatite record intrusion of a small
736 batches of fluid-rich melt between 1094 ± 11 and 1082 ± 5 Ma (Müller et al., 2017; Scherer et
737 al., 2001). These data imply regional scale fluid mobility after the peak of metamorphism and
738 deformation.
739 Rare lamprophyre dykes with near vertical attitude and non-foliated chilled margins
740 crosscut at high angle the regional foliation of the host gneiss. One such dyke yields an
741 intrusion age of 1033 ± 12 Ma and thus provides both a minimum bracket for the steep, high-
742 grade fabric of the host gneiss and the age of a batch of ultrapotassic mafic magmatism
743 (Bingen and Viola, 2018). The large non-foliated Herefoss granite pluton formed at 920 +16/-
744 27 Ma (Fig. 5) (Andersen et al., 2002a).
745 *3.4.4 Kongsberg–Idefjorden boundary zone*
746 The Kongsberg–Idefjorden boundary zone is marked by a c. 500 m thick amphibolite-facies
747 shear zone made of banded gneiss of mafic composition, characterized by steeply dipping
748 foliation bearing a moderately to steeply plunging lineation (Bingen and Viola, 2018). It
749 follows the lithological contact between metagreywackes of the Veme Complex and
750 orthogneisses of the Kongsberg Complex (Viola et al., 2016).

3.4.5 Kongsberg–Telemarkia boundary zone

The Sokna-Saggrenda Shear Zone (Fig. 2) (Starmer, 1985) is a N–S trending, east-dipping, up to 2 km thick multiphase shear zone. It is largely hosted within and along the eastern margin of a > 100 km long belt of foliated granite, dated between 1170 ± 11 and 1146 ± 5 Ma (Fig. 6) (Scheiber et al., 2015). This granite constitutes the footwall of the shear zone and is part the Telemarkia lithotectonic unit. Three post-1170 Ma ductile deformation phases have been identified in the shear zone (Scheiber et al., 2015). (i) The earliest structures accommodate top-to-the-west kinematics and relate to thrusting of Kongsberg over Telemarkia. (ii) These are selectively reactivated in a sinistral fashion along mylonitic to ultramylonitic shear zones. The sinistral shear zones possibly record the same deformation as the N–S trending, steeply dipping Hokksund-Solumsmo mylonite zones inside the Kongsberg lithotectonic unit, showing evidence for sinistral transpressive shearing. (iii) Extensional top-to-the-east sense of shear. A brittle zone overprinting this long-lived ductile deformation zone and traditionally referred to as the "Great Friction Breccia" (Starmer, 1985) probably represents a normal fault of Permian age (Larsen et al., 2008; Scheiber et al., 2015).

3.4.6 Bamble–Telemarkia boundary zone

The Kristiansand–Porsgrunn Shear Zone (Fig. 2) is a c. 1–2 km thick ductile to brittle shear zone juxtaposing the Bamble and Telemarkia lithotectonic units. It dips moderately to the southeast and is possibly connected with an offset of the Moho under the Skagerrak sea (Andersson et al., 1996). The shear zone is interpreted as a top-to-the-northwest thrust, later reactivated coaxially as an extensional shear zone (Henderson and Ihlen, 2004; Mulch et al., 2005; Starmer, 1991). Upper greenschist- to amphibolite-facies thrust-related structures are invariably northwest vergent. These structures are associated with tabular pegmatite bodies (Henderson and Ihlen, 2004). The shear zone overprints the 1132 ± 3 Ma Morkheia monzonite suite exposed in the Telemarkia footwall (Heaman and Smalley, 1994; Milne and

Starmer, 1982), and the 1140 ± 13 Ma Hovdefjell-Vegårshei metapluton exposed on the Bamble hangingwall (Bingen and Viola, 2018; Touret, 1987), implying that thrusting is younger than 1132 ± 3 Ma. Extension was accommodated by thin greenschist-facies shear zones with syn-kinematic muscovite porphyroblasts constraining the top-to-the-southeast deformation between 891 ± 3 and 880 ± 3 Ma ($^{40}Ar/^{39}Ar$ data) (Mulch et al., 2005). The contrast in titanite U–Pb ages between the Telemarkia footwall (c. 913 to 901 Ma) and Bamble hanging wall (c. 1107 to 1091 Ma) (Bingen et al., 1998; Cosca et al., 1998; deHaas et al., 2002a; Heaman and Smalley, 1994) underscores the importance of normal movement along the shear zone. A narrow, fully brittle, Permian, normal fault zone locally reactivates the Sveconorwegian ductile precursors.

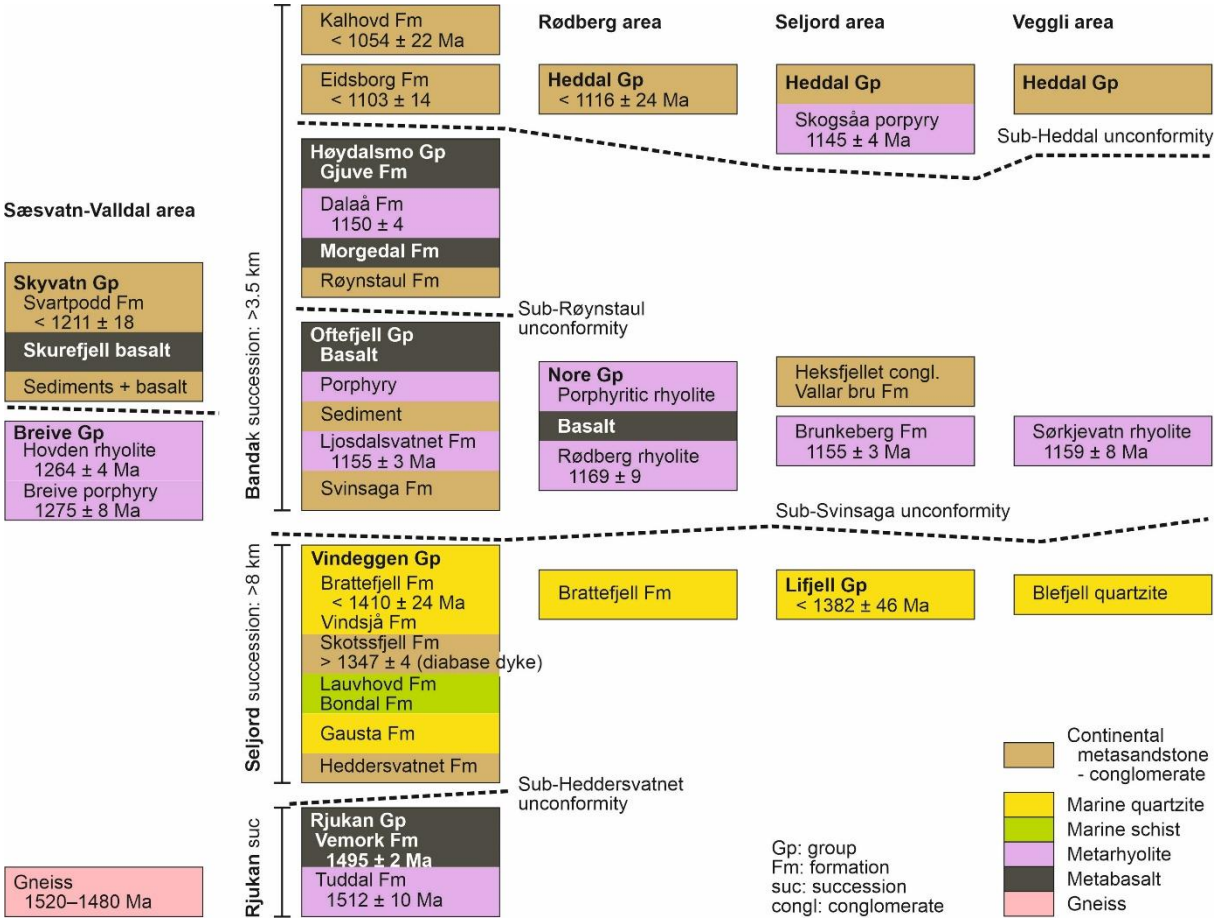

Figure 11. Generalized stratigraphic columns for the Telemark supracrustal rocks in central Telemark and supracrustal rocks in the Sæsvatn-Valldal area. These columns follow the archetypal subdivision into the Rjukan, Seljord and Bandak successions (Dons, 1960; Dons and Jorde, 1978; Sigmond, 1978), and integrate results of later mapping. Main sources of stratigraphic and geochronological data: Bingen et al. (2002), Bingen et al. (2003), Corfu and Laajoki (2008), Dons (1960; 1978), Laajoki et al. (2002), Laajoki and Corfu (2007), Köykkä and Lammingen (2011), Lamminen and Köykkä (2010), Lamminen (2011), Nordgulen (1999), Sigmond (1975, 1978, 1998), and Spencer et al. (2014).

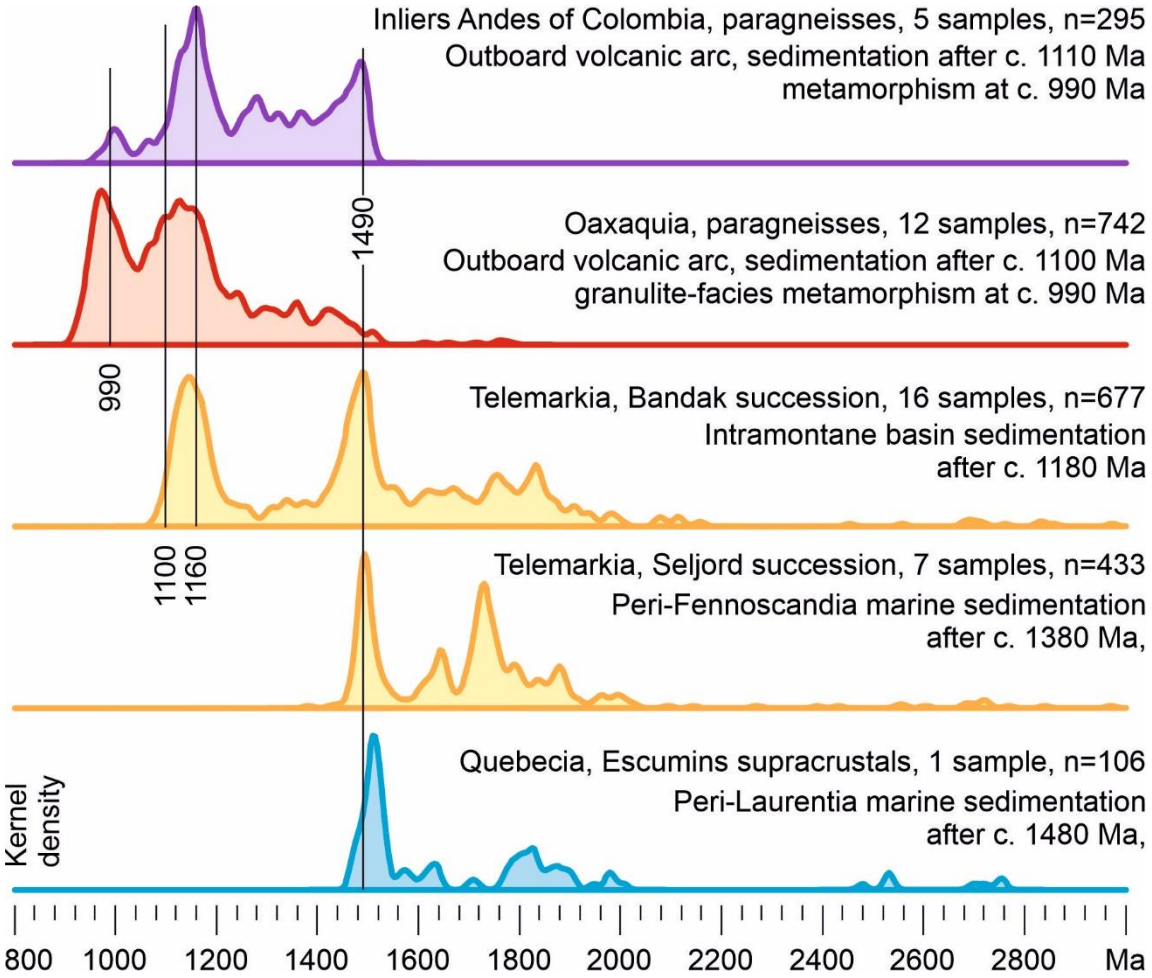

Figure 12. Kernel density estimators of detrital zircon ages in metasediments of the Telemarkia lithotectonic unit compared with paragneisses and metasediments in Quebecia, Oaxaquia, and inliers in the Andes of Colombia. The Seljord succession in Telemarkia and

the Port au Quilles formation in the Escumins supracrustals record marine peri-Baltica and peri-Laurentia sedimentation, respectively, after the 1520–1480 Ma continental generation. The main peak reflects sourcing in the juvenile c. 1520-1480 Ma volcanic arcs, while the diversity of older detrital zircons reflects sourcing from continental sources. The Bandak succession in Telemarkia deposited after c. 1180 Ma (Eidsborg Formation after c. 1100 Ma) and involved important recycling of the Seljord succession and younger magmatic rocks in continental intramontane environment. Contrasting with this situation, the Oaxaquia lithotectonic unit and the Inliers in the Andes of Colombia are interpreted as outboard volcanic arcs formed in the ocean between Laurentia, Amazonia and Baltica after c. 1460 Ma, and isolated almost entirely from continental sediment sources older than c. 1500 Ma. The plots are generated with "DensityPlotter" by (Vermeesch, 2012) with a bandwidth of 10 Ma. Data sources : Telemarkia, Bandak and Seljord successions: Bingen et al. (2001), de Haas et al. (1999), Lamminen (2011) and Spencer et al. (2014); Quebecia: Escumins supracrustal rocks, Port aux Quilles formation, Groulier et al. (2018b); Oaxaquia: granulite-facies paragneisses, Solari et al. (2014); inliers in the Andes of Colombia: parageneisses, Cardona et al. (2010) and Ibanez-Mejia et al. (2011).

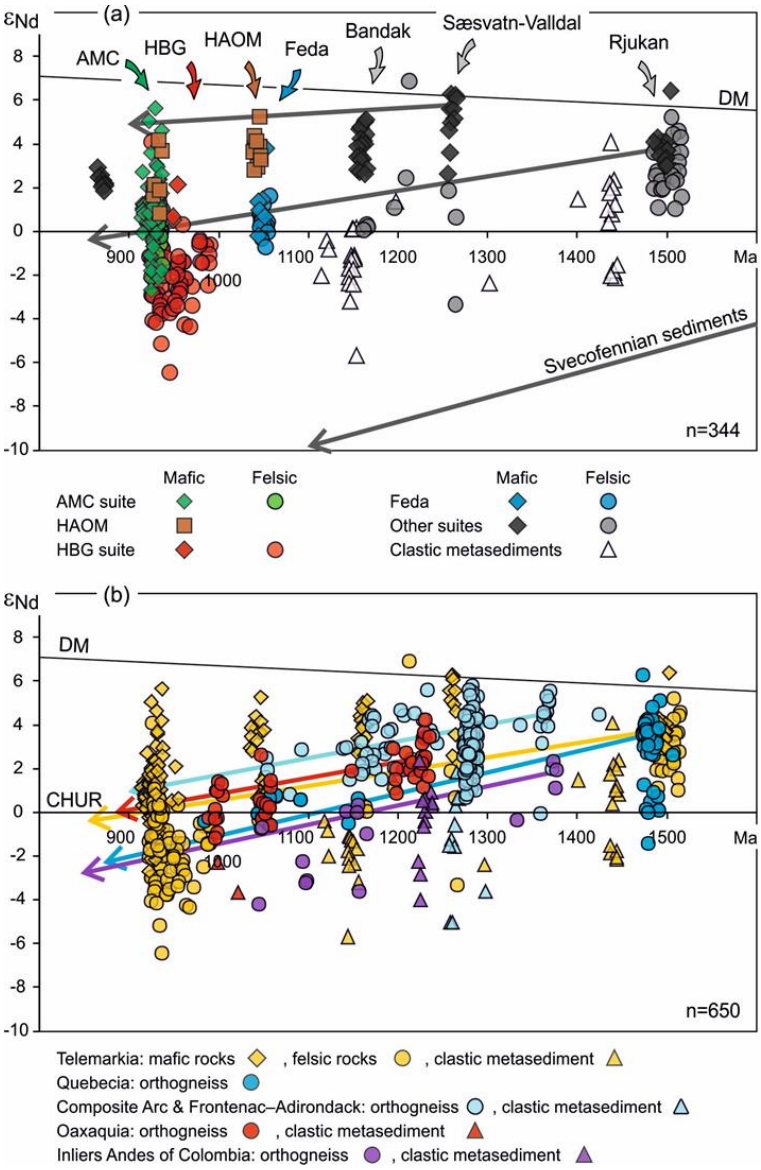

Figure 13. Neodymium isotopic composition of rock suites in the Telemarkia lithotectonic unit, expressed as ε_{Nd} (initial value) as a function of time. Each symbol represents one sample. Magmatic rocks are represented at their probable time of crystallization and metasedimentary rocks at their probable time of deposition (to improve legibility, each symbol is assigned a random scatter lower than ± 8 Ma along the time axis). Interpretations of the distribution of data are discussed in the text. (a) Rock suites in the Telemarkia lithotectonic unit. (b) Comparison between Telemarkia, Quebecia (Grenville orogen, Canada), the Composite Arc and Frontenac–Adirondack belt (Grenville orogen, Canada, USA), the Oaxaquia lithotectonic units (Mexico), and the inliers in the Andes of Colombia. These five lithotectonic units have

similar crustal evolution vectors. Sources of data: Hunnedalen dolerites at c. 870 Ma: (Maijer and Verschure, 1998); Rogaland AMC suite at 930 Ma: (Barling et al., 2000; Bolle et al., 2003a; Demaiffe et al., 1986; Menuge, 1988; Nielsen et al., 1996; Robins et al., 1997; Schiellerup et al., 2000); high-alumina orthopyroxene megacrysts (HAOM) in anorthosite plutons, 1040–930 Ma: (Bybee et al., 2014; Demaiffe et al., 1986); HBG granitoids, 985–925 Ma: (Andersen et al., 2001; Bogaerts et al., 2003; Demaiffe et al., 1990; Menuge, 1985, 1988; Vander Auwera et al., 2003; Vander Auwera et al., 2014a); Feda suite at 1050 Ma: (Bingen et al., 1993; Menuge, 1988; Vander Auwera et al., 2011); other magmatic rocks in Telemarkia: (Andersen et al., 2001; Brewer et al., 2002; Brewer et al., 2004; Brewer and Menuge, 1998; Menuge, 1985, 1988; Vander Auwera et al., 2003); metasedimentary rocks: (Andersen and Laajoki, 2003; deHaas et al., 1999); Oaxaquia: (Lawlor et al., 1999; Ruiz et al., 1988; Weber and Köhler, 1999) ; Inliers in the Andes of Colombia: (Cordani et al., 2005; Ibanez-Mejia et al., 2015); Quebecia: (Dickin, 2000; Dickin and Higgins, 1992; Groulier et al., 2018a; Groulier et al., 2018b); Composite Arc and Frontenac–Adirondack belt: (Chiarenzelli et al., 2010; Daly and McLelland, 1991; Dickin et al., 2010; Marcantonio et al., 1990; McLelland et al., 1993; Valentino et al., 2019).

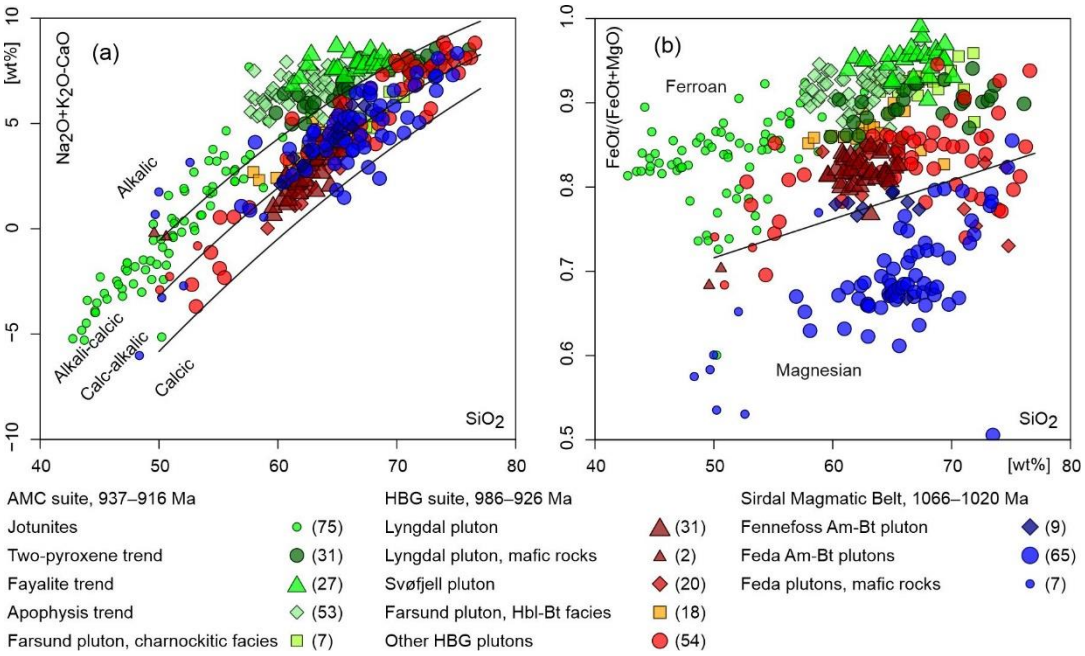

Figure 14. Comparison of the geochemical signature between three diagnostic magmatic suites intruded between 1066 and 916 Ma in the Telemarkia lithotectonic unit: c. 1050 Ma high-K calc-alkalic Feda plutonic suite of the Sirdal magmatic belt and 1030 Ma Fennefoss pluton (Bingen, 1989; Pedersen, 1981; Vander Auwera et al., 2011), 986–926 Ma hornblende-biotite granite (HBG) suite with ferro-potassic calc-alkalic to alkali-calcic signature (Bogaerts et al., 2003; Vander Auwera et al., 2003; Vander Auwera et al., 2014a) and the 937–916 Ma anorthosite-mangerite-charnockite (AMC) suite with ferro-potassic alkalic signature (Bolle and Duchesne, 2007; Charlier et al., 2010; Duchesne and Wilmart, 1997; Vander Auwera et al., 2014a; Vander Auwera et al., 1998; Wilmart et al., 1989). For the AMC suite, 3 different trends are recognized based on the mineralogy (two-pyroxene and fayalite trends) or their belonging to a specific intrusion (apophysis of the Bjerkreim-Sokndal intrusion).

3.5 Telemarkia lithotectonic unit

The western part of the Sveconorwegian orogen can be considered as one single lithotectonic unit, c. 230 x 300 km long, named Telemarkia (Fig. 2) (Bingen et al., 2005). The Telemarkia lithotectonic unit comprises low-grade supracrustal rocks preserved in several syncline structures, structurally overlying amphibolite- to granulite-facies gneiss complexes, and hosts

862 voluminous plutons (Fig. 4; Fig. 5.; Fig. 6). The gneiss complexes comprise orthogneisses
863 with subordinate paragneisses. The largest and most complete tract of supracrustal rocks,
864 called the Telemark supracrustal rocks, is exposed in a 60 km wide area in central Telemark
865 (Fig. 4; Fig. 6). Original mapping showed that stratigraphic relationships and deposition
866 structures are well preserved in the Telemark supracrustal rocks, and defined three groups or
867 successions separated by unconformities, which are, from bottom to top, the Rjukan, Seljord
868 and Bandak successions (Fig. 11, Fig. 12) (Dons, 1960; Dons and Jorde, 1978; Sigmond,
869 1978). Other supracrustal sequences are described in several other syncline structures, less
870 than 25 km wide, in the Ullensvang, Sauda, Grjotdokki-Nesflaten, Sæsvatn-Valldal and
871 Nissedal areas (Fig. 4).

872 *3.5.1 Telemarkian evolution*

873 Rapid generation of juvenile continental crust is recorded by voluminous magmatism between
874 1521 ± 6 and 1476 ± 13 Ma, hosted in both the low-grade successions and in the gneiss
875 complexes (Fig. 7) (Bingen et al., 2008a; Bingen et al., 2005; Laajoki and Corfu, 2007;
876 Pedersen et al., 2009; Roberts et al., 2013). This event is called the Telemarkian accretionary
877 orogeny and it is geographically zoned.

878 In the west, in the Suldal area, gneisses and granitoids are characterized by a calc-alkaline
879 geochemical signature, with s supra-chondritic Hf isotopic signature at 1500 Ma (average ε_{Hf}
880 = + 5.7; Fig. 8) (Pedersen et al., 2009; Roberts et al., 2013). These are interpreted to reflect
881 volcanic arc magmatism (the Suldal arc; Roberts et al., 2013).

882 In the east, in the Telemark area, magmatism is bimodal and typified by the Rjukan
883 bimodal metavolcanic rocks at the base of the Telemark supracrustal rocks (Vemork basalt vs.
884 Tuddal rhyolite dated between 1512 ± 10 and 1495 ± 2 Ma, Fig. 11) and coeval plutonism
885 (Bingen et al., 2005; Laajoki and Corfu, 2007). This magmatism is characterized by a within-
886 plate geochemical signature and moderately supra-chondritic Nd isotopic signatures (+1.1 <

887 $\varepsilon_{Nd(1500\ Ma)}$ < +4.3) (Fig. 13). It is interpreted to reflect back-arc rifting (the Rjukan rift basin),
888 continentwards of the active arc (Brewer and Menuge, 1998; Köykkä and Lamminen, 2011;
889 Lamminen and Köykkä, 2010; Roberts et al., 2013).

890 The Telemarkian orogenic event cannot be demonstrated to be associated with high-grade
891 metamorphism. The Seljord succession overlying the Rjukan succession is a c. 8 km thick,
892 shallow marine sedimentary succession, dominated by quartzite (Fig. 11, Fig. 12) (Köykkä
893 and Lamminen, 2011). The Seljord succession was deposited during a transgressive cycle,
894 interpreted as reflecting thermal subsidence after magmatism, between 1410 ± 24 Ma (detrital
895 zircon U–Pb data) and 1347 ± 4 Ma (U–Pb age of intrusive dolerite dyke ; Corfu and Laajoki,
896 2008; Köykkä and Lamminen, 2011; Lamminen and Köykkä, 2010).

897 *3.5.2 Pre- to early-Sveconorwegian evolution*

898 The Telemarkia lithotectonic unit hosts several generations of gneissic plutonic rocks in the
899 1280–1240, 1220–1180 and 1180–1145 Ma time intervals, with frequency maxima at c. 1280,
900 1260, 1210, 1170 and 1150 Ma (Fig. 6, Fig. 7) (Andersen et al., 2007; Bingen et al., 2003;
901 Corfu and Laajoki, 2008; Heaman and Smalley, 1994; Pedersen et al., 2009; Scheiber et al.,
902 2015).

903 In the southeast of the Telemarkia lithotectonic unit, a voluminous c. 60 x 120 km gneiss
904 complex consists of amphibolite-facies, NE–SW trending, moderately to weakly foliated
905 granitic gneiss and granitoids, named in different areas Drivheia gneiss (Heaman and
906 Smalley, 1994) and Vråvatn complex (Fig. 6) (Andersen et al., 2007). This complex is
907 dominated by c. 1220–1190 Ma plutonic rocks with a within-plate geochemical signature
908 (Andersen et al., 2007; Bingen and Viola, 2018; Heaman and Smalley, 1994) and a supra-
909 chondritic (radiogenic) Hf isotopic signature (+9 < ε_{Hf} < +10, in zircon from 4 samples, Fig.
910 8) approaching the depleted mantle reservoir value at 1210 Ma (ε_{Hf} = + 12) (Andersen et al.,
911 2007).

912 The Sæsvatn–Valldal and Nissedal supracrustal rocks are two low-grade basalt-dominated
913 successions (Fig. 6, Fig. 11), exposed in two c. 15 km wide syncline. Basalt is interlayered
914 with felsic volcanic and clastic sedimentary rocks and intruded by fine-grained granite sills
915 and dykes (Dons and Jorde, 1978; Sigmond, 1975). In the Sæsvatn–Valldal succession, the
916 basalts are overlying rhyolites and porphyries dated to between 1275 ± 8 and 1259 ± 2 Ma,
917 themselves unconformably overlying the 1520–1480 Ma gneissic basement (Bingen et al.,
918 2002; Brewer et al., 2004). In the Nissedal succession, the basalts overly the 1219 ± 8 to 1202
919 ± 9 Ma Vråvatn complex and host fine-grained granite sheets, one of which yields an
920 intrusion age of 1196 ± 6 Ma (Bingen and Viola, 2018). The Nissedal and Sæsvatn-Valldal
921 successions are interpreted as near-coeval bimodal (mafic dominated) continental successions
922 with an age close to 1210 Ma, coeval with the Drivheia and Vråvatn gneisses in the
923 underlying gneiss complex (Andersen et al., 2007; Heaman and Smalley, 1994).
924 In the Telemark supracrustal rocks, the c. 3.5 km thick Bandak succession rests over both
925 the Rjukan and Seljord successions (Köykkä, 2011; Laajoki et al., 2002), above a first order
926 unconformity locally decorated by a regolith (Köykkä and Laajoki, 2009) (Fig. 6, Fig. 11, Fig.
927 12). The succession includes at least two internal unconformities, implying active tectonism
928 during sedimentation (Laajoki, 2002; Laajoki et al., 2002). The lower part of the Bandak
929 succession consists of bimodal volcanic rocks interlayered with sediments (Köykkä, 2011).
930 The mafic rocks (Morgedal and Gjuve metabasalts) have a within-plate geochemical signature
931 (Brewer et al., 2002; Spencer et al., 2014). The felsic volcanic rocks range in age from 1169 ±
932 9 to 1145 ± 4 Ma (Bingen et al., 2003; Laajoki et al., 2002). The upper part of the Bandak
933 succession consists of exclusively sedimentary rocks. These are the Heddal Group, Eidsborg
934 Formation and Kalhovd Formation, deposited after 1116 ± 24, 1103 ± 14 and 1054 ± 22 Ma
935 respectively (Fig. 5, Fig. 11) (detrital zircon U–Pb data ; Bingen et al., 2003; deHaas et al.,
936 1999; Lamminen, 2011; Spencer et al., 2014).

The sedimentary rocks of the entire Bandak succession are generally immature, coarse-grained to conglomeratic, and of limited lateral extent. They are interpreted as alluvial fan-, braided fluvial- and locally eolian deposits, accumulated in continental fault-bounded intermontane extensional basins (Bingen et al., 2003; Köykkä, 2011; Lamminen, 2011; Spencer et al., 2014). Syn-sedimentary normal faults are well documented (Lamminen, 2011).

3.5.3 Sveconorwegian magmatism

After 70 Myr of quiescence, magmatism resumed at c. 1065 Ma with formation of the c. 50 km wide – 170 km long, orogen-parallel, NNW-SSE trending, Sirdal magmatic belt in the Agder area (Fig. 5) (Bingen et al., 2015; Coint et al., 2015; Granseth et al., 2020; Slagstad et al., 2013). This belt is a composite granitoid batholith, comprising mainly elongate and variably foliated plutons of granodiorite, granite and leucogranite. Slivers of heterogeneous gneiss interleaved within granitoid plutons are interpreted as xenoliths or panels of wall-rocks (Coint et al., 2015). The granitoids intruded under pressure conditions of 0.38–0.48 GPa (Coint et al., 2015) between 1066 ± 10 and 1020 ± 15 Ma (Bingen et al., 2015; Bingen and van Breemen, 1998a; Coint et al., 2015; Möller et al., 2002; Slagstad et al., 2018; Slagstad et al., 2013). A large portion of the belt comprises silica-rich biotite granite and leucogranite. Foliated plutons of biotite + amphibole K-feldspar-phyric quartz-monzonite to granodiorite are specifically called the Feda suite (1050 ± 8 Ma) and Fennefoss augen gneiss (1031 ± 2 Ma) (Fig. 5) (Bingen and van Breemen, 1998a). These are characterized by a magnesian, high-K, high-Sr-Ba, calc-alkaline geochemical signature and locally host ultrapotassic (lamprophyre) mafic layers and enclaves (Fig. 14) (Bingen et al., 1993; Bingen and van Breemen, 1998a).

After 985 Ma, large plutons with a distinctly ferroan geochemical signature were emplaced (Fig. 5, Fig. 14) (Andersen et al., 2001; Granseth et al., 2020; Vander Auwera et al., 2011). These plutons are weakly- to non-foliated, have sharp contacts to their wall-rock and are well

962 defined on aeromagnetic maps by positive anomalies (Slagstad et al., 2018). Two main
963 ferroan suites are defined: a ferro-potassic hornblende–biotite–granitoid (HBG) suite and an
964 orthopyroxene-bearing anorthosite–mangerite–charnockite (AMC) suite (Fig. 5, Fig. 14)
965 (Bogaerts et al., 2003; Duchesne and Wilmart, 1997; Vander Auwera et al., 2003; Vander
966 Auwera et al., 2011; Vander Auwera et al., 2014a). The HBG suite formed between 986 ± 2
967 and 926 ± 4 Ma and is exposed in the area of the Sirdal magmatic belt and eastwards
968 (Andersen et al., 2001; Andersen et al., 2007; Granseth et al., 2020; Jensen and Corfu, 2016;
969 Sigmond, 1985; Slagstad et al., 2018; Vander Auwera et al., 2011; Vander Auwera et al.,
970 2014a). The AMC suite formed between 937 ± 1 and 916 ± 9 Ma and is restricted to the
971 southwestern end of the Telemarkia lithotectonic unit (Fig. 5) (Bolle et al., 2018; Schärer et
972 al., 1996; Vander Auwera et al., 2011; Vander Auwera et al., 2014a). A few plutons (Farsund
973 and Kleivan plutons, 931 ± 2 and 936 ± 1 Ma) are composite HBG–AMC plutons, with
974 charnockitic and non-charnockitic facies, reflecting tapping of distinct sources into one pluton
975 (Vander Auwera et al., 2014a).

976 The Rogaland AMC suite (Fig. 5) consists of three large anorthosite plutons (Egersund-
977 Ogna, Håland-Helleren, Åna-Sira anorthosites), two satellite leuconorite plutons (Hidra and
978 Garsaknatt leuconorites), a layered intrusion (Bjerkreim-Sokndal layered intrusion), and
979 volumetrically minor sills and dykes of jotunite and ilmenite-norite, all emplaced during a
980 short lived magmatic event between c. 932 and 916 Ma (Charlier et al., 2006; Duchesne et al.,
981 1985; Duchesne et al., 1989; Schärer et al., 1996; Vander Auwera et al., 2011).

982 The Egersund-Ogna anorthosite pluton exhibits an isotropic core and a foliated margin,
983 characterized by a syn-magmatic fabric parallel to the contact. The centre of the pluton is
984 made up of anorthosite and leuconorite with a granulated matrix of plagioclase (An_{40}–An_{50}),
985 hosting 1–3 m large aggregates of plagioclase (up to An_{55}) and high-alumina orthopyroxene
986 megacrysts (HAOM, En_{75}) (Charlier et al., 2010). The high aluminium and chromium

contents (up to 8.5 wt% Al_2O_3 and 1500 ppm Cr) of the orthopyroxene megacrysts indicate a pressure of crystallization of c. 1.1 GPa for the megacrysts, contrasting with the ambient pressure of 0.5 GPa for the matrix minerals (2-3 wt% Al_2O_3 in matrix orthopyroxene). The anorthosite plutons intruded as a plagioclase-dominated crystal mush lubricated by melt, from the base of the crust (1.1 GPa) to the middle of the crust (0.5 GPa) (Barnichon et al., 1999; Charlier et al., 2010; Duchesne et al., 1999). The orthopyroxene megacrysts with the highest aluminum content (> 8 wt% Al_2O_3) define a Sm–Nd isochron with an age of 1041 ± 17 Ma (Bybee et al., 2014), pointing either to inheritance (Vander Auwera et al., 2014b) or protracted ponding of mafic magma at the base of the crust (Bybee et al., 2014).

The Bjerkreim-Sokndal layered intrusion (931 ± 7 Ma) can be subdivided into a layered lower part and a non-layered upper part. The lower part comprises five macrocyclic units of cumulates (Barling et al., 2000; Duchesne, 1972; Nielsen et al., 1996; Robins et al., 1997). The upper part comprises, fractionated and wall-rock-contaminated, mangerite and charnockite (Duchesne and Wilmart, 1997; Nielsen et al., 1996). The Bjerkreim-Sokndal intrusion intruded at pressure conditions of ≤ 0.5 GPa (Vander Auwera and Longhi, 1994). It forms a syncline (lopolith), the formation of which is attributed to gravity-driven subsidence of the central part of the intrusion (Bolle et al., 2000; Bolle et al., 2002; Paludan et al., 1994).

Undeformed pegmatites intruded between c. 914 and 900 Ma. They include the Evje-Iveland rare-mineral pegmatite field (Müller et al., 2017; Pasteels et al., 1979; Scherer et al., 2001; Seydoux-Guillaume et al., 2012).

3.5.4 Sveconorwegian metamorphism

As outlined above, the supracrustal rocks in the centre of the Telemarkia lithotectonic unit were affected by greenschist to epidote-amphibolite facies metamorphism and deformed by open to tight folding. Basalt in the Sæsvatn-Valldal succession (Fig. 6) was deformed under

epidote-amphibolite facies conditions at c. 1032 ± 2 Ma and faulted at 1017 ± 2 Ma (molybdenite Re-Os data; Stein and Bingen, 2002).

In the gneiss complexes, the metamorphic grade typically reached upper amphibolite-facies conditions, with widespread migmatitization between 1026 ± 14 and 1005 ± 7 Ma (zircon and monazite U–Pb data; Bingen et al., 2008b; Coint et al., 2015). Granitoids of the Sirdal magmatic belt (c. 1065–1020 Ma) are commonly moderately deformed (Coint et al., 2015). Locally, they contain zircons with rims recording a hydrothermal to metamorphic overprint at c. 1016 Ma (Knaben Mo district ; Bingen et al., 2015).

The metamorphic grade increases southwestwards towards the Rogaland AMC complex, structurally downwards, across to the N–S trending and E-dipping regional fabric (Fig. 5) (Bingen and van Breemen, 1998b; Maijer, 1987; Slagstad et al., 2018; Tobi et al., 1985). Metamorphism was coeval with the formation of lithological banding, tight to isoclinal folding and migmatitization. Two concentric granulite facies zones are defined: the orthopyroxene zone and the osumilite zone close to the AMC complex (Fig. 5). Osumilite is diagnostic of water poor, low-pressure, ultrahigh temperature (UHT; T > 900 °C) granulite-facies conditions (Harley, 2008; Holland et al., 1996).

Zircon and monazite U–Pb geochronology from a diversity of granulite-facies samples gave apparent ages spreading between c. 1045 and 900 Ma (Bingen et al., 2008b; Bingen and van Breemen, 1998b; Laurent et al., 2018a; Möller et al., 2002, 2003; Slagstad et al., 2018; Tomkins et al., 2005). Insight into the pressure-temperature-time evolution of this protracted metamorphism requires careful linkage of petrography, phase equilibrium modelling, geochronology and trace-element characterization of zircon and monazite. Typical samples inside the orthopyroxene zone reached peak conditions of 0.5 GPa – 880 °C between c. 1040 and 1010 Ma (Laurent et al., 2018b). Rims of neocrystallized zircon in such samples spread from 1045 to 955 Ma, supporting 90 Myr of melt-present conditions (Laurent et al., 2018a).

In the osumilite zone, the onset of migmatitization, associated with biotite and sulfide mineral breakdown, is recorded by sulfate-rich monazite cores in an osumilite-bearing paragneiss at 1034 ± 6 Ma (Laurent et al., 2016). In a (quartz- and garnet-free) sapphirine + orthopyroxene sample (Fig. 9; Ivesdal locality), a Y-rich monazite (5–7 wt% Y_2O_3) further constrains temperature higher than 900°C between 1029 ± 9 and 1006 ± 8 Ma (Laurent et al., 2018b), in accordance with zircon data (1010 ± 7 to 1006 ± 4 Ma) (Drüppel et al., 2013). The breakdown of the peak sapphirine + orthopyroxene assemblage into a cordierite + hercynite assemblage implies a clockwise P-T path with a decompression between 0.6 GPa – 920 °C and 4.5 GPa – 900°C (Fig. 9) (Blereau et al., 2017; Laurent et al., 2018b). This decompression is best captured by a garnet-bearing sample from the osumilite zone that contains Y-rich monazite recording garnet breakdown into cordierite + hercynite + orthopyroxene, pinning a robust P-T-t point at 0.4 GPa – 910 °C – 930 ± 6 Ma (Laurent et al., 2018b). Together, the data give evidence for two events of low-pressure granulite-facies metamorphism peaking at UHT conditions, the first event (M1) between c. 1030 and 1005 Ma, and the second (M2) at c. 930 Ma, associated with formation of osumilite (Blereau et al., 2017; Drüppel et al., 2013; Laurent et al., 2018b; Laurent et al., 2016). Minor exhumation (c. 6 km) took place between the two.

These two events were penecontemporaneous with magmatic activity (Laurent et al., 2018b; Slagstad et al., 2018). The first M1 event started with dehydration melting (c. 1034 Ma) coeval with intrusion of the Sirdal magmatic belt (c. 1065-1020 Ma) and associated underplating (c. 1040 Ma), and peaked at the end and after this magmatic event (1030–1005 Ma). The second M2 event (c. 930 Ma) was coeval with intrusion of the AMC suite. This correlation strongly suggests that magmatism and metamorphism had a common heat source in the mantle. The lag between magmatism and peak metamorphism for M1 may reflect temperature buffering by melt until melt migration effectively took place.

The M2 metamorphic event was followed by regional scale cooling, dated by titanite U–Pb data at 918 ± 2 Ma (Bingen and van Breemen, 1998b). Amphibole $^{40}Ar/^{39}Ar$ apparent ages scatter between 1059 ± 8 and 853 ± 3 Ma (Bingen et al., 1998). The main cluster at 871 ± 10 Ma overlaps with biotite Rb–Sr ages (Verschure et al., 1980) and is interpreted as a cooling age.

3.5.5 The Mandal-Ustaoset fault and shear zone

The Mandal-Ustaoset fault and shear zone is a N–S trending structure inside the Telemarkia lithotectonic unit (Fig. 2). It includes a precursor ductile shear zone and a set of later brittle normal faults (Sigmond, 1985). In its northern segment, it is an east dipping (c. 45°) normal (extensional) shear zone, juxtaposing the amphibolite-facies Hardangervidda gneiss complex in the west against the low-grade intramontane basin hosting the Kalhovd Formation (≤ 1054 ± 22 Ma) in the east (Sigmond and Ragnhildstveit, 2004). Towards the south, the Mandal-Ustaoset fault and shear zone merges into an amphibolite-facies N–S trending banded gneiss unit on the eastern side of an elongate pluton of the Feda suite (1049 ± 8 Ma, Mandal augen gneiss; Bingen and van Breemen, 1998a). The Mandal-Ustaoset fault and shear zone still requires detailed kinematic and geochronological characterization.

4 Discussion

4.1 U–Pb and Lu–Hf evidence for continental growth at the margin of Fennoscandia

The continental crust exposed in the Sveconorwegian orogen was formed after 1900 Ma (Åhäll and Connelly, 2008; Andersen et al., 2004a; Bingen et al., 2005; Bingen and Viola, 2018; Petersson et al., 2015b; Roberts and Slagstad, 2015; Roberts et al., 2013). The age of the dominant magmatic suites in the different lithotectonic units decreases towards the west (Fig. 7). The oldest major magmatic suites in each lithotectonic unit are dated between 1710 and 1660 Ma in the Eastern Segment, 1660 and 1520 Ma in the Idefjorden lithotectonic unit,

1575 and 1480 Ma in the Bamble and Kongsberg lithotectonic units, and 1520 and 1480 Ma in the Telemarkia lithotectonic unit. The Lu–Hf isotopic signature of igneous zircon in these magmatic suites (Fig. 8) becomes more radiogenic (more positive ε_{Hf} values) westward in the orogenic belt, with average initial ε_{Hf} values increasing from +3.0 in the Eastern Segment (1700 Ma) to +8.8 in the Bamble-Kongsberg lithotectonic units (1550 Ma), and back to +5.7 in the Telemarkia lithotectonic unit (1500 Ma; Fig. 8) (Andersen et al., 2002b; Pedersen et al., 2009; Petersson et al., 2015a; Petersson et al., 2015b; Roberts et al., 2013). The geochemical signature of these different magmatic suites generally ranges from calc-alkalic to alkali-calcic (references above), suggesting that the continental lithosphere was generated dominantly in a supra-subduction (accretionary) geodynamic setting between 1710 and 1480 Ma (Åhäll and Connelly, 2008; Andersen et al., 2004a; Petersson et al., 2015a; Petersson et al., 2015b; Roberts et al., 2013).

The weakly positive initial ε_{Hf} values in the Eastern Segment (Fig. 8) imply significant recycling of older Paleoproterozoic (Svecokarelian) continental crust in the genesis of the 1710–1660 Ma magmatic suites (Petersson et al., 2015a). The more positive initial ε_{Hf} values westwards imply, instead, that the four lithotectonic units to the west of the Mylonite Zone were generated in more juvenile volcanic arc and back arc environment, away from old Paleoproterozoic continental lithosphere (Andersen et al., 2002b; Petersson et al., 2015b; Roberts et al., 2013). The variability within and between these units can be accounted for by a change from an advancing to a retreating subduction system or, alternatively, a variable contribution of metasedimentary components incorporated in the subduction system along the oceanic lower plate (Andersen et al., 2002b; Petersson et al., 2015b; Roberts et al., 2013).

The age and isotopic trends of magmatism in the 1710–1480 Ma interval (Fig. 7, Fig. 8) are compatible with incremental westward growth of the continental lithosphere at the margin

of Fennoscandia. This is compatible with any orogenic model interpreting the lithotectonic units as endemic to the margin of Fennoscandia (Fig. 3 b, d, e, f).

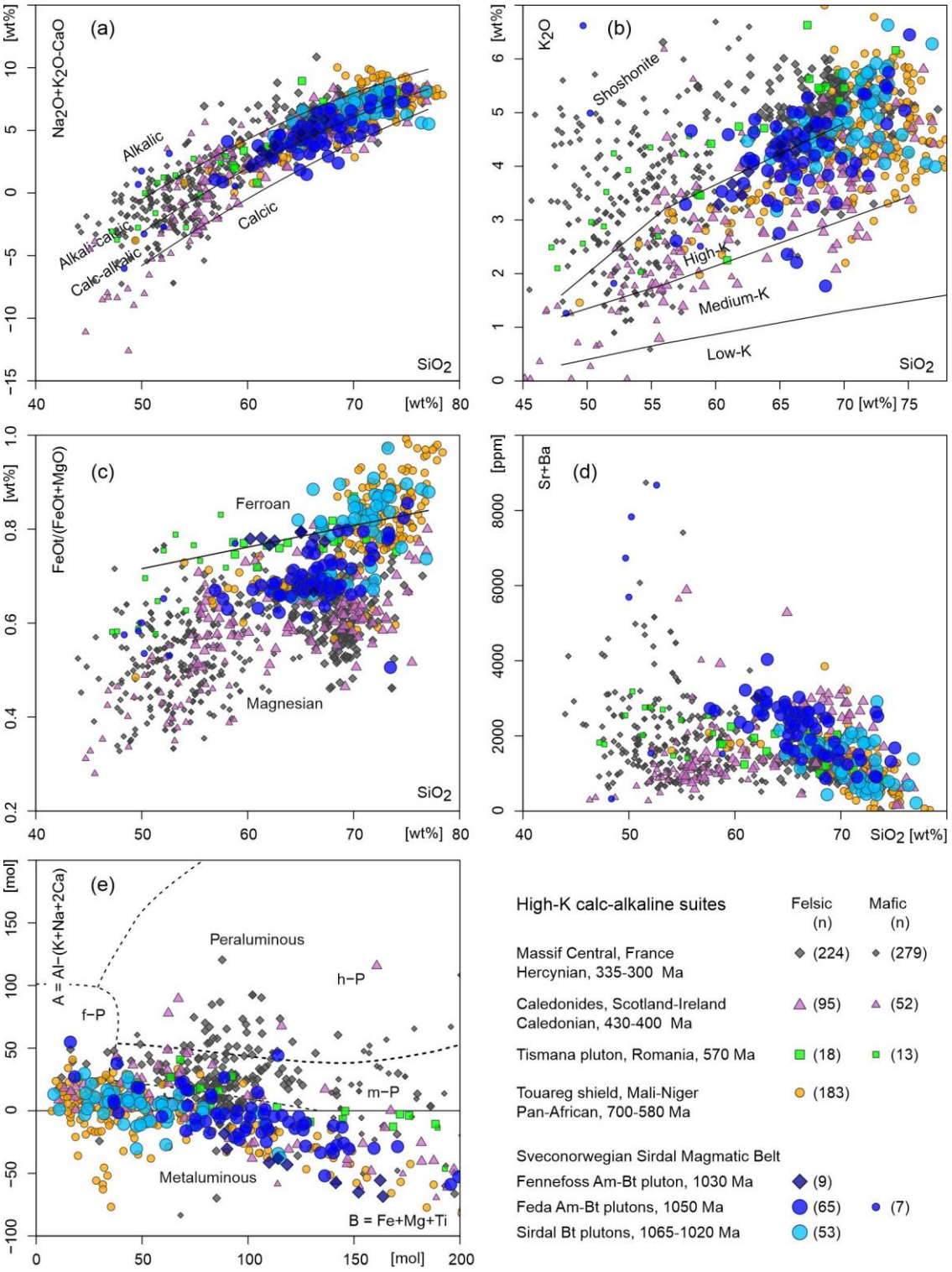

Figure 15. Comparison of the geochemical signature of the Sirdal magmatic belt (c. 1065–1020 Ma) in the Telemarkia lithotectonic unit, and syn-collisional high-K calc-alkaline magmatic suites in younger collision orogenic belts. Large symbols represent granitoids while small symbols represent associated minor mafic sills, dykes and enclaves. The Sirdal magmatic belt is divided into the magnesian amphibole-biotite Feda plutonic suite hosting minor volume of ultrapotassic enclaves, the ferroan amphibole-biotite-bearing Fennefoss pluton and more silica-rich biotite-bearing foliated plutons (Bingen, 1989; Pedersen, 1981; Slagstad et al., 2013; Vander Auwera et al., 2011). For comparison, the Hercynian high-K calc-alkaline plutons of the Massif Central in France associated with "vaugnerites" (compilation: Moyen et al., 2017), the Caledonian high-K, high Ba-Sr plutons of Scotland and Ireland associated with "appinites" (Clemens et al., 2009; Ghani and Atherton, 2006), the Neoproterozoic shoshonitic Tismana pluton in the Carpathians of Romania (Duchesne et al., 1998), and the Neoproterozoic high-K calc-alkalines suites of the Touareg Shield in Mali and Niger (Liégeois et al., 1998). The figure shows a broad overlap of the geochemistry between these different suites. (a) SiO_2 vs. Na_2O+K_2O-CaO diagram (Frost et al., 2001). (b) SiO_2 vs. K_2O diagram (Peccerillo and Taylor, 1976). (c) SiO_2 vs. FeO_{tot} / (FeO_{tot}+MgO) (Frost et al., 2001). (d) SiO_2 vs. Sr+Ba diagram showing the high Sr+Ba signature of high-K calc-alkaline suites, including the Feda plutons and their ultrapotassic mafic enclaves. (e) B-A diagram (B = Fe+Mg+Ti, A = Al-(K+Na+2Ca) (expressed in gram-atoms of each element in 100 gr of material) (Debon and Le Fort, 1983; Villaseca et al., 1998) (h-P: highly peraluminous, m-P: moderately peraluminous, l-P: low peraluminous, f-P: felsic peraluminous).

4.2 Significance of high-K calc-alkaline granite plutonism

Tracing past subduction systems largely relies on tracing a subduction-related geochemical signature in magmatic rocks. In the Telemarkia lithotectonic unit, a significant component of the large (50 x 170 km) orogen-parallel Sirdal magmatic belt (c. 1065–1020 Ma) has a calc-

alkaline geochemical signature (Bingen et al., 2015; Coint et al., 2015; Granseth et al., 2020; Slagstad et al., 2018; Slagstad et al., 2013). More specifically, the biotite + amphibole K-feldspar-phyric quartz-monzonite–granodiorite foliated plutons of the Feda suite are characterized by a high-K, high-Sr-Ba, magnesian, calc-alkalic geochemical trend (Fig. 14) (Bingen et al., 1993; Bingen and van Breemen, 1998a). They are associated with a small volume of ultrapotassic rocks. Calc-alkaline rocks are typically observed in active supra-subduction environment (Bateman and Chappell, 1979; Hervé et al., 2007; Pearce et al., 1984). However, high-K calc-alkaline suites are also typically representative of syn- to late-collision plutons and batholiths in collisional orogens (Fig. 15). They are well described in the Caledonian orogen (Bruand et al., 2014; Clemens et al., 2009; Ghani and Atherton, 2006; Neilson et al., 2009), the Hercynian orogen (Couzinié et al., 2016; Laurent et al., 2014; Laurent et al., 2017; Moyen et al., 2017) and the Pan-African orogens (Janoušek et al., 2010; Liégeois et al., 1998). These plutons are commonly associated with minor volumes of ultrapotassic rocks such as lamprophyre, appinite or vaugnerite (Fig. 15 b). The Sirdal magmatic belt and more specifically the Feda suite exhibits a complete overlap in major and trace element geochemical composition with syn- to late-collision high-K calc-alkaline plutons in collisional orogens (Fig. 15). Therefore, the belt could be reasonably interpreted as well as the product of syn- to late-collision magmatism.

To sum up, the geochemical signature of the Sirdal magmatic belt is not fully diagnostic of a geodynamic environment. There are two alternatives. (i) It records supra-subduction magmatism as part of an active subduction system in the 1065–1020 Ma time interval. This subduction was either dipping eastwards in the context of the models of protracted Andean margin (Fig. 3 e, f) (Slagstad et al., 2020; Slagstad et al., 2017; Slagstad et al., 2013) or was dipping westwards in the model of suturing along the Mylonite Zone at c. 990 Ma (Fig. 3 c) (Brueckner, 2009; Möller and Andersson, 2018; Petersson et al., 2015b). (ii) The Sirdal

magmatic belt represents syn-collision magmatism, therefore recording ongoing continent-continent collision between 1065 and 1020 Ma (Fig. 3 d).

4.3 Significance of massif-type anorthosite plutonism

Massif-type anorthosite plutons formed on Earth only in the Proterozoic. This peculiarity is inferred to relate directly or indirectly to the secular evolution of the temperature of the asthenosphere (Ashwal, 1993). The geodynamic context and petrogenesis of AMC plutonism remain controversial (Ashwal, 1993; Bédard, 2010; Duchesne et al., 1985; Emslie, 1985; Vander Auwera et al., 2011).

Petrologically, the AMC suite of Rogaland (Fig. 5; Fig. 14) can be accounted for by differentiation of several parental magmas ranging in composition from high-alumina basalt (anorthosite plutons) to ferro-basalt (Bjerkreim-Sokndal intrusion and jotunites) in anhydrous and reduced (QFM to QFM-1) conditions (Charlier et al., 2010; Duchesne and Wilmart, 1997; Duchesne et al., 1989; Robins et al., 1997; Vander Auwera and Longhi, 1994).

Here, we draw the attention to the fact that the AMC complex is almost entirely devoid of water-bearing minerals (Duchesne and Charlier, 2005; Longhi et al., 1999). Amphibole appears only very locally as a late-stage replacement mineral. The dry nature of the magmas as well as the water-poor to water-absent assemblages of the granulite-facies wall rock of the AMC plutons (Blereau et al., 2017; Drüppel et al., 2013; Laurent et al., 2018b) are objectively irreconcilable with the definition of magmatism in a supra-subduction setting (Grove et al., 2006). Supra-subduction magmatism is induced by fluids released from and fluxing above a subducting oceanic plate. It typically contains 1–6 wt % H_2O (Plank et al., 2013; Sobolev and Chaussidon, 1996; Wallace, 2005) and produces hornblende-bearing cumulates (Jagoutz and Schmidt, 2013). Therefore, in our opinion, models framing AMC magmatism in a supra-subduction setting (Fig. 3 e, f) (Bybee et al., 2014; Slagstad et al., 2013) are not realistic.

4.4 Sveconorwegian orogenic plateau

Evidence for the presence of a past orogenic plateau in Proterozoic orogens is largely indirect (Jamieson and Beaumont, 2013; Rey et al., 2001; Rivers, 2008, 2012; Vanderhaeghe, 2012). Today, following extension (collapse), exhumation and erosion, the Sveconorwegian orogen exposes widespread gneiss complexes characterized by ductile deformation accompanied by partial melting, compressional structures, and protracted upper amphibolite- to granulite-facies metamorphism, structurally overlain by discontinuous exposures of low-grade supracrustal rocks (Fig. 4). The supracrustal rocks are greenschist- to epidote-amphibolite-facies metavolcanic and metasedimentary sequences, exhibiting partially preserved primary structures and stratigraphic relationships. The age distribution of rocks in the supracrustal complexes matches that in the gneiss complexes. Transition between high-grade and low-grade rock occurs over short distances.

We interpret the gneiss complexes and supracrustal complexes as remnants of the infrastructure and superstructure of an orogenic plateau, respectively, now tectonically juxtaposed along extensional shear zones. Characterization of the geometry, kinematics and geochronology of these shear zones is still very fragmentary today. However, recent data support diffuse late-Sveconorwegian extensional tectonics (Persson-Nilsson and Lundqvist, 2014; Torgersen et al., 2018; Viola et al., 2011).

The sedimentary rocks in the supracrustal complexes offer a window into the surface environment at the time of deposition. As reviewed above, the supracrustal rocks deposited between 1280 and 1050 Ma reflect continental (above sea level) conditions, with evidence for sediment accumulation in fault-bounded intermontane extensional basins (Bingen et al., 2003; Köykkä, 2011; Lamminen, 2011; Spencer et al., 2014). Gneiss complexes in the Bamble and Kongsberg lithotectonic units were exhumed to upper-crustal level after the early-Sveconorwegian orogenic phase (1150–1120 Ma) and, therefore, they can be regarded as part of the orogenic superstructure during the main Sveconorwegian orogeny (after 1065 Ma).

Plutons, produced by partial melting of the lower and middle crust, can be anticipated to accumulate mainly at the transition between ductile and brittle crust (Brown, 2013). In an orogenic plateau, they will accumulate between the infrastructure and superstructure. The Sveconorwegian orogen exposes Sveconorwegian plutons increasing in abundance westwards and mainly hosted in gneiss complexes (Fig. 5). Plutons intruded between 1065 and 920 Ma, define a consistent pressure of intrusion of 0.4–0.5 GPa (Table 1). This suggests a rather constant depth of c. 16 km for the boundary between the infrastructure and superstructure, through time during the main Sveconorwegian orogeny. Additionally, this is consistent with a model of stable orogenic plateau extending over large areas in the orogen.

4.5 End of convergence and collapse of the orogenic plateau

The switch between plate convergence and plate divergence is a fundamental parameter of orogeny. However, it is not trivial to constrain in time, because evidence for compression or extension are distinct in the infrastructure and superstructure of an orogenic plateau. The last undisputable evidence for convergence in the Sveconorwegian orogen corresponds to eclogite facies metamorphism dated at 988 ± 6 Ma in the Eastern Segment (Möller et al., 2015). Several observations, however, indicate that compression continued after this point in the middle crust (infrastructure), probably to at least c. 930 Ma. (i) In the Eastern Segment, the internal section and the eclogite-bearing ductile nappe are folded by east-verging to recumbent folds and later upright folds, recording continued high-grade E–W contraction (Möller and Andersson, 2018; Möller et al., 2015; Piñán-Llamas et al., 2015; Tual et al., 2015). Zircon carries a record of these events between c. 978 and 961 Ma. (ii) In the Telemarkia lithotectonic unit, plutons of the HBG suite exhibit a petrofabric, which is largely controlled by wall-rock ductile deformation during emplacement (Bolle et al., 2018). A study of the anomaly of magnetic susceptibility (AMS) of the Holum, Kleivan, and Sjelset plutons in the Agder area provided evidence for regional E–W compression during intrusion, at 957 ±

7, 936 ± 1 and 932 ± 1 Ma respectively (Fig. 5) (Bolle et al., 2010; Bolle et al., 2003b; Bolle et al., 2018). (iii) In the frontal wedge of the orogen, dykes attributed to the c. 980–945 Ma Blekinge-Dalarna dolerite swarm (Fig. 5) are known to be displaced along discrete ductile shear zones with top-to-east reverse sense of shear. This suggests that thrusting along the Sveconorwegian front took place as late as after c. 945 Ma (Stephens and Wahlgren, 2020a; Wahlgren et al., 1994).

In contrast with this evidence, dykes and sills intruded along brittle structures suggest coeval extension in the upper crust (superstructure). (i) In the Idefjorden lithotectonic unit, WNW–ESE trending mafic to felsic intrusions suggest a phase of NNE-SSW extension between c. 951 and 915 Ma (Fig. 5) (Årebäck et al., 2008; Hellström et al., 2004; Scherstén et al., 2000; Wahlgren et al., 2015). (ii) In the internal section of the Eastern Segment, pegmatite dykes crosscutting the gneiss fabric suggest relaxation between c. 961 and 934 Ma (Andersson et al., 1999; Möller et al., 2007; Möller and Söderlund, 1997; Söderlund et al., 2008b; Söderlund et al., 2002) (iii) In the frontal wedge and the foreland of the orogen, the N-S trending Blekinge-Dalarna dolerites document a phase of E–W extension between c. 978 and 946 Ma (Fig. 5) (Gong et al., 2018; Ripa and Stephens, 2020d; Söderlund et al., 2005).

This cumulatively suggests that the Sveconorwegian orogenic plateau was sustained and grew eastwards until c. 930 Ma, in an overall convergent orogen. Evidence of compression in the ductile middle crust (infrastructure) to c. 930 Ma contrasts with evidence for extension in the same time interval in the brittle upper crust (superstructure), and in the brittle foreland of the orogen.

5 Review of Sveconorwegian orogenic models

In light of the evidence summarised and discussed above, we now review and discuss the orogenic models sketched in Fig. 3 are discussed in more detail in the following.

5.1 Early-Sveconorwegian collision-accretion with suture in Bamble-Kongsberg

The oldest known Sveconorwegian high-grade metamorphism (1150–1120 Ma) is recorded in the Kongsberg and Bamble lithotectonic units, in the centre of the Sveconorwegian orogen. This metamorphism could be interpreted to reflect crustal thickening during an early-Sveconorwegian collision. This interpretation leads to the conceptual model of Fig. 3 a involving collision or accretion of an exotic Telemarkia microcontinent to the Idefjorden lithotectonic unit between 1150 and 1120 Ma, closing an intervening ocean and forming the Bamble-Kongsberg orogenic wedge (Bingen et al., 2008c; Bingen et al., 2005). At least two arguments rule out the closure of an oceanic realm. (i) The Mesoproterozoic magmatism exhibits a significant age overlap between the Bamble–Kongsberg, Telemarkia and Idefjorden lithotectonic units. Specifically, the 1520–1480 Ma magmatic suites, which are prominant in the Telemarkia lithotectonic unit, extend well into the Bamble, Kongsberg and Idefjorden lithotectonic units, thus representing a stitching element of these units around c. 1500 Ma (Fig. 7). (ii) The granulite-facies low-K calc-alkaline Tromøy Complex in Bamble was formerly interpreted as an early-Sveconorwegian, c. 1200 Ma old, oceanic volcanic arc (Andersen et al., 2004a; Andersen et al., 2002b; Knudsen and Andersen, 1999). However, new data demonstrate that the magmatic protolith of the Tromøy Complex is Gothian (1575 ± 44 to 1544 ± 14 Ma) (Bingen and Viola, 2018), meaning that no evidence for remnants of early-Sveconorwegian oceanic lithosphere is known in the Bamble lithotectonic unit. There is therefore no actual geological support for the conceptual model sketched in Fig. 3 a.

5.2 Early-Sveconorwegian wrench tectonics

The Bamble and Kongsberg lithotectonic units have been referred to as shear belts in the literature mostly because of widespread, steep shear foliation zones and penetrative lithological banding (Starmer, 1991). This intense deformation has inspired tectonic models (Fig. 3 b) involving long distance early-Sveconorwegian strike-slip transport of the

Telemarkia lithotectonic unit relative to the Idefjorden lithotectonic unit, at the margin of Fennoscandia, generating a Bamble–Kongsberg transpressional shear belt (Andersen et al., 2004a; Bingen et al., 2008c; deHaas et al., 1999; Lamminen and Köykkä, 2010). However, recent field data from the tectonic boundaries between the Bamble, Kongsberg, Telemarkia and Idefjorden lithotectonic units, and from the centre of the Bamble and Kongsberg lithotectonic units (Bingen and Viola, 2018; Henderson and Ihlen, 2004; Scheiber et al., 2015) highlight orthogonal compression and rule out significant wrench tectonics, thus excluding orogen-scale strike-slip transport. A component of sinistral strike-slip shearing is indeed recorded by some of the mylonite zones within the Kongsberg lithotectonic unit (Scheiber et al., 2015). These are, however, compatible with transpressional deformation ensuing only after the peak of orthogonal deformation and high-grade metamorphism (1150–1120 Ma).

5.3 Collisional orogeny with suture along the Mylonite Zone

The Mylonite Zone is a major Sveconorwegian east-southeastward-verging shear zone, juxtaposing the Eastern Segment beneath the Idefjorden lithotectonic unit. The geological records of these two units are significantly distinct and, as a consequence, several authors have argued that the Mylonite Zone may represent a suture zone. An oceanic domain would have closed at c. 990 Ma between the Eastern Segment, representing the Fennoscandia continent as lower plate, and distal terranes formed outboard of the Fennoscandia margin in the west as upper plate (the four western lithotectonic units of the orogen named together ‘Sveconorwegia’; Fig. 3 c) (Andersson et al., 2002a; Austin Hegardt et al., 2005; Brueckner, 2009; Cornell et al., 2000; Möller and Andersson, 2018; Möller et al., 2015; Petersson et al., 2015b). This model envisions the pre-990 Ma (pre-collision) magmatism and metamorphism west of the Mylonite Zone as formed in a supra-subduction setting, above a west-dipping subduction zone. At least four arguments support this model. (i) The magmatic records in the Eastern Segment and in the Idefjorden lithotectonic unit are distinct (Fig. 7). Magmatic suites

do not extend across the Mylonite Zone. (ii) Hallandian metamorphism between 1465 and 1385 Ma is documented only east of the Mylonite Zone (Fig. 6) (Söderlund et al., 2002; Ulmius et al., 2015). (iii) The Sveconorwegian metamorphism in the Eastern Segment reached eclogite-facies conditions at c. 990 Ma (Möller et al., 2015), significantly after granulite-facies metamorphism in the Idefjorden hanging wall at c. 1050 Ma (Söderlund et al., 2008a). Eclogite-facies metamorphism could record continental burial after closure of an ocean basin (Möller and Andersson, 2018; Möller et al., 2015). (iv) The Lu–Hf isotopic signature of magmatic rocks in the 1780–1480 Ma interval documents a geochemical disconnect across the Mylonite Zone, with an average ε_{Hf} = +3.0 in the Eastern Segment at 1700 Ma against +4.8 in the Idefjorden lithotectonic unit at 1570 Ma (Petersson et al., 2015a; Petersson et al., 2015b) (Fig. 8). This difference implies a lower contribution of old continental crust in the genesis of the magmatic rocks in the Idefjorden lithotectonic unit.

These four pro-arguments, however, are balanced by counterarguments. Specifically (i) the Orust dolerites (1457 ± 6 Ma) in the Idefjorden lithotectonic unit (Åhäll and Connelly, 1998) overlap in age with 1465–1385 Ma Hallandian granitic to charnockitic plutonism in the Eastern Segment. (ii) The Lu–Hf isotopic signature of early-Sveconorwegian magmatism between 1225 and 1180 Ma is distinctly supra-chondritic in both the Eastern Segment (bimodal magmatism along the Sveconorwegian front; $+1.2 < \varepsilon_{Hf} < + 6.6$) and the Telemarkia lithotectonic unit (Vråvatn Complex; $+9 < \varepsilon_{Hf} < + 10$; Fig. 8) (Andersen et al., 2007; Petersson et al., 2015a; Söderlund et al., 2005). This signature attests to coeval depleted mantle derived magmatism on both side of the Mylonite Zone before the presumed ocean closure at 990 Ma. (iii) The Mylonite Zone (or geological units in its direct proximity) does not contain any remnants or slivers of pre- to early-Sveconorwegian (1340–1080 Ma) marine sedimentary sequences, oceanic lithosphere, oceanic volcanic arc, or ultramafic rocks, such that no suture zone can be directly constrained.

To conclude, closure of an oceanic basin along the Mylonite Zone at c. 990 Ma represents a plausible model (Fig. 3 c) (Möller and Andersson, 2018). However, the evidence is not conclusive at this point of research. In the following text, we do not select this model as the most probable.

5.4 Non-collisional (Andean type) orogeny

In the non-collisional (Andean type) orogenic models (Fig. 3 e, f), the Sveconorwegian orogen represents an active margin of Fennoscandia, evolving from at least 1280 Ma to after 900 Ma, above an oceanic plate subducting to the east into a trench situated to the west of the exposed orogen (Falkum and Petersen, 1980; Slagstad et al., 2013). The geological record in the Sveconorwegian orogen is explained by changes in the conditions of subduction, such as trench position, subduction angle, convergence rate, convergence direction and age of the oceanic lithosphere. This model is an adaptation of the tectonic switching model (Collins, 2002; Haschke et al., 2002), which is based on the observation that a retreating or steepening oceanic subduction is associated with an extensional tectonic regime and abundant magmatism in the (supra-subduction) upper plate, while an advancing or flattening subduction is associated with compression, metamorphism and magmatic quiescence.

Different versions of the non-collisional (Andean type) model have been proposed by Slagstad et al. (2020; 2018; 2017; 2013) and Granseth et al. (2020). These models offer an elegant and flexible framework for the orogeny. However, we think that they are irreconcilable with a number of key features and concepts. (i) In its simple expression, the tectonic switching model predicts either extension or compression in the upper (supra-subduction) plate. During the main Sveconorwegian orogeny, voluminous magmatism (mafic and felsic) in the Telemarkia lithotectonic unit would indicate a retreating subduction trench between 1065 and 1020 Ma, while HP granulite facies metamorphism in the Idefjorden lithotectonic unit (Söderlund et al., 2008a) would indicate an advancing trench in the same

time interval, in contradiction with the model. (ii) Conceptually, an eastwards oceanic subduction to the west of the orogen can hardly represent the driving force for westwards underthrusting of the Eastern Segment at c. 990 Ma to eclogite-facies conditions. Considering the presumably weak rheology of the lithosphere in the Telemarkia lithotectonic unit around 990 Ma, it is unlikely that compressive stresses from a plate subducting west of the orogen could be effectively transmitted at least 400 km to the east to the Eastern Segment. (iii) The Sveconorwegian magmatism (1065–915 Ma) does not represent typical volcanic arc magmatism. The geochemical signature and petrology of magmatic suites can be related to lower crustal sources and partial melting conditions (Granseth et al., 2020; Vander Auwera et al., 2008; Vander Auwera et al., 2011), rather than to an active subduction. The geochemical signature of the Sirdal magmatic belt (1065–1020 Ma) can be interpreted in both a collisional setting or a supra-subduction setting (see above). The magmatism between 985 and 915 Ma lacks a subduction signature and the dry nature of AMC magmatism is not compatible with a supra-subduction setting (see above). The magmatism between 935 and 915 Ma is exposed over a zone at least 350 km wide, much larger than a typical volcanic arc. The geographical polarity of the magmatism in the 935–915 Ma time interval, involving dry plutonism of the AMC suite in the west and water-bearing plutonism of the HBG suite in the east is opposite to what should be expected from an east dipping subduction system.

For these different reasons, we remain sceptical that an oceanic subduction in the hinterland of the orogen could have steered tectonic forces and magmatism inside the orogen during the main Sveconorwegian orogeny (1065–900 Ma). The non-collisional models proposed by Slagstad et al. (2020; 2018) omit to propose specific tectonic driving forces, either oceanic subduction or continental subduction-delamination inside the orogen, to explain the metamorphism with high-pressure signature in the Bamble–Kongsberg lithotectonic units (1150–1120 Ma), Idefjorden lithotectonic unit (c. 1050 Ma) and Eastern Segment (c. 990 Ma).

In a recent version of the non-collisional model (Slagstad et al., 2020), the margin of Fennoscandia is proposed to have been fragmented (into micro-continents) by extension before c. 1150 Ma and re-amalgamated during the Sveconorwegian orogeny between c. 1150 and 980 Ma to form the Sveconorwegian orogen. However, as discussed previously in this chapter, there is no evidence between the lithotectonic units for (i) marine sediment sequences that could represent marine basins, (ii) ophiolites or oceanic volcanic arcs that could represent oceanic basins, or (iii) ultramafic bodies that could represent exhumed hyperextended domains. As noted earlier, the low-K calc-alkaline Tromøy Complex in Bamble (Andersen et al., 2004a) should not be interpreted as an early-Sveconorwegian oceanic volcanic arc (Bingen and Viola, 2018).

5.5 Collisional orogeny with suture west of the orogen

The Grenville orogen is the archetypal example of a large (> 600 km wide) and hot Mesoproterozoic collisional orogen (Fig. 1) (Gower et al., 2008; Jamieson and Beaumont, 2013; Rivers, 2008, 2012). The Grenville orogeny was long lived (> 110 Myr). It propagated from a weak Proterozoic lithosphere into the cratonic Archean foreland, with thrusting along two orogen parallel, continuous, crustal-scale shear zones (the Allochthon Boundary Thrust and Grenville Front) and two main phases of orogenic convergence (the Ottawan, 1090–1020 Ma, and Rigolet, 1010–980 Ma, phases; Fig. 1). Protracted high-temperature–low-pressure high-grade metamorphism in the hinterland, associated with both crustal- and mantle-derived magmatism, was coeval with comparatively short-lived high-pressure metamorphism in thick thrust slices towards the foreland (Groulier et al., 2018a; Indares, 2020; Rivers, 2008). The first order architecture of the Sveconorwegian orogen and its orogenic evolution are comparable to that of the Grenville orogen (Cawood and Pisarevsky, 2017; Gower, 1985; Gower et al., 2008; Hoffman, 1991; Rivers, 2008, 2012). An analogy in the geodynamic evolution is therefore natural.

In the collisional models (Fig. 3 d), closure of (one or several) oceanic basin(s) to the west of the exposed orogen was followed by the collision of Baltica (Fennoscandia) with (one or several) continental plate(s) at and after 1065 Ma (Bingen et al., 2008c; Bogdanova et al., 2008; Cawood and Pisarevsky, 2017; Gower et al., 2008; Ibanez-Mejia et al., 2011; Li et al., 2008; Pisarevsky et al., 2014; Stephens and Wahlgren, 2020b; Weber et al., 2010). Consumption of these oceanic basins involved subduction and formation of volcanic arcs, either at the margin of Fennoscandia or in an outboard position prior to final collision. During collision, the Sveconorwegian orogen was situated in the upper plate position, on the Fennoscandia side of the main suture zone.

Here are some key features supporting the collisional model for the main Sveconorwegian orogeny (1065–900 Ma). (i) The Sveconorwegian orogen is c. 550 km wide, i.e. wider than any present-day Andean orogen. It exhibits a c. 550 km wide zone of convergent tectonics (1065–930 Ma) and a c. 350 km wide zone of syn-orogenic magmatism (Fig. 5). (ii) The orogen has the structure of an extended (collapsed) orogenic plateau, with the juxtaposition of high-grade gneiss complexes representing a middle crustal infrastructure, against low-grade supracrustal rocks representing a brittle superstructure, and plutons representing the product of lower- to middle-crustal melting during orogeny (Fig. 4) (Andersen et al., 2001; Granseth et al., 2020; Vander Auwera et al., 2011). The gneiss complexes carry evidence for protracted (> 110 Myr) middle-crustal high-temperature-low-pressure metamorphism (Bingen et al., 2008b; Blereau et al., 2017; Laurent et al., 2018a; Laurent et al., 2018b; Slagstad et al., 2018). (iii) High pressure granulite- and eclogite-facies rocks attest to crustal thickening, up to c. 70 km, between c. 1050 and 990 Ma (Möller and Andersson, 2018; Söderlund et al., 2008a). After peak metamorphism, these rocks were incorporated and overprinted into the middle-crustal infrastructure. They were probably more abundant in the orogen than what is apparent from their exposure. (iv) The orogenic zone grew towards the foreland, in a stepwise fashion

with time. This process involved thrusting along crustal scale shear zones (Mylonite Zone and Sveconorwegian front). This pattern is typical of collision orogens (Royden et al., 2008). (v) The orogenic zone lacks evidence for syn-orogenic marine sedimentary sequences, in spite of a largely exposed superstructure (Fig. 4), and therefore was above sea-level during the entire orogeny.

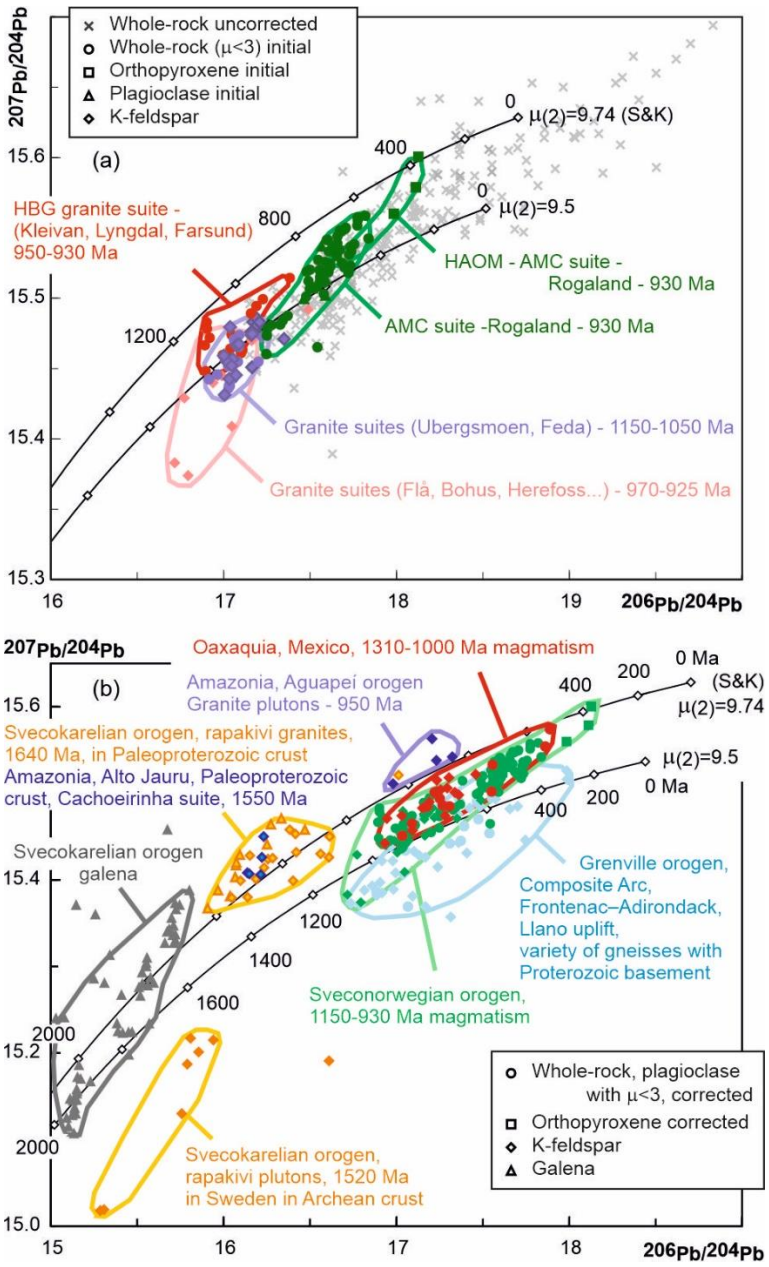

Figure 16. Common Pb isotopic composition in the $^{206}Pb/^{204}Pb$ vs. $^{207}Pb/^{204}Pb$ diagram, with reference growth curves of terrestrial common Pb ($\mu_{(2)}$ = 9.74 (Stacey and Kramers, 1975) and

$\mu_{(2)}$ = 9.5, with $\mu = {}^{238}U/{}^{204}Pb$). (a) Compilation of data from the Sveconorwegian orogen. Highlighted symbols represent initial ratio of plutonic suites dated between 1150 and 930 Ma. Initial ratio (ratio corrected for U decay since intrusion) is calculated for analyses of K-feldspar, plagioclase, orthopyroxene and whole-rock with $\mu < 3$. The initial ratio of plutonic rocks defines a short trend below the reference growth curve of Stacey and Kramers (1975). High alumina orthopyroxene megacrysts (HAOM) hosted in the anorthosite plutons are situated at the radiogenic (upper-right) end of the trend. They are interpreted to represent a mafic, mantle-derived, underplate, formed at c. 1040 Ma and remelted at c. 930 Ma. The granite plutons partly sourced from metasedimentary protoliths, like the Flå and Bohus muscovite-bearing plutons, are situated at the less radiogenic (lower-left) end of the trend. The hornblende-biotite granite plutons, ranging from c. 1150 to 930 Ma, sourced from metaigneous protoliths, cluster in the centre of the trend (Andersen, 1997; Andersen et al., 2001; Andersen et al., 1994; Andersen and Munz, 1995; Bingen et al., 1993; Vander Auwera et al., 2014a; Weis, 1986). (b) Compilation of initial isotopic compositions for Baltica (Fennoscandia) and selected late-Mesoproterozoic orogenic belts. Data for the Sveconorwegian orogen are copied from panel (a). A variety of ortho- and paragneisses from the hinterland of the Grenville orogen, including the Composite Arc (Ontario), Frontenac-Adirondack (Ontario) and Llano uplift (Texas) overlap with the data of the Sveconorwegian orogen, as well as orthogneisses from the Oaxaquia lithotectonic unit (Mexico) (Cameron et al., 2004; DeWolf and Mezger, 1994). Granite plutons (950 Ma) in the Aguapei Belt in Amazonia are characterized by a more radiogenic ^{207}Pb signature than coeval rocks in the Sveconorwegian orogen, consistent with involvement of an older Paleoproterozoic basement in this orogen (Geraldes et al., 2001). Data for rapakivi granite plutons from Fennoscandia on Paleoproterozoic and Archean basement, as well as Paleoproterozoic galena deposits from the

Svecokarelian orogen are shown for reference (Andersson et al., 2002b; Rämö, 1991; Vaasjoki, 1981).

5.6 Conjugate margins in Rodinia

In classical Rodinia assembly models, Laurentia and Baltica were probably already contiguous at low latitudes at c. 1260 Ma as part of Nuna (Columbia), facing an ocean, the Mirovoio ocean (Buchan et al., 2000; Evans and Mitchell, 2011; Pisarevsky et al., 2014; Zhang et al., 2012). Opening of the Asgard sea (north of Baltica; Fig. 1), clockwise rotation and drift of Baltica relative to Laurentia, and consumption of the Mirovoio ocean (south of Baltica) led to collision of Amazonia with Laurentia and Baltica, involving three sequential tectonic phases (Bogdanova et al., 2008; Cawood and Pisarevsky, 2017; Gower et al., 2008; Hynes and Rivers, 2010; Ibanez-Mejia et al., 2011; Johansson, 2009; Li et al., 2008; Pisarevsky et al., 2014; Roberts, 2013; Tohver et al., 2004a; Weber et al., 2010). (i) Collision between Amazonia and the southwestern part of Laurentia starting at c. 1200 Ma and generating the Llano section of the Grenville orogen and the Sunsás orogen (Fig. 1). (ii) Sinistral transpression between Amazonia and Laurentia, between c. 1150 and 1050 Ma, generating the Grenville orogen. (iii) Collision between Amazonia and Baltica at c. 1060 Ma, following closure of the intervening oceans, producing the Sveconorwegian and Putumayo orogens (Fig. 1) (Boger et al., 2005; Ibanez-Mejia et al., 2011; Tohver et al., 2004b; Tohver et al., 2005).

Following Cawood et al. (2010), a subduction system was initiated along the northern open margin of Rodinia (Asgard sea; Fig. 1) after the Amazonia–Laurentia–Baltica collision (i.e. after 1000 Ma). In this model, Tonian sediments sequences and volcanic and plutonic rocks hosted in variably far-travelled nappes of the Caledonides of NE Greenland, Scandinavia, Svalbard and Scotland (Augland et al., 2014; Cawood and Pisarevsky, 2017; Cawood et al., 2015; Corfu, 2019; Cutts et al., 2009; Kalsbeek et al., 2000; Kirkland et al., 2006, 2007) are

interpreted as fragments of an accretionary orogen, the Valhalla orogen, at the margin of Rodinia (Fig. 1). An orogenic phase, including magmatism, metamorphism, and deformation (Renlandian) took place between 980 and 910 Ma (Cawood et al., 2010), therefore overlapping with metamorphism in the Sveconorwegian orogen (Table 1).

Several Mesoproterozoic basement inliers in the Andes of Colombia (Garzón, Las Minas) and in Mexico (Oaxaquia lithotectonic unit) are characterized by high-grade metamorphism, dated consistently between 1000 and 980 Ma (Zapotecan-Putumayo orogenies). These lithotectonic units are interpreted as oceanic volcanic arcs formed in ocean tracts between Laurentia, Amazonia and Baltica (after c. 1460 Ma) (Fig. 12 a, b) and involved in the collision zone between these plates (Fig. 1) (Cardona et al., 2010; Cordani et al., 2005; Ibanez-Mejia et al., 2015; Ibanez-Mejia et al., 2011; Jiménez-Mejía et al., 2006; Keppie et al., 2003; Keppie and Ortega-Gutiérrez, 2010; Weber and Köhler, 1999; Weber et al., 2010).

In archetypal Rodinia reconstructions (Fig. 1), the hinterland of the Sveconorwegian orogen is facing Mesoproterozoic basement inliers in the Andes of Colombia (Garzón, Las Minas) and in Mexico (Oaxaquia lithotectonic unit) and the hinterland of the Grenville orogen. The isotopic signature of these units is compared in a εNd vs. time diagram (Fig. 13 b). The Quebecia and Telemarkia lithotectonic units, located in the hinterland of the exposed Grenville and Sveconorwegian orogens respectively, represent coeval continental growth zones generated by volcanic arc and back arc magmatism between c. 1520 and 1480 Ma (Pinwarian and Telemarkian phases; Table 1; Fig. 13 b) (Dickin and Higgins, 1992; Groulier et al., 2018b). These units are characterized by very similar isotopic evolution trends starting from close to the Depleted Mantle reservoir at and after 1520 Ma and decreasing along a continental recycling trend to near-chondritic value at c. 1000 Ma. The basement inliers in the Andes of Colombia (Garzón, Las Minas) and in Mexico (Oaxaquia lithotectonic unit) define evolution trends starting at c. 1380 Ma and 1300 Ma, respectively, that overlap with the

1519 Telemarkia trend (Ibanez-Mejia et al., 2015; Lawlor et al., 1999; Weber and Köhler, 1999). In
1520 the hinterland of the Grenville Belt, the Composite Arc and Frontenac–Adirondack
1521 lithotectonic units define the most juvenile trend, starting at c. 1380 Ma (Fig. 13 b) (Daly and
1522 McLelland, 1991; Dickin et al., 2010; Marcantonio et al., 1990). These units are interpreted as
1523 marginal or outboard volcanic arcs, back-arcs and microcontinents assembled (or
1524 reassembled) to Laurentia early during the Grenvillian orogeny (Shawinigan phase, 1190–
1525 1140 Ma) (Carr et al., 2000; Hanmer et al., 2000; Rivers, 2008). Interestingly, the 1280-1200
1526 Ma magmatism in the Composite Arc (Elzevirian) has a Nd isotopic signature approaching
1527 that of the Depleted Mantle reservoir (Carr et al., 2000; Corfu and Easton, 1995; Corriveau
1528 and van Breemen, 2000; Dickin and McNutt, 2007), very similar to the one of coeval 1280–
1529 1200 Ma continental magmatism in the Sveconorwegian orogen (Sæsvatn–Valldal bimodal
1530 volcanism) (Brewer et al., 2004).

1531 In the $^{206}Pb/^{204}Pb$ vs. $^{207}Pb/^{204}Pb$ diagram (Fig. 16), the initial isotopic composition of
1532 Sveconorwegian plutonic rocks intruded between 1150 and 930 Ma defines a short trend
1533 below the evolution curve of terrestrial common Pb of Stacey and Kramers (1975) ($\mu_{(2)}$ =
1534 9.74). Ortho- and paragneisses from the hinterland of the Grenville Belt, including the
1535 Composite Arc (Ontario), Frontenac-Adirondack (Ontario) and Llano uplift (Texas) and
1536 orthogneisses from the Oaxaquia lithotectonic unit (Mexico) overlap with the data of the
1537 Sveconorwegian orogen (Cameron et al., 2004; DeWolf and Mezger, 1994).

1538 To summarize, Nd and Pb isotopic data (Fig. 13; Fig. 16) and detrital zircon data (Fig. 12)
1539 underscore the existence of juvenile lithotectonic units generated at and after c. 1520 Ma
1540 exposed in the hinterland of the Grenville and Sveconorwegian orogens and the basement
1541 inliers in the Andes of Colombia (Garzón, Las Minas) and in Mexico (Oaxaquia lithotectonic
1542 unit). These isotopic data therefore support to join these lithotectonic units in the core of the
1543 collision zone between Laurentia, Amazonia and Baltica, in a classical Rodinia reconstruction

(Fig. 1). These data also suggest that, in the collision model of Fig. 3 d, the continental margin colliding with the Sveconorwegian orogen possessed a weak lithosphere similar to the one of the Telemarkia lithotectonic unit (as opposed to a stronger cratonic lithosphere).

6 Model of large, hot and long-duration continental collision

The previous discussion argues for a collisional model for the main Sveconorwegian orogeny. Here, we further develop a model of large, hot and long-duration continent-continent collision starting at c. 1065 Ma, wherein the five lithotectonic units of the orogen are endemic to Fennoscandia (Fig. 3 d). The plate tectonic interpretation of the pre-collision evolution between 1280 and 1080 Ma is still largely speculative. The model is fitted into a classical Rodinia assembly framework (Fig. 1), involving an Amazonia-Laurentia-Baltica collision, as discussed previously. However, the model is based upon evidence from within the exposed Sveconorwegian orogen (and its foreland) and therefore independent of Rodinia models.

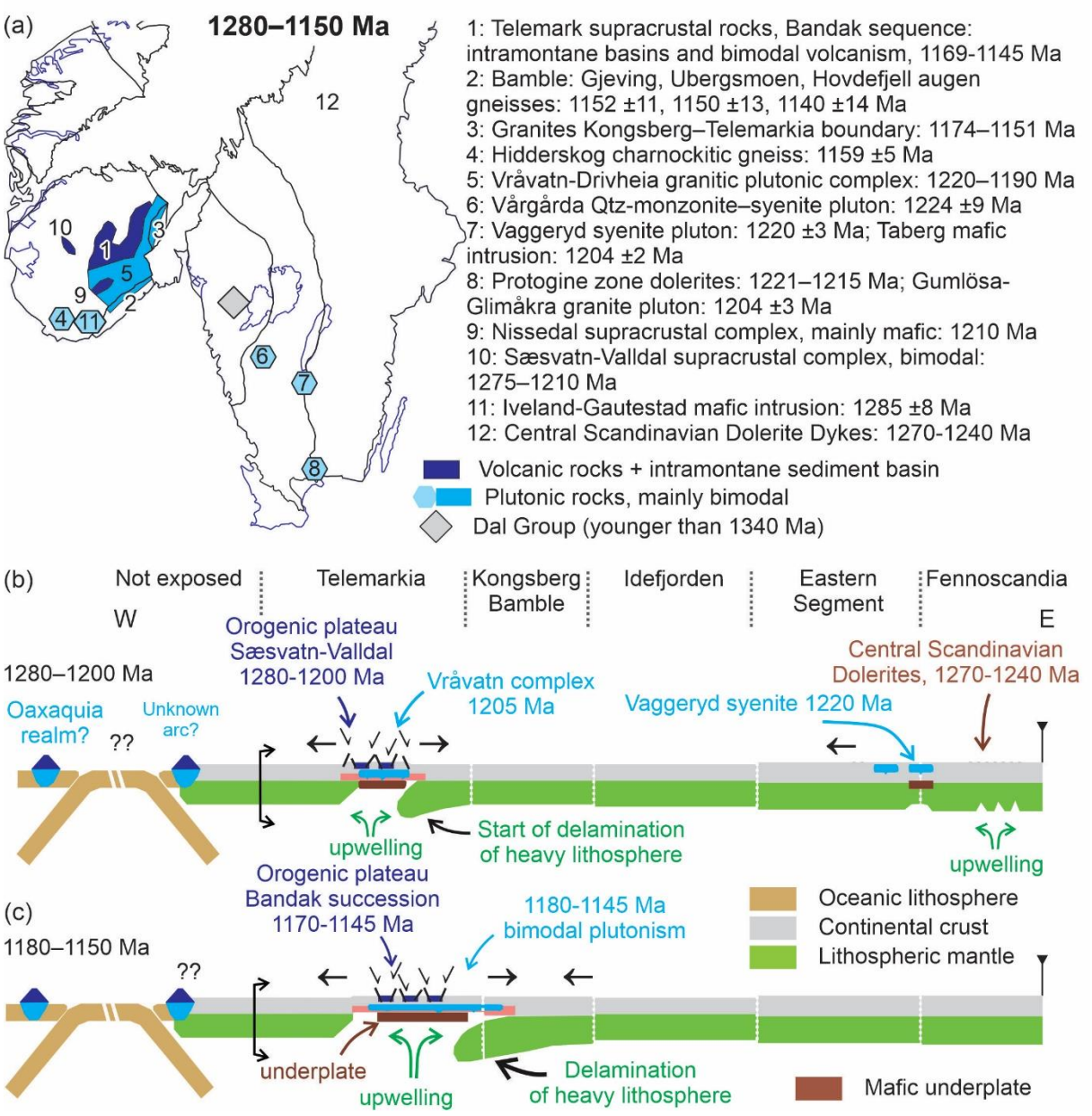

Figure 17. Schematic geodynamic model for the 1280–1150 Ma time interval. (a) Sketch map of the Sveconorwegian orogen, with position and list of plutonic and supracrustal complexes. (b, c) Interpretative E-W cross sections of the Sveconorwegian orogen and speculative linkage westwards. The exposed part of the orogen is limited by an arrowed bracket. The limit between lithotectonic units is schematically represented by a white vertical dashed line. References and explanations in the text.

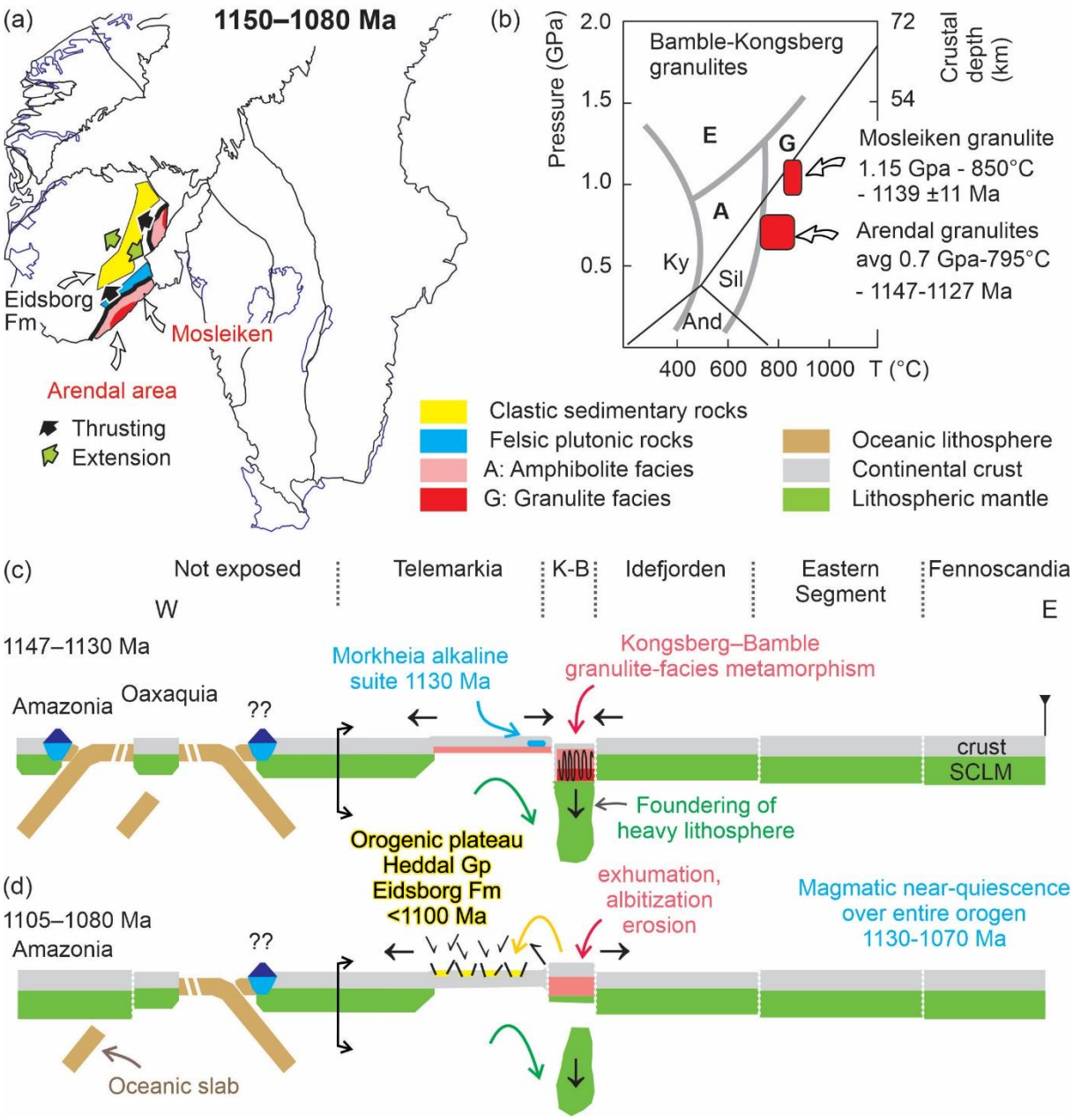

Figure 18. Schematic geodynamic model for the 1150–1080 Ma time interval. (a) Sketch map of the Sveconorwegian orogen, with distribution of metamorphism, magmatism and clastic sediment basins. (b) Pressure-temperature diagram with fields of the main metamorphic facies following Spear (1993): E: eclogite facies, G: granulite facies, A: amphibolite facies. (c, d) Interpretative E-W cross sections of the Sveconorwegian orogen and speculative linkage westwards. Explanations and references in the text.

6.1 1280–1080 Ma, pre-collision: lithospheric mantle delamination

The geological record for the pre- to early-Sveconorwegian 1280-1080 Ma time interval is very distinct in the Telemarkia, Kongsberg–Bamble and Idefjorden lithotectonic units. Abundant bimodal magmatism between 1280 and 1145 Ma, and protracted (upper) crustal extension in Telemarkia between 1280 and 1080 Ma (Fig. 17; Fig. 18) contrast with amphibolite- to granulite-facies metamorphism and shortening in the Kongsberg–Bamble lithotectonic units between 1150 and 1120 Ma (Fig. 18). Except for a few dolerite dykes, the Idefjorden lithotectonic unit is lacking evidence for magmatism, metamorphism and deformation between 1280 and 1080 Ma, and therefore it is regarded as having played the role of a passive buttress during this time interval. There is no evidence for closure of marine or oceanic basins between the Telemarkia, Kongsberg–Bamble and Idefjorden lithotectonic units (Scheiber et al., 2015). These different features cannot be explained by a simple model of regional scale inversion from extension to compression at c. 1150 Ma, as one would anticipate compression structures to be located in the weakest Telemarkia lithosphere, or distributed evenly throughout the Telemarkia, Bamble and Kongsberg lithotectonic units.

In Fig. 17, we propose that upwelling of asthenosphere and development of an orogenic plateau started at c. 1280 Ma in the Telemarkia lithotectonic unit. Repeated pulses of bimodal magmatism between 1280 and 1145 Ma provide evidence for upwelling and decompression melting of asthenospheric mantle (Fig. 7). The most prominent mafic volcanic rocks (Fig. 11; Sæsvatn–Valldal, Nissedal, Morgedal and Gjuve metabasalts) exhibit a within-plate geochemical signature and supra-chondritic Nd isotopic signature ($+2.6 < \varepsilon_{Nd} < +6.3$) implying sourcing in the asthenosphere (Fig. 13 a) (Brewer et al., 2002; Brewer et al., 2004; Spencer et al., 2014). The voluminous felsic gneisses of the Vråvatn Complex (1220–1190 Ma) have Hf isotopic signature of zircon ($+9 < \varepsilon_{Hf} < +10$) also close to the depleted mantle reservoir at 1210 Ma ($\varepsilon_{Hf} = +12$) (Fig. 8) (Andersen et al., 2007). These values indicate that

1598 the Vråvatn Complex was not produced principally by partial melting of the Telemarkian
1599 (1520–1480 Ma) crust. Rather, it was probably produced by partial melting of a mafic lower
1600 crust or mafic underplate, itself produced shortly before in the depleted mantle (a maximum
1601 of some 50 Mys before 1210 Ma; Andersen et al., 2007). The earliest magmatism between
1602 1280 and 1190 Ma occurred in the centre of the Telemarkia lithotectonic unit (Vråvatn,
1603 Nissedal, Sæsvatn–Valldal, Iveland-Gautestdad; Fig. 6; Fig. 17) while younger magmatism
1604 between 1170 and 1140 Ma is more abundant towards the periphery of the lithotectonic unit
1605 (mainly eastwards and southwards) and is well recorded into the Kongsberg and Bamble
1606 lithotectonic units. This geographic distribution suggests that mantle upwelling affected
1607 progressively a larger area between c. 1280 and 1145 Ma (Fig. 17).

1608 Upwelling of hot asthenosphere at c. 1280 Ma induced partial melting at the base of the
1609 crust. This weakening of the lower crust possibly initiated decoupling between the crust and
1610 the lithospheric mantle and progressive delamination of the lithospheric mantle between c.
1611 1280 and 1145 Ma. Alternatively, protracted upwelling of asthenosphere between 1280 and
1612 1145 Ma progressively induced convective removal (or displacement) of the continental
1613 lithospheric mantle. Both interpretations resulted in uplift, formation of a plateau and
1614 extension in the crust (Dewey, 1988; Li et al., 2016).

1615 Evidence for an orogenic plateau involving uplift and extension in the upper crust is
1616 provided by the sedimentology of low-grade sedimentary rocks deposited between 1260 and
1617 1080 Ma in Telemarkia. The sediments of the Bandak succession are high-energy immature
1618 deposits, accumulated in continental (above sea level) intermontane basins (Bingen et al.,
1619 2003; Köykkä, 2011; Lamminen, 2011; Spencer et al., 2014). The limited lateral extent of the
1620 basin infills, the existence of at least two major internal unconformities in the Bandak
1621 succession, and the direct evidence for normal syn-sedimentary growth faults, suggest active
1622 extension during accumulation (Fig. 11; Fig. 12) (Laajoki, 2002; Laajoki et al., 2002;

Lamminen, 2011). This orogenic plateau does not satisfy to the definition of a Tibetan orogenic plateau, as evidence for crustal thickening and protracted metamorphism is lacking in the 1280–1080 Ma time interval inside the Telemarkia lithotectonic unit.

Compression in the Kongsberg–Bamble lithotectonic units in the interval between 1150 and 1120 Ma can be explained by compression at the margin of the plateau and foundering (subduction) below the Kongsberg–Bamble lithotectonic units of the lithospheric mantle slab delaminated below Telemarkia (Fig. 18). We suggest that the pull effect of foundering generated subsidence in the crust, high-grade metamorphism (up to 1.15 GPa) and deformation with lithological banding and commonly steep lineation in Kongsberg–Bamble between 1150 and 1120 Ma.

Eventual breakoff of the mantle slab triggered exhumation of the Bamble and Kongsberg lithotectonic units after 1120 Ma (Fig. 18 d). The volumetrically minor alkaline Morkheia monzonite suite, located just north of the Bamble–Telemarkia boundary zone, may record this event with local melting of a sliver of lithospheric mantle at c. 1134–1130 Ma (Fig. 18 c) (Heaman and Smalley, 1994). Exhumation to upper crustal levels (1105–1080 Ma) was associated with northwestwards thrusting of Bamble and westwards thrusting of the Kongsberg onto Telemarkia and reworking of plutons emplaced shortly before the foundering process (Henderson and Ihlen, 2004; Scheiber et al., 2015). Exhumation of the Bamble and Kongsberg lithotectonic units after 1105 Ma was associated with fluid-rock interaction, albitization and scapolitization (Engvik et al., 2017). Erosion provided the clastic material stored in the Heddal Group and Eidsborg Formation in Telemarkia (Fig. 6; Fig. 11; Fig. 12; Fig. 18).

The plate tectonic context and paleogeographic setting of this pre- to early-Sveconorwegian asthenosphere upwelling, plateau development and sub-continental lithospheric mantle delamination model is difficult to assess. The asthenosphere upwelling

could be related to a deep mantle plume, similar to the ones that generated the four mafic dyke swarms of the Central Scandinavian dolerites in the cratonic center of Fennoscandia between c. 1271 and 1246 Ma (Brander et al., 2011; Söderlund et al., 2006), and dolerites along the Sveconorwegian front (Protogine zone dolerites) between 1221 and 1215 Ma (Söderlund et al., 2005) (Fig. 17). Alternatively, in recent paleogeographic models (Cawood and Pisarevsky, 2017), the Sveconorwegian orogen (Telemarkia–Bamble–Kongsberg lithotectonic units) is located in a continent back-arc position on the Fennoscandia side of an active volcanic arc, in the 1280–1080 Ma interval, during consumption of the oceans between Baltica, Amazonia and Laurentia (Fig. 17; Fig. 18) (Bingen et al., 2003; Brewer et al., 2002; Roberts and Slagstad, 2015; Slagstad et al., 2017; Spencer et al., 2014). This arc would be located to the west of the exposed orogenic belt and possibly disappeared by tectonic erosion (Spencer et al., 2014). A Cenozoic analogue to this Mesoproterozoic evolution would be plateau building and lithospheric delamination in the Colorado Plateau and the North American Cordillera (Bao et al., 2014; Levander et al., 2011).

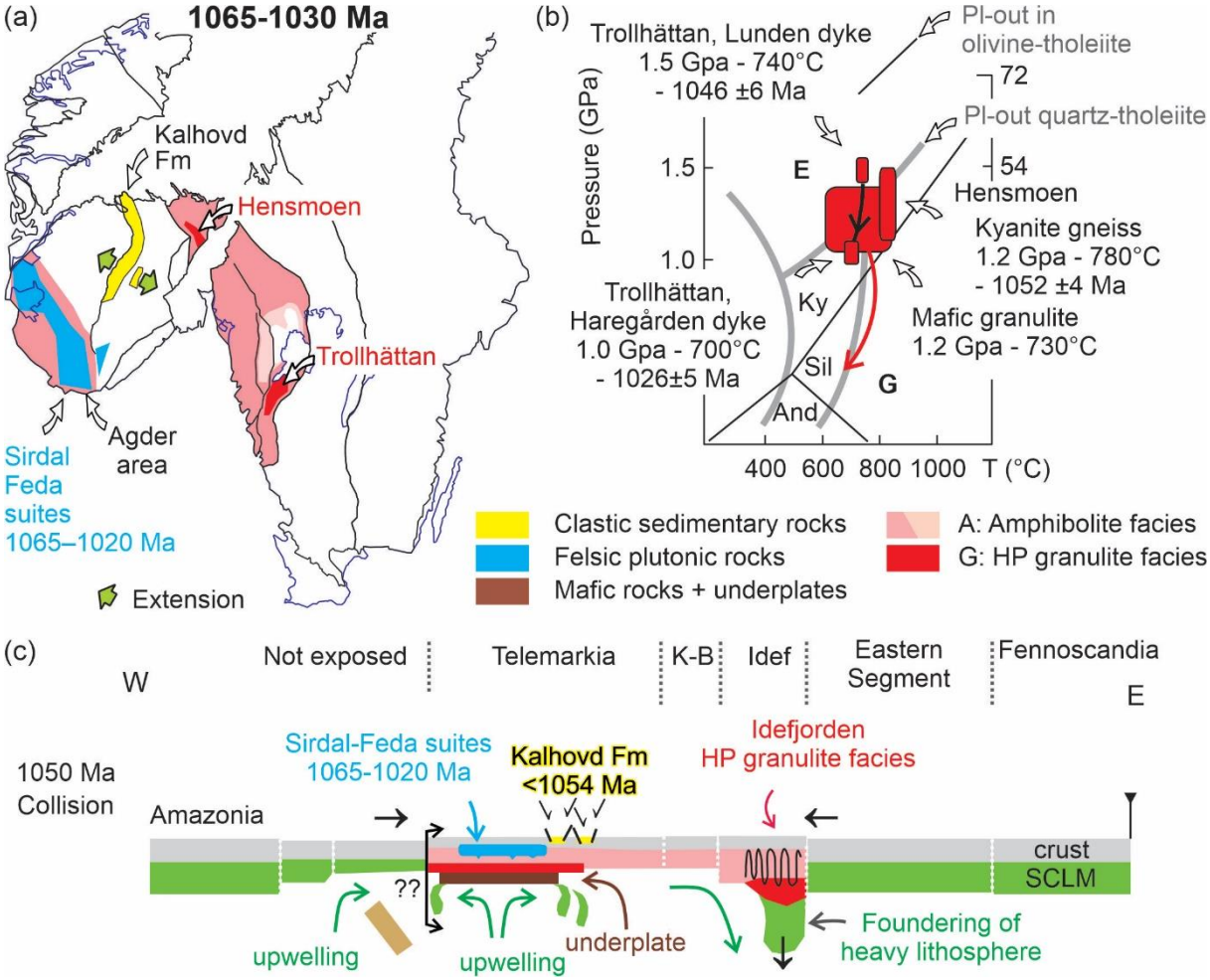

Figure 19. Schematic geodynamic model for the 1065–1030 Ma time interval. (a) Sketch map of the Sveconorwegian orogen, with distribution of metamorphism, magmatism and clastic sediment basins. (b) Pressure-temperature diagram. (c) Interpretative E-W cross section. Explanations and references in the text.

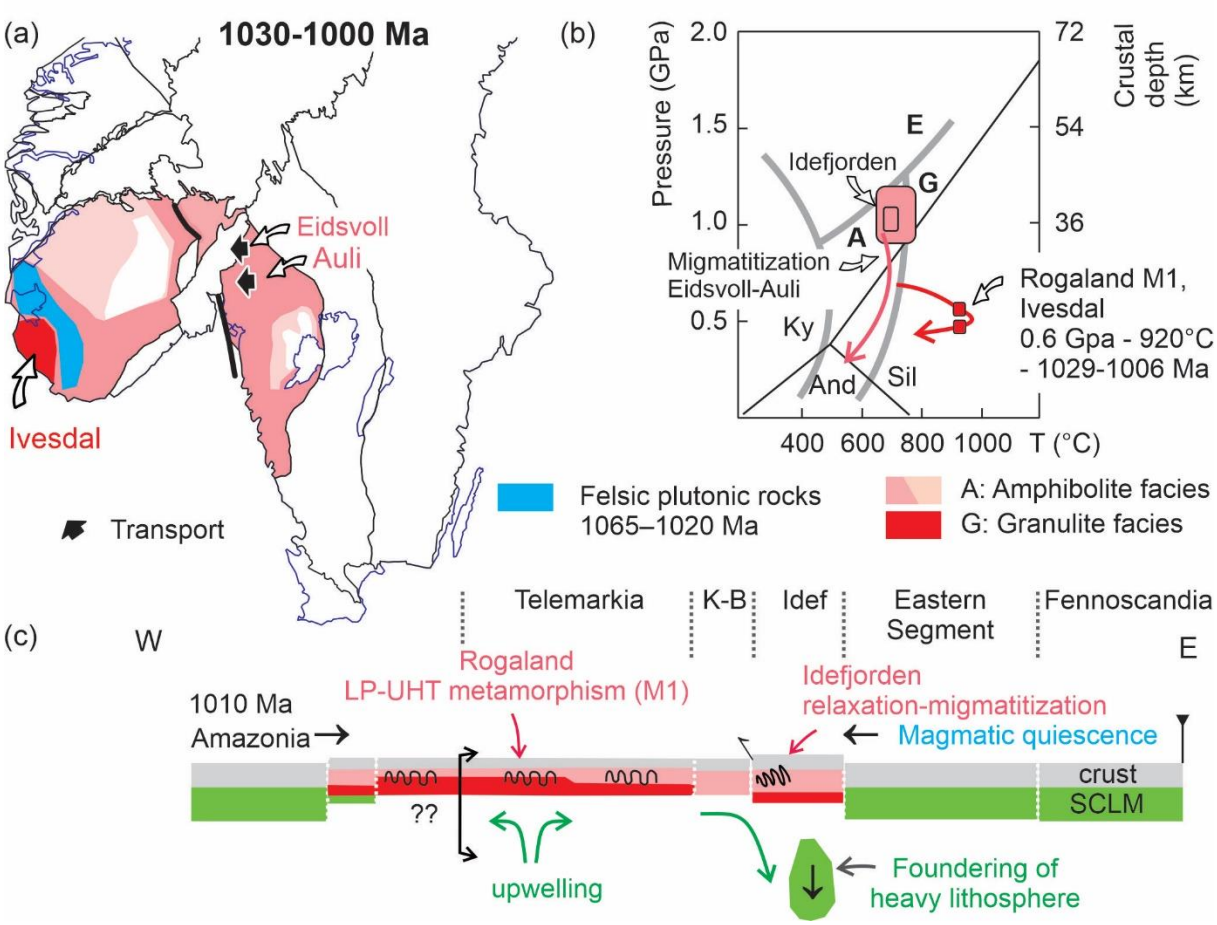

Figure 20. Schematic geodynamic model for the 1030–1000 Ma interval. (a) Sketch map of the Sveconorwegian orogen, with distribution of metamorphism and magmatism. (b) Pressure-temperature diagram. (c) Interpretative E-W cross section. Explanations and references in the text.

6.2 1065–1000 Ma: main Sveconorwegian continental collision

After a period of quiescence, the orogenic zone grew substantially around 1065 Ma, both eastwards (continentwards) and westwards, to include the entire Idefjorden and Telemarkia lithotectonic units (Fig. 19; Fig. 20). Widespread compressional deformation, high-grade metamorphism, partial melting and magmatism are recorded in these units between 1065 and 1000 Ma (Agder phase). Little is recorded in the Kongsberg–Bamble lithotectonic units, which were exhumed to high crustal levels (superstructure) and juxtaposed as reflected by

their current position before 1080 Ma. High-pressure granulite facies metamorphism in the Idefjorden lithotectonic unit, dated to c. 1050 Ma, contrasts with the voluminous granite magmatism of the Sirdal magmatic belt (1065–1020 Ma) and low-pressure granulite-facies metamorphism (1045–990 Ma) culminating at UHT conditions (1030–1005 Ma) in the west of the Telemarkia lithotectonic unit (Fig. 5; Fig. 19; Fig. 20). The width of the orogenic zone (minimum of 460 km), the large volume of magmatism with syn- to late-collision geochemical signature (Sirdal magmatic belt), the paired belts of high-pressure (towards the foreland) vs. high-temperature (towards the hinterland) metamorphism, and the structural evidence for convergence suggests that the Sveconorwegian orogeny entered the main phase of continent-continent collision around 1065 Ma.

In Fig. 19, we propose that collision resulted in the formation of a Tibetan-style orogenic plateau (Jamieson and Beaumont, 2013) extending from the Telemarkia to the Idefjorden lithotectonic units. The infrastructure of this orogenic plateau is defined by widespread gneiss complexes characterized by partial melting, compressive ductile deformation and amphibolite- to granulite-facies metamorphism between 1050 and 1000 Ma. Evidence from the superstructure of this plateau is scanty, simply because little upper crustal rocks younger than 1050 Ma are preserved. The N–S trending Kalhovd Formation consists of unconformable conglomerate and immature sandstone, deposited after c. 1054 Ma, in a continental (above sea level) intermontane basin (Fig. 5; Fig. 11; Fig. 19; Fig. 20). This basin was downfaulted along the Mandal-Ustaoset fault zone, possibly during deposition, recording extension after c. 1054 Ma in the upper crust in the centre of the Telemarkia lithotectonic unit.

Dynamic of the mantle in the collision zone would be simulated by a “pro-plate” (upper-plate) Tibetan-style delamination numerical models by Li et al. (2016). In Fig. 19, we propose that mantle upwelling under the Telemarkia lithotectonic unit was counterbalanced by mantle downwelling and lithospheric mantle delamination and foundering under the Idefjorden

lithotectonic unit. In the Idefjorden lithotectonic unit, the crust was pulled down by a lithospheric mantle slab to reach peak high-pressure low-temperature granulite facies conditions (c. 1.2–1.5 GPa, 740–780 °C) between c. 1052 and 1046 Ma (Fig. 19) (Bingen et al., 2008b; Söderlund et al., 2008a). The crust in the Idefjorden lithotectonic unit was not affected by orogenic processes before 1050 Ma and therefore could reach high-pressure conditions before melting. Decoupling between the mantle slab and the crust (breakoff) probably took place when partial melting reactions were activated in the lower crust. During exhumation, widespread migmatitization (including muscovite-, biotite- and amphibole-dehydration melting) is observed at regional scale between c. 1040 and 1000 Ma in the Idefjorden lithotectonic unit (Fig. 10; Fig. 20; Table 2). Migmatitization took place in convergent setting; east of the Oslo rift, it is associated with a well-defined top-to-west direction of transport (Viola et al., 2011). Lamprophyre dykes, close to the boundary between the Kongsberg and Idefjorden lithotectonic units, attests to local melting of lithospheric mantle material at c. 1030 Ma (Bingen and Viola, 2018), and is consistent with a model of foundering of the lithospheric mantle around 1030 Ma.

In the Telemarkia lithotectonic unit (Agder area), the NNW-SSE trending Sirdal magmatic belt attests to voluminous crustal melting between c. 1065 and 1020 Ma (Fig. 5; Fig. 19) (Bingen et al., 2015; Coint et al., 2015; Granseth et al., 2020; Slagstad et al., 2013). As discussed earlier, it contains high-K calc-alkaline quartz-monzonite–granodiorite plutons associated with minor ultrapotassic rocks (Fig. 7; Fig. 15) (Bingen et al., 1993; Bingen and van Breemen, 1998a). Such calc-alkaline granitoids can be derived by partial melting of lower crustal mafic metaigneous rocks. Enrichment in K and other large ion lithophile elements (LILE) implies either that this crustal source was previously enriched in LILE or that the melts were mixed with ultrapotassic lamprophyric melts, themselves generated from lithospheric mantle previously enriched in LILE. The most straightforward interpretation is

that this lithospheric mantle source was part of a mantle wedge enriched in LILE by supra-subduction fluids between 1520 and 1480 Ma. It would then become part of a subcontinental lithospheric mantle after 1480 Ma, and finally, it would melt during collision between 1065 and 1020 Ma, heated during orogeny. Two observations support this three stage model: i) the 1065–1020 Ma Sirdal magmatic belt overlaps geographically with the 1520-1480 Ma Suldal magmatic arc (Roberts et al., 2013); ii) the near-chondritic Nd isotopic signature of the Feda suite granitoids ($-1 < \varepsilon_{Nd} < +1.5$) and ultrapotassic enclaves ($+1 < \varepsilon_{Nd} < +1.5$) are lying on the evolution vector of the crust generated at 1520-1480 Ma (Fig. 13 a). A similar interpretation is provided for near-coeval (1063 ± 3 Ma) high-Sr-Ba quartz-monzonite plutons in the Quebecia lithotectonic unit of the Grenville orogen (Michaud pluton hosted in the c. 1500 Ma Escumins supracrustal rocks)(Groulier et al., 2018a).

Voluminous melting of the crust clearly requires an appropriate heat source. The high-alumina orthopyroxene megacrysts (HAOM) and plagioclase megacrysts hosted in the c. 930 Ma anorthosite plutons constrain mafic magmatism at the base of the crust at 1041 ± 17 Ma coeval with formation of the Sirdal magmatic belt (Bybee et al., 2014; Slagstad et al., 2018; Vander Auwera et al., 2014b). The supra-chondritic Nd isotopic values for the megacrysts ($+2.8 < \varepsilon_{Nd(1041\ Ma)} < +5.3$) trace the source of this magmatism to the asthenosphere (Fig. 13 a). Here we suggest that upwelling of hot asthenosphere in the collision zone generated asthenospheric melts, produced underplates (with HAOM), reheated and destabilized the lithospheric mantle, and generated minor lamprophyre melts (from this lithospheric mantle) (Fig. 19; Fig. 20). Heating of the crust produced granitoids of the Sirdal magmatic belt. After extraction of these melts, protracted heating in the crust resulted in a first phase of granulite-facies metamorphism (M1), reaching ultra-high temperature conditions (0.7–0.5 GPa, 900–950 °C) between 1030 and 1005 Ma (Fig. 20) (Blereau et al., 2017; Drüppel et al., 2013; Laurent et al., 2018b).

The HAOM hosted in the anorthosites record a pressure of crystallization of 1.1 GPa and an age of 1041 ± 17 Ma (Bybee et al., 2014; Charlier et al., 2010). These numbers imply a crustal thickness of at least 42 km around 1040 Ma, corresponding to a moderate crustal overthickening relative to the standard 30 km. The regional folding observed at various scales in the Telemarkia lithotectonic unit, also requires at least one phase of compression between 1030 and 1000 Ma.

In Fig. 17 to Fig. 20, the Oaxaquia and inliers of in the Andes of Columbia, which contain evidence of high-grade metamorphism between 1050 and 980 Ma, are represented speculatively as volcanic arcs in the ocean between, Amazonia Laurentia and Baltica (Fig. 8, Fig. 12; Fig. 13; Fig. 16). They were first accreted to Amazonia (Putumayo) before colliding with Baltica around 1050 Ma (Fig. 19; Fig. 20) (Ibanez-Mejia et al., 2011; Lawlor et al., 1999; Weber et al., 2010). In this framework, the Telemarkia–Kongsberg–Bamble units are indeed situated in a back-arc domain, in the time interval between 1280 and 1080 Ma, before closure of all oceans, and they ended-up in upper plate position at c. 1065 Ma during collision with Amazonia (Fig. 18; Fig. 19; Fig. 20). Upwelling of hot asthenosphere in the collision zone was possibly promoted by break-off all oceanic lithospheric plates to the west of the orogen when subductions ceased (Fig. 19).

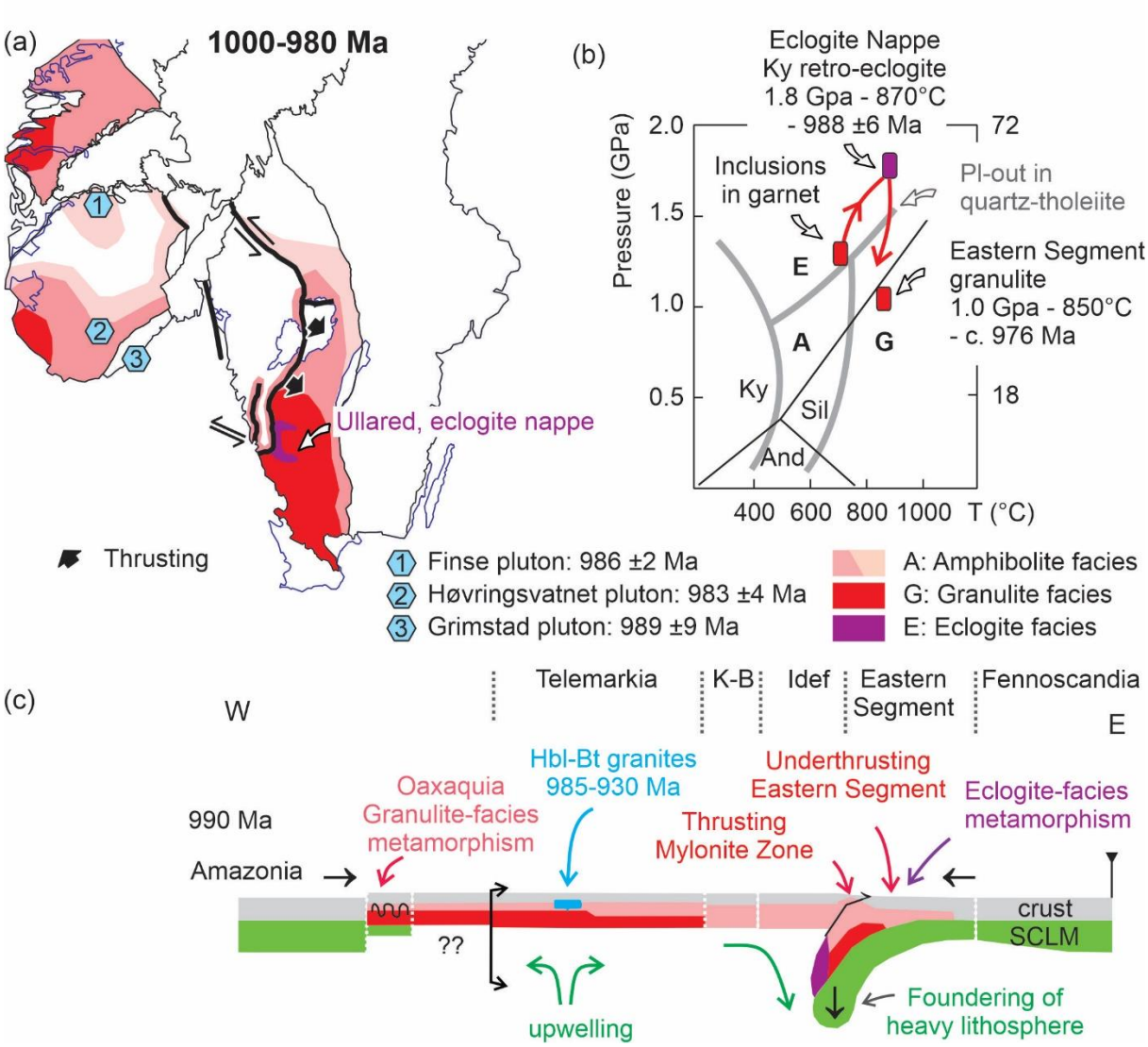

Figure 21. Schematic geodynamic model for the 1000–980 Ma time interval. (a) Sketch map of the Sveconorwegian orogen, with distribution of metamorphism and magmatism. (b) Pressure-temperature diagram. (c) Interpretative E-W cross section. Explanations and references in the text.

6.3 1000–920 Ma: long-duration growth of the collision zone

At c. 1000 Ma, orogeny propagated to the east, all the way into the Eastern Segment. Continued high-temperature low-pressure metamorphism in the west of the collision zone and voluminous magmatism contrast with high pressure metamorphism in the east, suggesting that

the western part was characterized by protracted mantle upwelling while the eastern part by underthrusting and mantle downwelling. In Fig. 21, Fig. 22 and Fig. 23, we propose that the Tibetan-style orogenic plateau grew towards the foreland to includes the Eastern Segment and covered the entire orogen. The Eastern Segment offers a nice example of how crust underthrust to high-pressure conditions is incorporated into a melt-lubricated middle-crustal infrastructure of an orogenic plateau. We suggest that the orogenic plateau was sustained to c. 930 Ma before it collapsed.

6.3.1 Eastward growth of orogenic plateau

The Eastern Segment was a cold lithospheric segment of Fennoscandia foreland affinity, unaffected by Sveconorwegian orogenic processes before 1000 Ma. At this point in time, it was underthrust as a slab towards the west beneath the Mylonite Zone during convergence (Fig. 21) (Möller and Andersson, 2018; Möller et al., 2015). The deepest underthrust western part of the slab reached eclogite-facies conditions corresponding to a depth of c. 70 km (1.65–1.9 GPa, 850–900°C) at c. 990 Ma (Fig. 5; Fig. 21 b), while the adjacent part of the slab (now the internal section) reached high-pressure granulite-facies conditions (1.1 GPa, 850°C; Fig. 21 b) (Möller et al., 2015; Piñán-Llamas et al., 2015; Tual et al., 2017). Preservation of prograde zoning in garnet in eclogites attests to faster-than-equilibration prograde metamorphism (Möller, 1998; Tual et al., 2017). In Fig. 21, we propose that this underthrust crustal slab was pulled down by foundering of the dense subcontinental lithospheric mantle. Breakoff of the lithospheric mantle slab triggered exhumation after c. 980 Ma (Fig. 22). Exhumation took place in two steps (Fig. 22). During the first step, the eclogitized westernmost part of the Eastern Segment was detached from the deepest part of the segment and exhumed with an overall eastward vergence, as a single and coherent (eclogite-bearing) ductile nappe to an intermediate depth of c. 35–40 km (1.1 GPa), where it was juxtaposed to the granulite-facies internal section. This process is interpreted as eastwards extrusion during

overall E-W convergence (Möller and Andersson, 2018; Möller et al., 2015; Piñán-Llamas et al., 2015; Tual et al., 2015). During the second step, the eclogite-bearing nappe and the granulite-facies internal section were exhumed together, also with an overall eastwards vergence. Accurate geochronology of these two steps remains difficult to establish. Breakoff of the lithospheric mantle slab was probably facilitated by partial melting in the crust. East vergent exhumation was clearly lubricated by abundant partial melting. The crystallization of these leucosome melts is dated between c. 978 and 961 Ma inside the eclogite-bearing nappe (Andersson et al., 2002a; Möller et al., 2015) and between c. 976 and 965 Ma, i.e. in a coeval time interval, in the granulite-facies internal section (Andersson et al., 2002a; Hansen et al., 2015; Möller et al., 2007; Piñán-Llamas et al., 2015; Söderlund et al., 2002).

The Blekinge-Dalarna dolerite dyke swarm intruded in the upper crust in the foreland of the orogen between c. 978 and 946 Ma (Gong et al., 2018; Ripa and Stephens, 2020d; Söderlund et al., 2005). This mafic magmatism is characterized by a within-plate geochemical signature and supra-chondritic Hf isotopic signature ($+1 < \varepsilon_{Hf} < +5$). It is evidence for asthenosphere upwelling and decompression melting under the cratonic lithosphere of the foreland (Gong et al., 2018; Ripa and Stephens, 2020d; Söderlund et al., 2005). The upwelling may represent a dynamic response in the asthenosphere of the breakoff and foundering of the lithospheric mantle slab under the Eastern Segment at and after c. 980 Ma (Fig. 22).

Eastwards thrusting in the frontal wedge and along the Sveconorwegian front represents a final spasm of the orogeny. Both $^{40}Ar/^{39}Ar$ data and the observation that Blekinge-Dalarna dolerite dykes are sheared in the frontal wedge suggest that it took place after c. 945 Ma (Andréasson and Dallmeyer, 1995; Page et al., 1996a; Stephens and Wahlgren, 2020a; Ulmius et al., 2018).

6.3.2 Sustained orogenic plateau west of the Mylonite Zone

Little tectonic activity or metamorphism is dated in the central part of the orogen (western part of the Idefjorden lithotectonic unit, Kongsberg and Bamble lithotectonic units and eastern part of the Telemarkia lithotectonic unit) between c. 980 and 930 Ma, suggesting that this part of the orogen behaved passively during this time interval. In the west, in the orthopyroxene zone of Rogaland, a scatter of zircon rim U–Pb ages between 1045 and 955 Ma is interpreted as evidence for protracted high-grade metamorphism with melt-present conditions in the middle crust (0.45–0.55 GPa) (Fig. 22) (Blereau et al., 2017; Laurent et al., 2018a; Slagstad et al., 2018). In Fig. 22, we propose that the orogenic plateau formed between 1050 and 1000 Ma west of the Mylonite Zone was sustained throughout the orogeny to c. 930 Ma.

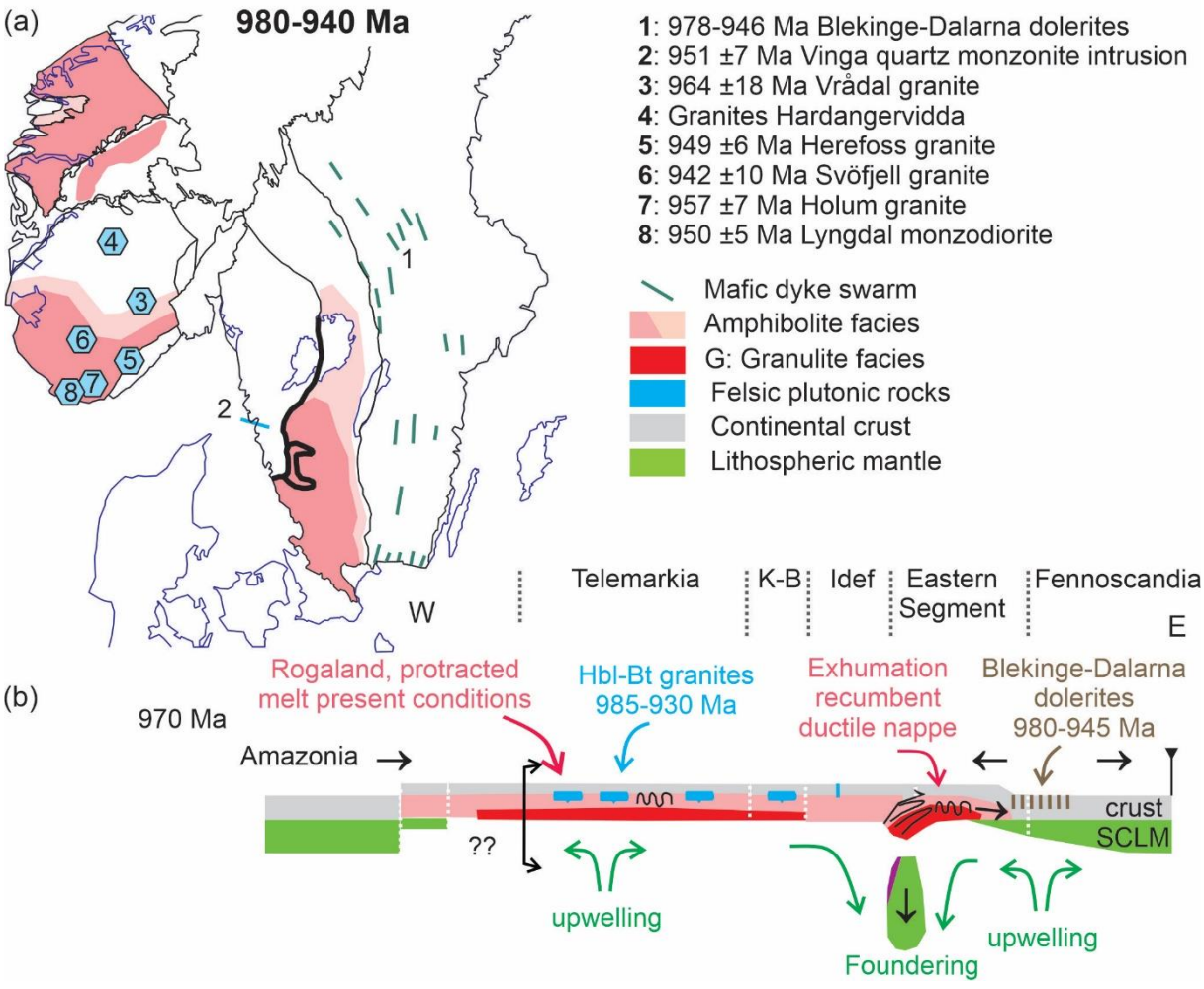

Figure 22. Schematic geodynamic model for the 980–940 Ma time interval. (a) Sketch map of the Sveconorwegian orogen, with distribution of metamorphism and magmatism. (b) Interpretative E-W cross section. WGR: Western Gneiss Region. Explanations and references in the text.

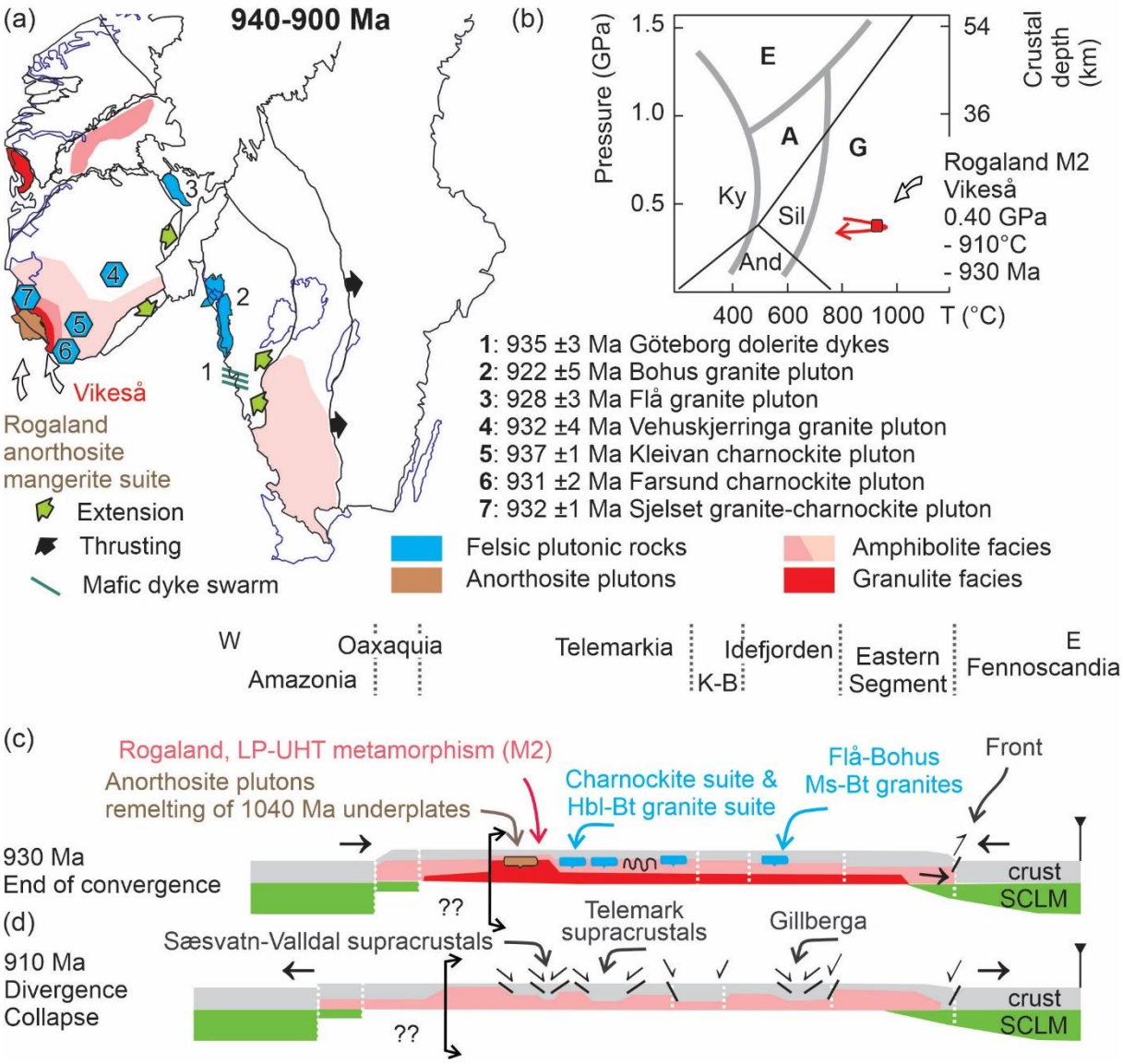

Figure 23. Geodynamic model for the 940–900 Ma time interval. (a) Sketch map of the Sveconorwegian orogen, with distribution of metamorphism and magmatism. (b) Pressure-temperature diagram. (c, d) Interpretative E-W cross sections. Explanations and references in the text.

6.3.3 Late-Sveconorwegian magmatism and associated metamorphism

The volume of late-Sveconorwegian magmatism increases dramatically westwards in the orogen (Fig. 5; Fig. 7; Fig. 22; Fig. 23). In the Eastern Segment, minor pegmatite and granite bodies formed between c. 961 and 935 Ma during regional cooling (Möller et al., 2007; Söderlund et al., 2008b). In the Idefjorden lithotectonic unit, the large biotite + muscovite-bearing Flå and Bohus granite plutons (c. 932–922 Ma) (Eliasson et al., 2003; Eliasson and Schöberg, 1991; Lamminen et al., 2011) carry a distinctly peraluminous signature (S-type) and sub-chondritic epsilon Nd values ($-8.4 < \varepsilon_{Ndi} < -2.7$) (Andersen et al., 2001). These properties imply a metasedimentary source, most probably in the hosting Stora Le-Marstrand complex ($-8.0 < \varepsilon_{Nd930} < -3.0$) (Åhäll and Daly, 1989). In the Telemarkia lithotectonic unit, large plutons of the HBG granite suite emplaced between c. 985 and 926 Ma (Fig. 22; Fig. 23). There is a significant spread in geochemical and isotopic composition, reflecting a diversity of sources and petrogenesis (Andersen et al., 2001; Granseth et al., 2020; Vander Auwera et al., 2011). The HBG suite is characterized by a distinctly ferroan geochemical signature (Fig. 14). Experimental petrology and geochemical modelling of the representative Lyngdal pluton in Vest Agder (Bogaerts et al., 2006; Vander Auwera et al., 2008), suggest that this granodiorite crystallized at shallow conditions corresponding to pressures between 0.2 and 0.4 GPa from a wet (5–6 wt% H_2O), oxydized (QFM +1) and hot (c. 975 °C) magma. This magma can be generated by partial melting of an amphibole-rich mafic source (with c. 1.5 wt% H_2O). The near-chondritic to sub-chondritic Nd isotopic signature of the HBG plutons ($-6.4 < \varepsilon_{Ndi} < +1.9$, n = 7; $-2.0 < \varepsilon_{Hfi} < +1.7$, n = 10) overlaps with the evolution trend of the crust generated at 1520-1480 Ma (Fig. 8; Fig. 13). This implies sources isotopically similar to those of the Sirdal magmatic belt. However, the geographical overlap between the

HBG suite and the Sirdal magmatic belt suggests that more refractory lower crustal sources were exploited at higher temperature after 985 Ma for the HBG suite (Granseth et al., 2020; Vander Auwera et al., 2008).

To the west of the Sirdal magmatic belt, the AMC suite formed between 932 and 915 Ma in a crust previously metamorphosed to granulite conditions (1030–1005 Ma). The AMC suite is ferroan and alkalic (Fig. 14). Constraints from experimental petrology indicate that the high alumina basalt parental to the anorthosite plutons is characterized by a too low Mg# (molar Mg/(Mg+Fe) = 0.52) and crystallizes too sodic plagioclase (An55) to be generated by melting of a mantle peridotite (HLCA and TJ compositions; Duchesne et al., 1999; Longhi, 2005; Longhi et al., 1999). Instead, its composition is situated on the thermal divide of the plagioclase + pyroxene liquidus surface at 1.0 to 1.3 GPa, imposing that it was produced by partial melting of a gabbronoritic source (Longhi, 2005; Longhi et al., 1999). Experiments show that compositionally adequate melts in equilibrium with plagioclase and orthopyroxene are found in a temperature range between c. 1180 and 1250 °C at c. 1.1 GPa (Fram and Longhi, 1992; Longhi et al., 1999; Vander Auwera and Longhi, 1994). The Sm–Nd isochron of 1041 ± 17 Ma defined by the high-aluminium orthopyroxene megacrysts (HAOM) hosted in the anorthosite plutons (Bybee et al., 2014) suggests that these megacrysts are restitic crystals from a lower crustal source (Vander Auwera et al., 2014b). The isochron implies that the gabbronoritic source formed at c. 1040 Ma as an underplate (1.1 GPa) and was remelted at c. 930 Ma to form the parental magmas of the AMC suite (Vander Auwera et al., 2014b). Isotopically, this two stage model is realistic, with overlapping positive epsilon Nd values for the megacrysts ($+3.1 < \varepsilon_{Nd(930\ Ma)} < +5.9$) and mafic rocks in the AMC suite ($\varepsilon_{Nd(930\ Ma)} < +5.8$) (Fig. 13). However, the wide range of Nd isotopic composition of differentiated rocks in the AMC suite ($-2.8 < \varepsilon_{Nd(930\ Ma)} < +5.8$), implies a variety of lower crustal sources and crustal contaminants in the suite, all of them characterized by low water content (Barling et al., 2000;

Duchesne and Wilmart, 1997). This two-stage model requires that hot asthenosphere was upwelling just under the crust around 930 Ma in order to extensively remelt (high degree of partial melting) gabbronoritic layers of the 1040 Ma underplate. Heat transfer from the mantle and the anorthosite plutons to the crust resulted in a second phase of ultra-high temperature granulite-facies metamorphism (M2; 0.35–0.5 GPa, 900–950 °C, c. 930 Ma) (Laurent et al., 2018b). Using a conservative geothermal gradient of 20 °C/km, extrapolation of a 900 °C temperature at 0.4 GPa (15 km depth; M2) to the base of the crust at 1.1 GPa (41.5 km depth) indeed yield a temperature of 1420 °C, compatible with the presence of asthenosphere at the base of the crust at c. 930 Ma.

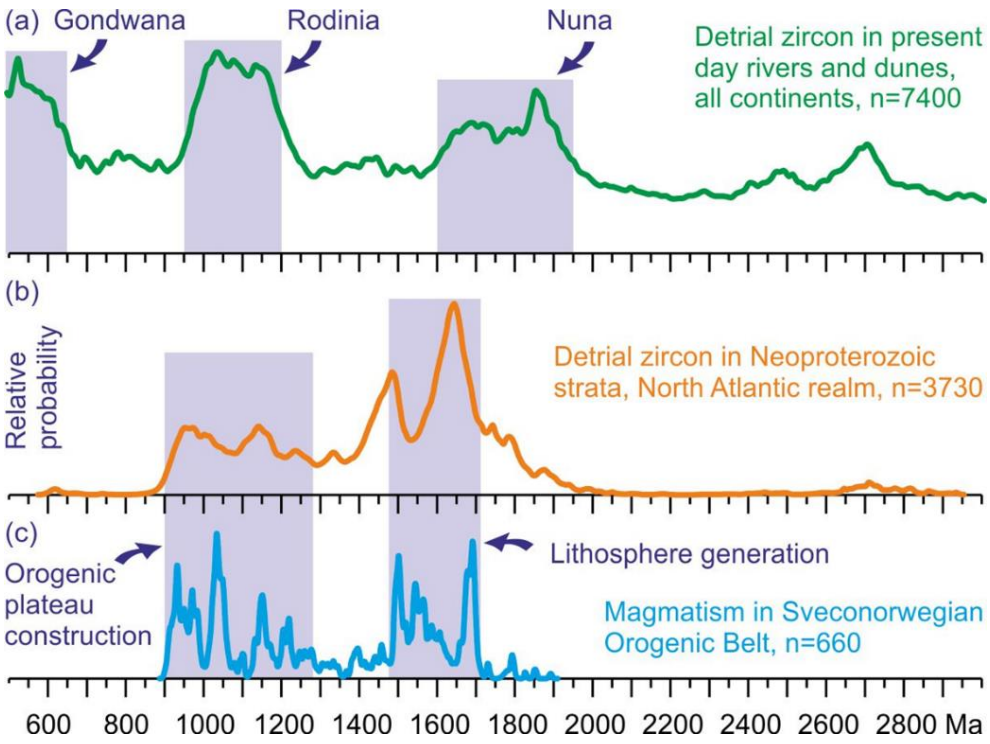

Figure 24. Erosion of the Sveconorwegian orogen. (a) Relative probability diagrams of detrital zircons in present day river sediments and dunes. Peaks in this distribution are attributed to formation of supercontinents Nuna, Rodinia and Gondwana. Compilation of Campbell and Allen (2008). (b) Relative probability diagrams of detrital zircons in Neoproterozoic clastic sediments in the North Atlantic realm, deposited in marine and

continental environment mainly during the Tonian and Cryogenian. The compilation includes 3730 detrital zircons from the Moine Supergroup in Scotland (Kirkland et al., 2008b), Caledonian Lower and Middle Allochthons in Norway and Sweden (Be'eri-Shlevin et al., 2011; Bingen et al., 2011; Gee et al., 2015; Kirkland et al., 2007, 2008a; Lamminen et al., 2015; Zhang et al., 2015, 2016), Timanides in N Norway (Zhang et al., 2015), Northwestern terrane in Svalbard (Pettersson et al., 2009) and Eleonore Bay Supergroup in E Greenland (Sláma et al., 2011). Only analyses with discordance < 5% are selected; the $^{206}Pb/^{238}U$ age is selected for zircon younger than 1500 Ma and the $^{206}Pb/^{207}Pb$ age for older zircons. (c) Relative probability diagram for magmatic events in the entire Sveconorwegian orogen. The time intervals for continental lithosphere generation and orogenic plateau development are highlighted. The similitude in the age distribution between magmatic events in the Sveconorwegian orogen and the Neoproterozoic strata argues for sourcing in the Sveconorwegian orogen for these sediments and important transport of detritus northwards and westwards.

6.4 Post 920 Ma: late- to post-Sveconorwegian collapse and sedimentation

The orogenic plateau developed during the Sveconorwegian orogeny (Fig. 17 to Fig. 23) could not be sustained when convergence came to a halt sometime after c. 930 Ma, and it collapsed. As noted earlier, syn- to late-Sveconorwegian plutons (1066–920 Ma) exposed today define a rather uniform depth of intrusion of c. 16 km (0.4–0.5 GPa, Table 1) (Charlier et al., 2010; Coint et al., 2015; Eliasson et al., 2003; Vander Auwera et al., 2014a; Vander Auwera and Longhi, 1994). Removal of this c. 16 km thick overburden took place by a combination of late- to post-Sveconorwegian erosion and extensional tectonics.

Mapping and characterization of extensional shear zones that could explain exhumation of amphibolite-facies gneiss complexes (infrastructure of the orogenic plateau) relative to low-

grade supracrustal rocks (superstructure) are still in their infancy (Persson-Nilsson and Lundqvist, 2014; Torgersen et al., 2018; Viola et al., 2011). Extensional reactivation of the main shear zones in the orogen, including the Sveconorwegian Front, the Mylonite Zone and the Bamble-Telemarkia boundary zone, are documented between c. 930 and 860 Ma by muscovite and biotite $^{40}Ar/^{39}Ar$ data (Andréasson and Dallmeyer, 1995; Mulch et al., 2005; Page et al., 1996b; Viola et al., 2011). Extension was associated with regional cooling, as documented by regional scale titanite U–Pb and amphibole, muscovite and biotite $^{40}Ar/^{39}Ar$ data (Bingen et al., 1998; Connelly et al., 1996; Johansson et al., 2001; Page et al., 1996a; Page et al., 1996b; Söderlund et al., 1999; Ulmius et al., 2018; Verschure et al., 1980; Wang et al., 1998).

Pegmatite bodies represent the youngest magmatism of regional significance in the orogen between c. 914 and 900 Ma (Hetherington and Harlov, 2008; Müller et al., 2015; Müller et al., 2017; Pasteels et al., 1979; Scherer et al., 2001; Seydoux-Guillaume et al., 2012). Pegmatites are locally abundant in the gneiss complexes of the Telemarkia and Idefjorden lithotectonic units. In the Telemarkia lithotectonic unit, they formed shortly after the regional scale titanite U–Pb age of c. 918 Ma, interpreted to record regional cooling below c. 600 °C. The pegmatites are not genetically related to any exposed granite pluton and therefore they represent small individual batches of fluid-rich melt sourced locally in the gneiss complexes (Müller et al., 2015; Müller et al., 2017). Their relation to the extensional collapse of the orogen and the source(s) of fluids necessary to generate the fluid-rich melts remain enigmatic.

Absence of widespread late-Sveconorwegian sedimentation inside the orogen is suggested by a lack of post-Sveconorwegian sedimentary cover below the sub-Cambrian peneplain in southern Norway and Sweden (Gabrielsen et al., 2015). The Neoproterozoic Visingsö Group deposited between c. 885 and 740 Ma along the Sveconorwegian Front is directly and unconformably overlying Paleoproterozoic basement (Loron and Moczydłowska, 2018;

Moczydłowska et al., 2018; Pulsipher and Dehler, 2019). These observations suggest that the Sveconorwegian orogen was erodible, i.e. above sea level, at the end of the Sveconorwegian orogeny.

The rock record supportive for clastic transport towards the Fennoscandia foreland is only local (Almesåkra Group) (Ripa and Stephens, 2020d). However, thermochronological data suggest heating of the foreland up to c. 220 °C some 150 km east of the Sveconorwegian Front between 944 Ma and 851 Ma, which corresponds to burial of the present day surface to c. 7 km (Guenthner et al., 2017). Clastic transport towards the north and west of the Sveconorwegian orogen is, instead, quite well established, as Neoproterozoic continental and marine sediments abound in Caledonian parautochthons and allochthons, Svalbard, and the Timanides (Nystuen et al., 2008). These sediment sequences contain detrital zircons with age between 1700 and 1500 Ma and 1280 and 900 Ma (Bingen et al., 2011; Gee et al., 2015; Kirkland et al., 2007; Kirkland et al., 2008b; Pettersson et al., 2009; Sláma et al., 2011; Strachan et al., 1995; Strachan et al., 2013; Zhang et al., 2015). These sequences can be, at least partly, sourced directly from within the Sveconorwegian orogen (Fig. 24).

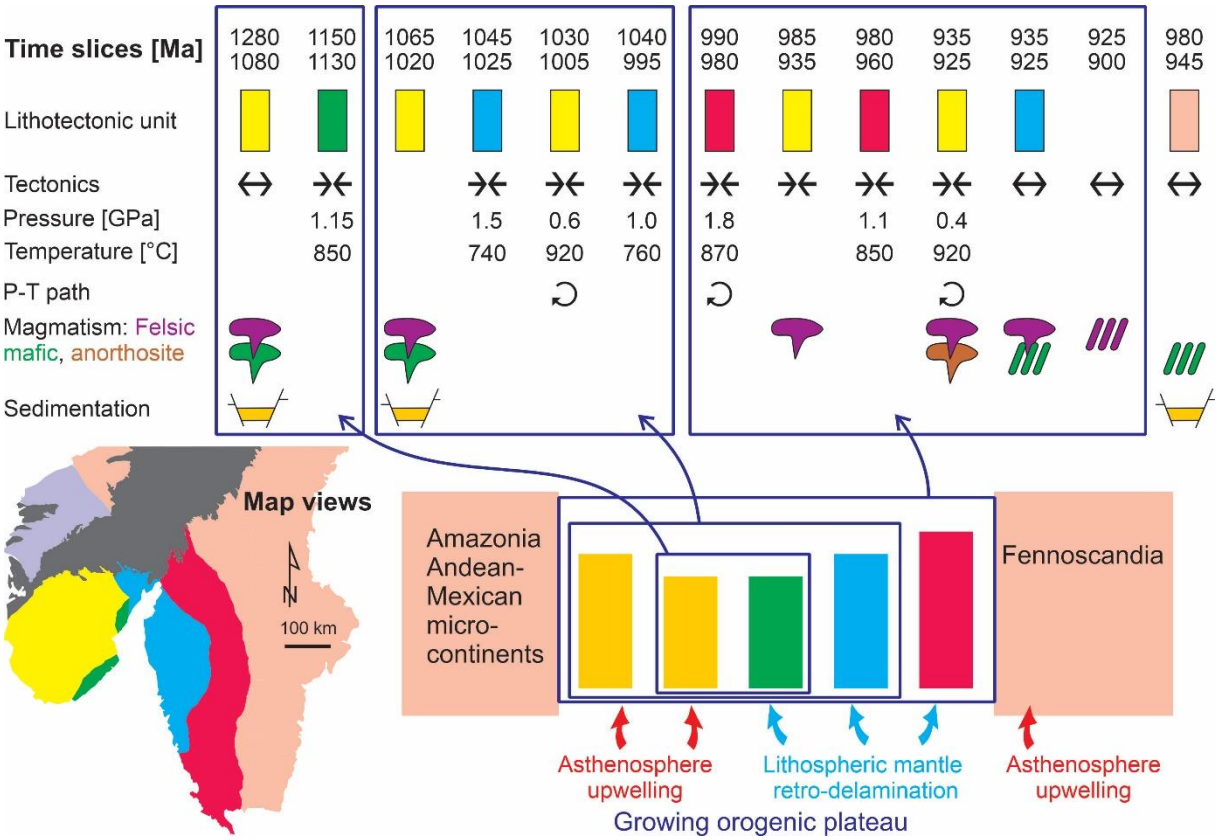

Figure 25. Summary matrix of Sveconorwegian orogeny. The first line provides the time slices of events. Line 2 represents the lithotectonic units colour coded following the inset map at the bottom. Line 3 (Tectonics) indicates if the tectonic regime is compressional or extensional in the specific time interval and geographic location. Note that for the time interval between 1280 and 1080 Ma, the tectonic regime is extensional in Telemarkia while it is compressional in the Bamble and Kongsberg Lithotectonic Units. Lines 4-5 (Pressure-Temperature) provides the conditions of peak metamorphism and line 6 (P-T path) indicates where this metamorphism follows a clockwise P-T path. Line 7 (magmatism) records plutonic events, with color coding for felsic (purple), mafic (green) or anorthosite (brown). Line 9 records known sedimentation in intermontane basins or foreland basins. The bottom-right figure is a interpretative transect in map view through the orogen between the Amazonia hinterland and Fennoscandia foreland, showing the three step growth of the orogenic plateau from the centre of the orogen. This three steps growth is associated with three steps of retro-delamination of the sub-continental lithospheric mantle (SCLM) towards the foreland, as

recorded by metamorphism with a high-pressure signature. The western part of the orogen is characterized by upwelling and shallow asthenosphere during the entire orogenic period. Explanations in the text.

---

7 Conclusions

Published models attempting to explain the tectonic evolution of the Sveconorwegian orogeny vary widely even with respect to their first-order features and boundary conditions. They range from end-members involving continental collision between Fennoscandia and another continent to accretion in the absence of collision (Fig. 3). This variation reflects the difficulty to translate the observed geological record and the analytical data into geodynamic processes in the Proterozoic.

Based on a review of data and concepts, we favour a model of large, hot and long-duration continental collision at the margin of Fennoscandia between c. 1065 and 920 Ma, as synthesized in Fig. 17 to Fig. 23, and by a matrix in Fig. 25. The plate tectonic setting of the pre-collision events, between 1280 and 1080 Ma, remains uncertain, although it was possibly a continental back arc setting (Fig. 17; Fig. 18). Although not strictly necessary, the model is adjusted into a classical Rodinia assembly framework, involving a Baltica–Laurentia–Amazonia collision (Fig. 1; Fig. 8, Fig. 12; Fig. 13; Fig. 16).

The width of the orogenic zone, the evidence for protracted and widespread crustal melting and high-temperature metamorphism reaching UHT conditions, the evidence for high pressure metamorphism recording crustal thickening, the growth of the orogenic zone towards the foreland, the juxtaposition of low-grade supracrustal rocks and high-grade gneiss complexes, and the lack of syn-orogenic marine sedimentary sequence, argue for a collisional orogeny. We suggest that an orogenic plateau started to form around 1280 Ma in the Telemarkia lithotectonic unit, first as a Cordillera-style (back-arc) orogenic plateau, and that it grew

stepwise both towards the hinterland and foreland, as a Tibetan-style (collisional) orogenic plateau. Shallow asthenosphere conditions were maintained in the western part of the orogenic belt at least up to c. 930 Ma, when the formation of anorthosite plutons took place by remelting of mafic underplates themselves formed at c. 1040 Ma. Formation of the orogenic plateau was paired with retro-delamination and foundering of the sub-continental lithospheric mantle. This process is recorded by compression and regional metamorphism with an increasingly higher pressure signature towards the foreland followed by exhumation. Three stages of lithosphere foundering are inferred, one at c. 1150–1120 Ma under the Bamble and Kongsberg Lithotectonic units, one at c. 1050 Ma under the Idefjorden lithotectonic unit and one at c. 990 Ma under the Eastern Segment. In the Eastern Segment, peak conditions reached eclogite facies conditions (1.8 GPa-870 °C) and exhumation of eclogite-bearing units was aided by extrusion of a ductile nappe lubricated by partial melting, within an overall compressional setting. The increasing peak pressure recorded in time and space reflects increasing mechanical coupling between the lower crust and colder lithospheric mantle, as the delamination process progressed toward the Fennoscandia craton.

After c. 930 Ma, convergence came to a halt, the orogenic plateau collapsed, and 16 km of overburden was removed by extension and erosion.

8 Declaration of interests

The authors declare that they have no known competing financial interests or personal relationships that could have appeared to influence the work reported in this paper.

9 Acknowledgements

The Geological Survey of Norway provided project time to perform this research. T. Horscroft and M. Santosh are thanked for handling this publication. Mike Stephens and Aphrodite Indares provided very constructive review of the manuscript.

10 References

Åhäll, K.I., Connelly, J.N., 1998. Intermittent 1.53-1.13 Ga magmatism in western Baltica; age constraints and correlations within a postulated supercontinent. Precambrian Research 92, 1-20.

Åhäll, K.I., Connelly, J.N., 2008. Long-term convergence along SW Fennoscandia: 330 m.y. of Proterozoic crustal growth. Precambrian Research 161, 452-474.

Åhäll, K.I., Cornell, D.H., Armstrong, R., 1998. Ion probe zircon dating of metasedimentary units across the Skagerrak: new constraints for early Mesoproterozoic growth of the Baltic Shield. Precambrian Research 87, 117-134.

Åhäll, K.I., Daly, J.S., 1989. Age, tectonic setting and provenance of Östfold-Marstrand Belt supracrustals: westward crustal growth of the Baltic Shield at 1760 Ma. Precambrian Research 45, 45-61.

Åhäll, K.I., Gower, C.F., 1997. The Gothian and Labradorian orogens: variations in accretionary tectonism along a late Paleoproterozoic Laurentia–Baltica margin. GFF 119, 181-191.

Åhäll, K.I., Larson, Å., 2000. Growth-related 1.85-1.55 Ga magmatism in the Baltic Shield; a review addressing the tectonic characteristics of Svecofennian, TIB 1 -related, and Gothian events. GFF 122, 193-206.

Åhäll, K.I., Samuelsson, L., Persson, P.O., 1997. Geochronology and stuctural setting of the 1.38 Ga Torpa granite; implications for charnockite formation in SW Sweden. Geologiska Föreningens i Stockholm Förhandlingar 119, 37-43.

Ahlin, S., Austin Hegardt, E., Cornell, D., 2006. Nature and stratigraphic position of the 1614 Ma Delsjön augen granite-gneiss in the Median Segment of south-west Sweden. GFF 128, 21-32.

2075 Andersen, T., 1997. Radiogenic isotope systematics of the Herefoss granite, South
2076 Norway: an indicator of Sveconorwegian (Grenvillian) crustal evolution in the Baltic shield.
2077 Chemical Geology 135, 139-158.
2078 Andersen, T., Andersson, U.B., Graham, S., Åberg, G., Simonsen, S.L., 2009. Granitic
2079 magmatism by melting of juvenile continental crust: new constraints on the source of
2080 Palaeoproterozoic granitoids in Fennoscandia from Hf isotopes in zircon. Journal of the
2081 Geological Society of London 166, 233-247.
2082 Andersen, T., Andresen, A., Sylvester, A.G., 2001. Nature and distribution of deep crustal
2083 reservoirs in the southwestern part of the Baltic Shield: evidence from Nd, Sr and Pb isotope
2084 data on late Sveconorwegian granites. Journal of the Geological Society of London 158, 253-
2085 267.
2086 Andersen, T., Andresen, A., Sylvester, A.G., 2002a. Timing of late- to post-tectonic
2087 Sveconorwegian granitic magmatism in South Norway. Norges geologiske undersøkelse
2088 Bulletin 440, 5-18.
2089 Andersen, T., Griffin, W.L., Jackson, S.E., Knudsen, T.L., Pearson, N.J., 2004a. Mid-
2090 Proterozoic magmatic arc evolution at the southwest margin of the Baltic shield. Lithos 73,
2091 289-318.
2092 Andersen, T., Griffin, W.L., Pearson, N.J., 2002b. Crustal evolution in the SW part of the
2093 Baltic Shield: the Hf isotope evidence. Journal of Petrology 43, 1725-1747.
2094 Andersen, T., Griffin, W.L., Sylvester, A.G., 2007. Sveconorwegian crustal underplating in
2095 southwestern Fennoscandia: LAM-ICPMS U-Pb and Lu-Hf isotope evidence from granites
2096 and gneisses in Telemark, southern Norway. Lithos 93, 273-287.
2097 Andersen, T., Hagelia, P., Whitehouse, M.J., 1994. Precambrian multi-stage crustal
2098 evolution in the Bamble sector of south Norway: Pb isotopic evidence from a

2099 Sveconorwegian deep-seated intrusion. Chemical Geology (Isotope Geoscience Section) 116,
2100 327-343.
2101 Andersen, T., Laajoki, K., 2003. Provenance characteristics of Mesoproterozoic
2102 metasedimentary rocks from Telemark, South Norway: a Nd-isotope mass-balance model.
2103 Precambrian Research 126, 95-122.
2104 Andersen, T., Laajoki, K., Saeed, A., 2004b. Age, provenance and tectonostratigraphic
2105 status of the Mesoproterozoic Blefjell quartzite, Telemark sector, southern Norway.
2106 Precambrian Research 135, 217-244.
2107 Andersen, T., Munz, I.A., 1995. Radiogenic whole-rock lead in Precambrian
2108 metasedimentary gneisses from South Norway: evidence of Sveconorwegian LILE mobility.
2109 Norsk Geologisk Tidsskrift 75, 156-168.
2110 Andersson, J., Möller, C., Johansson, L., 2002a. Zircon chronology of migmatite gneisses
2111 along the Mylonite Zone (S Sweden): a major Sveconorwegian terrane boundary in the Baltic
2112 Shield. Precambrian Research 114, 121-147.
2113 Andersson, J., Söderlund, U., Cornell, D., Johansson, L., Möller, C., 1999.
2114 Sveconorwegian (-Grenvillian) deformation, metamorphism and leucosome formation in SW
2115 Sweden, SW Baltic Shield: constraints from a Mesoproterozoic granite intrusion. Precambrian
2116 Research 98, 151-171.
2117 Andersson, M., Lie, J.E., Husebye, E.S., 1996. Tectonic setting of post-orogenic granites
2118 within SW Fennoscandia based on deep seismic and gravity data. Terra Nova 8, 558-566.
2119 Andersson, U.B., Neymark, L.A., Billström, K., 2002b. Petrogenesis of Mesoproterozoic
2120 (Subjotnian) rapakivi complexes of central Sweden: implications for U-Pb zircon ages, Nd, Sr
2121 and Pb isotopes. Transactions of the Royal Society of Edinburgh, Earth Sciences 92, 201-228.
2122 Andréasson, P.G., Dallmeyer, R.D., 1995. Tectonothermal evolution of high-alumina rocks
2123 within the Protogine Zone, southern Sweden. Journal of Metamorphic Geology 13, 461-474.

Andréasson, P.G., Rodhe, A., 1994. Ductile and brittle deformation within the Protogine Zone, southern Sweden: a discussion. Geologiska Föreningens i Stockholm Förhandlingar 116, 115-117.

Appelquist, K., Brander, L., Johansson, Å., Andersson, U.B., Cornell, D., 2011. Character and origin of variably deformed granitoids in central southern Sweden: implications from geochemistry and Nd isotopes. Geological Journal 46, 597-618.

Appelquist, K., Cornell, D., Brander, L., 2008. Age, tectonic setting and petrogenesis of the Habo Volcanic Suite: Evidence for an active continental margin setting for the Transscandinavian Igneous Belt. GFF 130, 123-138.

Årebäck, H., Andersson, U.B., Petersson, J., 2008. Petrological evidence for crustal melting, unmixing, and undercooling in an alkali-calcic, high-level intrusion: the late Sveconorwegian Vinga intrusion, SW Sweden. Mineralogy and Petrology 93, 1-46.

Årebäck, H., Stigh, J., 2000. The nature and origin of an anorthosite associated ilmenite-rich leuconorite, Hakefjorden Complex, south-west Sweden. Lithos 21, 247-267.

Ashwal, L.D., 1993. Anorthosites. Springer-Verlag, Berlin.

Augland, L.E., Andresen, A., Corfu, F., Agyei-Dwarko, N.Y., Larionov, A.N., 2014. The Bratten-Landegode gneiss complex: a fragment of Laurentian continental crust in the Uppermost Allochthon of the Scandinavian Caledonides, in: Corfu, F., Gasser, D., Chew, D.M. (Eds.), New perspectives on the Caledonides of Scandinavia and related areas. Geological Society, London, Special Publications, pp. 633-654.

Austin Hegardt, E., 2010. Pressure, temperature and time constraints on tectonic models for southwestern Sweden, Department of Earth Science. University of Gothenburg, p. 91.

Austin Hegardt, E., Cornell, D.H., Claesson, L., Simakov, S., Stein, H.J., Hannah, J.L., 2005. Eclogites in the central part of the Sveconorwegian Eastern Segment of the Baltic Shield: support for an extensive eclogite terrane. GFF 127, 221-232.

2149 Austin Hegardt, E., Cornell, D.H., Hellström, F.A., Lundqvist, I., 2007. Emplacement age
2150 of the mid-Proterozoic Kungsbacka Bimodal Suite, SW Sweden. GFF 129, 227-234.
2151 Bao, X.W., Eaton, D.W., Guest, B., 2014. Plateau uplift in western Canada caused by
2152 lithospheric delamination along a craton edge. Nature Geoscience 7, 830-833.
2153 Barling, J., Weis, D., Demaiffe, D., 2000. A Sr-, Nd- and Pb-isotopic investigation of the
2154 transition between two megacyclic units of the Bjerkreim–Sokndal layered intrusion, south
2155 Norway. Chemical Geology 165, 47-65.
2156 Barnichon, J.D., Havenith, H., Hoffer, B., Charlier, R., Jongmans, D., Duchesne, J.C.,
2157 1999. The deformation of the Egersund-Ogna anorthosite massif, south Norway: finite-
2158 element modelling of diapirism. Tectonophysics 303, 109-130.
2159 Bateman, P.C., Chappell, B.W., 1979. Crystallization, fractionation, and solidification of
2160 the Tuolumne Intrusive Series, Yosemite National Park, California. Geological Society of
2161 America Bulletin 90, 465-482.
2162 Be'eri-Shlevin, Y., Gee, D.G., Claesson, S., Ladenberger, A., Majka, J., Kirkland, C.L.,
2163 Robinson, P., Frei, D., 2011. Provenance of Neoproterozoic sediments in the Särv nappes
2164 (Middle Allochthon) of the Scandinavian Caledonides: LA-ICP-MS and SIMS U-Pb dating of
2165 detrital zircons. Precambrian Research 187, 181-200.
2166 Beaumont, C., Nguyen, M.H., Jamieson, R.A., Ellis, S., 2006. Crustal flow modes in large
2167 hot orogens. Geological Society, London, Special Publications 268, 91-145.
2168 Beckman, V., Möller, C., Söderlund, U., Andersson, J., 2017. Zircon growth during
2169 progressive recrystallization of gabbro to garnet amphibolite, Eastern Segment,
2170 Sveconorwegian orogen. Journal of Petrology 58, 167-187.
2171 Bédard, J., 2010. Parental magmas of Grenville Province massif-type anorthosites, and
2172 conjectures about why massif anorthosites are restricted to the Proterozoic. Earth and

Environmental Science Transactions of the Royal Society of Edinburgh - Earth Sciences 100, 77-103.

Bergerat, F., Angelier, J., Andreasson, P.G., 2007. Evolution of paleostress fields and brittle deformation of the Tornquist Zone in Scania (Sweden) during Permo-Mesozoic and Cenozoic times. Tectonophysics 444, 93-110.

Bergman, S., Högdahl, K., Nironen, M., Ogenhall, E., Sjöström, H., Lundqvist, L., Lahtinen, R., 2008. Timing of Palaeoproterozoic intra-orogenic sedimentation in the central Fennoscandian Shield; evidence from detrital zircon in metasandstone. Precambrian Research 161, 231-249.

Bergström, U., Stephens, M.B., Wahlgren, C.H., 2020. Chapter 16 - Polyphase (1.6–1.5 and 1.1–1.0 Ga) deformation and metamorphism of Proterozoic (1.7–1.1 Ga) continental crust, Idefjorden terrane, Sveconorwegian orogen. Geological Society, London, Memoirs 50, 397-434.

Berthelsen, A., 1980. Towards a palinspastic tectonic analysis of the Baltic Shield, in: Cogne, J., Slansky, M. (Eds.), Geology of Europe, from Precambrian to the post-Hercyninan sedimentary basins. Mémoires du B.R.G.M., Paris, pp. 5-21.

Bingen, B., 1989. Geochemistry of Sveconorwegian augen gneisses from SW Norway at the amphibolite-granulite facies transition. Norsk Geologisk Tidsskrift 69, 177-189.

Bingen, B., Andersson, J., Söderlund, U., Möller, C., 2008a. The Mesoproterozoic in the Nordic countries. Episodes 31, 29-34.

Bingen, B., Belousova, E.A., Griffin, W.L., 2011. Neoproterozoic recycling of the Sveconorwegian orogenic belt: detrital-zircon data from the Sparagmite basins in the Scandinavian Caledonides. Precambrian Research 189, 347-367.

Bingen, B., Birkeland, A., Nordgulen, Ø., Sigmond, E.M.O., 2001. Correlation of supracrustal sequences and origin of terranes in the Sveconorwegian orogen of SW

Scandinavia: SIMS data on zircon in clastic metasediments. Precambrian Research 108, 293-318.

Bingen, B., Boven, A., Punzalan, L., Wijbrans, J., Demaiffe, D., 1998. Hornblende $^{40}Ar/^{39}Ar$ geochronology across terrane boundaries in the Sveconorwegian province of S Norway. Precambrian Research 90, 159-185.

Bingen, B., Corfu, F., Stein, H.J., Whitehouse, M.J., 2015. U-Pb geochronology of the syn-orogenic Knaben molybdenum deposits, Sveconorwegian orogen, Norway. Geological Magazine 152, 537-556.

Bingen, B., Davis, W.J., Hamilton, M.A., Engvik, A., Stein, H.J., Skår, Ø., Nordgulen, Ø., 2008b. Geochronology of high-grade metamorphism in the Sveconorwegian belt, S Norway: U-Pb, Th-Pb and Re-Os data. Norwegian Journal of Geology 88, 13-42.

Bingen, B., Demaiffe, D., Hertogen, J., Weis, D., Michot, J., 1993. K-rich calc-alkaline augen gneisses of Grenvillian age in SW Norway: mingling of mantle-derived and crustal components. The Journal of Geology 101, 763-778.

Bingen, B., Mansfeld, J., Sigmond, E.M.O., Stein, H.J., 2002. Baltica-Laurentia link during the Mesoproterozoic: 1.27 Ga development of continental basins in the Sveconorwegian Orogen, southern Norway. Canadian Journal of Earth Sciences 39, 1425-1440.

Bingen, B., Nordgulen, Ø., Sigmond, E.M.O., Tucker, R.D., Mansfeld, J., Högdahl, K., 2003. Relations between 1.19-1.13 Ga continental magmatism, sedimentation and metamorphism, Sveconorwegian province, S Norway. Precambrian Research 124, 215-241.

Bingen, B., Nordgulen, Ø., Viola, G., 2008c. A four-phase model for the Sveconorwegian orogeny, SW Scandinavia. Norwegian Journal of Geology 88, 43-72.

Bingen, B., Skår, Ø., Marker, M., Sigmond, E.M.O., Nordgulen, Ø., Ragnhildstveit, J., Mansfeld, J., Tucker, R.D., Liégeois, J.P., 2005. Timing of continental building in the Sveconorwegian orogen, SW Scandinavia. Norwegian Journal of Geology 85, 87-116.

Bingen, B., van Breemen, O., 1998a. Tectonic regimes and terrane boundaries in the high-grade Sveconorwegian belt of SW Norway, inferred from U-Pb zircon geochronology and geochemical signature of augen gneiss suites. Journal of the Geological Society of London 155, 143-154.

Bingen, B., van Breemen, O., 1998b. U-Pb monazite ages in amphibolite- to granulite-facies orthogneisses reflect hydrous mineral breakdown reactions: Sveconorwegian Province of SW Norway. Contributions to Mineralogy and Petrology 132, 336-353.

Bingen, B., Viola, G., 2018. The early-Sveconorwegian orogeny in southern Norway: tectonic model involving delamination of the sub-continental lithospheric mantle. Precambrian Research 313, 170-204.

Bird, P., 1979. Continental delamination and the Colorado Plateau. Journal of Geophysical Research: Solid Earth 84, 7561-7571.

Blereau, E., Johnson, T.E., Clark, C., Taylor, R.J.M., Kinny, P.D., Hand, M., 2017. Reappraising the P–T evolution of the Rogaland–Vest Agder Sector, southwestern Norway. Geoscience Frontiers 8, 1-14.

Bogaerts, M., Scaillet, B., Liégeois, J.P., Vander Auwera, J., 2003. Petrology and geochemistry of the Lyngdal granodiorite (Southern Norway) and the role of fractional crystallization in the genesis of Proterozoic ferro-potassic A-type granites. Precambrian Research 124, 149-184.

Bogaerts, M., Scaillet, B., Vander Auwera, J., 2006. Phase equilibria of the Lyngdal granodiorite (Norway): implications for the origin of metaluminous ferroan granitoids. Journal of Petrology 47, 2405-2431.

Bogdanova, S., Bingen, B., Gorbatschev, R., Kheraskova, T., Kozlov, V., Puchkov, V., Volozh, Y., 2008. The East European Craton (Baltica) before and during the assembly of Rodinia. Precambrian Research 160, 23-45.

Boger, S.D., Raetz, M., Giles, D., Etchart, E., Fanning, C.M., 2005. U–Pb age data from the Sunsas region of Eastern Bolivia, evidence for the allochthonous origin of the Paragua Block. Precambrian Research 139, 121-146.

Bolle, O., Demaiffe, D., Duchesne, J.C., 2003a. Petrogenesis of jotunitic and acidic members of an AMC suite (Rogaland anorthosite province, SW Norway): a Sr and Nd isotopic assessment. Precambrian Research 124, 185-214.

Bolle, O., Diot, H., Duchesne, J.C., 2000. Magnetic fabric and deformation in charnockitic igneous rocks of the Bjerkreim–Sokndal layered intrusion (Rogaland, Southwest Norway). Journal of Structural Geology 22, 647-667.

Bolle, O., Diot, H., Liégeois, J.P., Vander Auwera, J., 2010. The Farsund intrusion (SW Norway): a marker of late-Sveconorwegian (Grenvillian) tectonism emplaced along a newly defined major shear zone. Journal of Structural Geology 32, 1500-1518.

Bolle, O., Diot, H., Trindade, R.I.F., 2003b. Magnetic fabrics in the Holum granite (Vest-Agder, southernmost Norway): implications for the late evolution of the Sveconorwegian (Grenvillian) orogen of SW Scandinavia. Precambrian Research 121, 221-249.

Bolle, O., Diot, H., Vander Auwera, J., Dembele, A., Schittekat, J., Spassov, S., Ovtcharova, M., Schaltegger, U., 2018. Pluton construction and deformation in the Sveconorwegian crust of SW Norway: Magnetic fabric and U-Pb geochronology of the Kleivan and Sjelset granitic complexes. Precambrian Research 305, 247-267.

Bolle, O., Duchesne, J.C., 2007. The Apophysis of the Bjerkreim-Sokndal layered intrusion (Rogaland anorthosite province, SW Norway): A composite pluton build up by

2270 tectonically-driven emplacement of magmas along the margin of an AMC igneous complex.
2271 Lithos 98, 292-312.
2272 Bolle, O., Trindade, R.I.F., Bouchez, J.L., Duchesne, J.C., 2002. Imaging downward
2273 granitic magma transport in the Rogaland Igneous Complex, SW Norway. Terra Nova 14, 87-
2274 92.
2275 Bouvier, A., Vervoort, J.D., Patchett, P.J., 2008. The Lu-Hf and Sm-Nd isotopic
2276 composition of CHUR: Constraints from unequilibrated chondrites and implications for the
2277 bulk composition of terrestrial planets. Earth and Planetary Science Letters 273, 48-57.
2278 Brander, L., Appelquist, K., Cornell, D., Andersson, U.B., 2012. Igneous and metamorphic
2279 geochronologic evolution of granitoids in the central Eastern Segment, southern Sweden.
2280 International Geology Review 54, 509-546.
2281 Brander, L., Söderlund, U., 2009. Mesoproterozoic (1.47-1.44 Ga) orogenic magmatism in
2282 Fennoscandia; baddeleyite U-Pb dating of a suite of massif-type anorthosite in S Sweden.
2283 International Journal of Earth Sciences 98, 499-516.
2284 Brander, L., Söderlund, U., Bingen, B., 2011. Tracing the 1271-1246 Ma Central
2285 Scandinavian Dolerite Group mafic magmatism in Fennoscandia: U-Pb baddeleyite and Hf
2286 isotope data on the Moslätt and Børgefjell dolerites. Geological Magazine 148, 632-643.
2287 Brewer, T.S., Åhäll, K.I., Darbyshire, D.P.F., Menuge, J.F., 2002. Geochemistry of late
2288 Mesoproterozoic volcanism in southwestern Scandinavia: implications for Sveconorwegian
2289 /Grenvillian plate tectonic models. Journal of the Geological Society of London 159, 129-144.
2290 Brewer, T.S., Åhäll, K.I., Menuge, J.F., Storey, C.D., Parrish, R.R., 2004. Mesoproterozoic
2291 bimodal volcanism in SW Norway, evidence for recurring pre-Sveconorwegian continental
2292 margin tectonism. Precambrian Research 134, 249-273.
2293 Brewer, T.S., Daly, J.S., Åhäll, K.I., 1998. Contrasting magmatic arcs in the
2294 Palaeoproterozoic of the south-western Baltic Shield. Precambrian Research 92, 297-315.

Brewer, T.S., Menuge, J.F., 1998. Metamorphic overprinting of Sm-Nd isotopic systems in volcanic rocks: the Telemark Supergroup, southern Norway. Chemical Geology 145, 1-16.

Broekmans, M.A., Nijland, T.G., Jansen, J.B.H., 1994. Are stable isotopic trends in amphibolite to granulite facies transitions metamorphic of diagenetic? - An answer for the Arendal area (Bamble sector, S.E. Norway) from mid-Proterozoic carbon bearing rocks. American Journal of Science 294, 1135-1165.

Brown, M., 2006. Duality of thermal regimes is the distinctive characteristic of plate tectonics since the Neoarchean. Geology 34, 961-964.

Brown, M., 2013. Granite: From genesis to emplacement. Geological Society of America Bulletin 125, 1079-1113.

Bruand, E., Storey, C., Fowler, M., 2014. Accessory mineral chemistry of high Ba–Sr granites from northern Scotland: Constraints on petrogenesis and records of whole-rock signature. Journal of Petrology 55, 1619-1651.

Brueckner, H.K., 2009. Subduction of continental crust, the origin of post-orogenic granitoids (and anorthosites?) and the evolution of Fennoscandia. Journal of the Geological Society of London 166, 753-762.

Buchan, K.L., Mertanen, S., Park, R.G., Pesonen, L.J., Elming, S.-Å., Abrahamsen, N., Bylund, G., 2000. Comparing the drift of Laurentia and Baltica in the Proterozoic: the importance of key palaeomagnetic poles. Tectonophysics 319, 167-198.

Bybee, G.M., Ashwal, L.D., Shirey, S.B., Horan, M., Mock, T., Andersen, T.B., 2014. Pyroxene megacrysts in Proterozoic anorthosites: Implications for tectonic setting, magma source and magmatic processes at the Moho. Earth and Planetary Science Letters 389, 74-85.

Cagnard, F., Barbey, P., Gapais, D., 2011. Transition between “Archaean-type” and “modern-type” tectonics: Insights from the Finnish Lapland Granulite Belt. Precambrian Research 187, 127-142.

Cameron, K.L., Lopez, R., Ortega-Gutiérrez, F., L, S.A., Keppie, J.D., Schulze, C., 2004. U-Pb geochronology and Pb isotopic compositions of leached feldspars: constraints on the origin and evolution of Grenville rocks from eastern and southern Mexico. Geological Society of America Memoirs 197, 755-769.

Campbell, I.H., Allen, C.M., 2008. Formation of supercontinents linked to increases in atmospheric oxygen. Nature Geoscience 1, 554-558.

Cardona, A., Chew, D., Valencia, V.A., Bayona, G., Miskovic, A., Ibañez-Mejía, M., 2010. Grenvillian remnants in the Northern Andes: Rodinian and Phanerozoic paleogeographic perspectives. Journal of South American Earth Sciences 29, 92-104.

Carr, S.D., Easton, R.M., Jamieson, R.A., Culshaw, N.G., 2000. Geologic transect across the Grenville orogen of Ontario and New York. Canadian Journal of Earth Sciences 37, 193-216.

Cawood, P.A., Pisarevsky, S.A., 2017. Laurentia-Baltica-Amazonia relations during Rodinia assembly. Precambrian Research 292, 386-397.

Cawood, P.A., Strachan, R., Cutts, K., Kinny, P.D., Hand, M., Pisarevsky, S., 2010. Neoproterozoic orogeny along the margin of Rodinia: Valhalla orogen, North Atlantic. Geology 38, 99-102.

Cawood, P.A., Strachan, R.A., Merle, R.E., Millar, I.L., Loewy, S.L., Dalziel, I.W.D., Kinny, P.D., Jourdan, F., Nemchin, A.A., Connelly, J.N., 2015. Neoproterozoic to early Paleozoic extensional and compressional history of East Laurentian margin sequences: the Moine Supergroup, Scottish Caledonides. Geological Society of America Bulletin 127, 349-371.

Cecys, A., Benn, K., 2007. Emplacement and deformation of the ca. 1.45 Ga Karlshamn granitoid pluton, southeastern Sweden, during ENE-WSW Danopolonian shortening. International Journal of Earth Sciences 96, 397-414.

Cecys, A., Bogdanova, S., Janson, C., Bibikova, E., Kornfält, K.A., 2002. The Stenshuvud and Tåghusa granitoids: new representative of Mesoproterozoic magmatism in southern Sweden. GFF 124, 149-162.

Chardon, D., Gapais, D., Cagnard, F., 2009. Flow of ultra-hot orogens: A view from the Precambrian, clues for the Phanerozoic. Tectonophysics 477, 105-118.

Charlier, B., Duchesne, J.C., Vander Auwera, J., 2006. Magma chamber processes in the Tellnes ilmenite deposit (Rogaland Anorthosite Province, SW Norway) and the formation of Fe-Ti ores in massif-type anorthosites. Chemical Geology 234, 264-290.

Charlier, B., Duchesne, J.C., Vander Auwera, J., Storme, J.Y., Maquil, R., Longhi, J., 2010. Polybaric fractional crystallization of high-alumina basalt parental magmas in the Egersund-Ogna massif-type anorthosite (Rogaland, SW Norway) constrained by plagioclase and high-alumina orthopyroxene megacrysts. Journal of Petrology 51, 2515-2546.

Chen, M., Niu, F., Tromp, J., Lenardic, A., Lee, C.T.A., Cao, W., Ribeiro, J., 2017. Lithospheric foundering and underthrusting imaged beneath Tibet. Nature Communications 8, 15659.

Chiarenzelli, J., Lupulescu, M., Cousens, B., Thern, E., Coffin, L., Regan, S., 2010. Enriched Grenvillian lithospheric mantle as a consequence of long-lived subduction beneath Laurentia. Geology 38, 151-154.

Christoffel, C.A., Connelly, J.N., Åhäll, K.I., 1999. Timing and characterization of recurrent pre-Sveconorwegian metamorphism and deformation in the Varberg-Halmstad region of SW Sweden. Precambrian Research 98, 173-195.

Clemens, J.D., Darbyshire, D.P.F., Flinders, J., 2009. Sources of post-orogenic calcalkaline magmas: The Arrochar and Garabal Hill–Glen Fyne complexes, Scotland. Lithos 112, 524-542.

Clough, P.W., Field, D., 1980. Chemical variation in metabasites from a Proterozoic amphibolite-granulite transition zone, S Norway. Contributions to Mineralogy and Petrology 73, 277-286.

Coint, N., Slagstad, T., Roberts, N.M.W., Marker, M., Røhr, T., Sørensen, B.E., 2015. The Late Mesoproterozoic Sirdal Magmatic Belt, SW Norway:Relationships between magmatism and metamorphism and implications for Sveconorwegian orogenesis. Precambrian Research 265, 57-77.

Collins, W.J., 2002. Hot orogens, tectonic switching, and creation of continental crust. Geology 30, 535-538.

Connelly, J.N., Åhäll, K.I., 1996. The Mesoproterozoic cratonization of Baltica – new age constraints from SW Sweden, in: Brewer, T.S. (Ed.), Precambrian crustal evolution in the North Atlantic Region. Geological Society, London, Special Publications, pp. 261-273.

Connelly, J.N., Berglund, J., Larson, S.Å., 1996. Thermotectonic evolution of the Eastern Segment of southwestern Sweden: tectonic constraints from U-Pb geochronology, in: Brewer, T.S. (Ed.), Precambrian crustal evolution in the North Atlantic Region. Geological Society, London, Special Publications, pp. 297-313.

Cooper, D.C., Field, D., 1977. The chemistry and origins of Proterozoic low-potash, high-iron, charnockitic gneisses from Tromøy, South Norway. Earth and Planetary Science Letters 35, 105-115.

Cordani, U.G., Cardona, A., Jimenez, D.M., Liu, D., Nutman, A.P., 2005. Geochronology of Proterozoic basement inliers in the Colombian Andes: Tectonic history of remnants of a fragmented Grenville belt. Geological Society, London, Special Publications 246, 329-346.

Corfu, F., 2019. The Sognefjell volcanic-subvolcanic complex – A late Sveconorwegian arc imbricated in the central Norwegian Caledonides. Precambrian Research 331, 105353.

Corfu, F., Easton, R.M., 1995. U-Pb geochronology of the Mazinaw terrane, an imbricate segment of the Central Metasedimentary Belt, Grenville Province, Ontario. Canadian Journal of Earth Sciences 32, 959-976.

Corfu, F., Laajoki, K., 2008. An uncommon episode of mafic magmatism at 1347 Ma in the Mesoproterozoic Telemark supracrustals, Sveconorwegian orogen - Implications for stratigraphy and tectonic evolution. Precambrian Research 160, 299-307.

Cornell, D., Årebäck, H., Scherstén, A., 2000. Ion microprobe discovery of Archaean and Early Proterozoic zircon xenocrysts in southwest Sweden. GFF 122, 377-383.

Corriveau, L., van Breemen, O., 2000. Docking of the Central Metasedimentary Belt to Laurentia in geon 12: evidence from the 1.17–1.16 Chevreuil intrusive suite and host gneisses, Quebec. Canadian Journal of Earth Sciences 37, 253-269.

Cosca, M.A., Mezger, K., Essene, E.J., 1998. The Baltica-Laurentia connection: Sveconorwegian (Grenvillian) metamorphism, cooling, and unroofing in the Bamble Sector, Norway. The Journal of Geology 106, 539-552.

Cosca, M.A., O'Nions, R.K., 1994. A re-examination of the influence of composition on argon retentivity in metamorphic calcic amphiboles. Chemical Geology 112, 39-56.

Couzinié, S., Laurent, O., Moyen, J.F., Zeh, A., Bouilhol, P., Villaros, A., 2016. Post-collisional magmatism: crustal growth not identified by zircon Hf-O isotopes. Earth and Planetary Science Letters 456, 182-195.

Cutts, K.A., Hand, M., Kelsey, D.E., Wade, B., Strachan, R.A., Clark, C., Netting, A., 2009. Evidence for 930 Ma metamorphism in the Shetland Islands, Scottish Caledonides: implications for Neoproterozoic tectonics in the Laurentia-Baltica sector of Rodinia. Journal of the Geological Society of London 166, 1033-1047.

Dahlgren, S., Bogoch, R., Magaritz, M., Michard, A., 1993. Hydrothermal dolomite marbles associated with charnockitic magmatism in the Proterozoic Bamble Shear Belt, south Norway. Contributions to Mineralogy and Petrology 113, 394-409.

Daly, J.S., McLelland, J.M., 1991. Juvenile Middle Proterozoic crust in the Adirondack Highlands, Grenville province, northeastern North America. Geology 19, 119-122.

Dalziel, I.W.D., 1997. Neoproterozoic-Paleozoic geography and tectonics: reviews, hypothesis, environmental speculations. Geological Society of America Bulletin 109, 16-42.

Debon, F., Le Fort, P., 1983. A chemical-mineralogical classification of common plutonic rocks and associations. Transactions of the Royal Society of Edinburgh, Earth Sciences 73, 135-149.

deHaas, G.J.L.M., Andersen, T., Vestin, J., 1999. Detrital zircon geochronology: new evidence for an old model for accretion of the SW Baltic Shield. The Journal of Geology 107, 569-586.

deHaas, G.J.L.M., Nijland, T.G., Andersen, T., Corfu, F., 2002a. New constraints on the timing of deposition and metamorphism in the Bamble sector, south Norway: zircon and titanite U-Pb data from the Nelaug area. GFF 124, 73-78.

deHaas, G.J.L.M., Nijland, T.G., Valbracht, P.J., Maijer, C., Verschure, R., Andersen, T., 2002b. Magmatic versus metamorphic origin of olivine-plagioclase coronas. Contributions to Mineralogy and Petrology 143, 537-550.

Demaiffe, D., Bingen, B., Wertz, P., Hertogen, J., 1990. Geochemistry of the Lyngdal hyperites (SW Norway): comparison with the monzonorites associated with the Rogaland anorthosite complex. Lithos 24, 237-250.

Demaiffe, D., Michot, J., 1985. Isotope geochronology of the Proterozoic crustal segment of southern Norway: a review, in: Tobi, A.C., Touret, J.L. (Eds.), The deep Proterozoic crust in the north Atlantic provinces. Reidel, Dordrecht, pp. 411-433.

Demaiffe, D., Weis, D., Michot, J., Duchesne, J.C., 1986. Isotopic constraints on the genesis of the Rogaland anorthositic suite (SW Norway). Chemical Geology 57, 167-179.

Dewey, J.F., 1988. Extensional collapse of orogens. Tectonics 7, 1123-1139.

DeWolf, C.P., Mezger, K., 1994. Lead isotope analyses of leached feldspars: Constraints on the early crustal history of the Grenville Orogen. Geochimica et Cosmochimica Acta 58, 5537-5550.

Dhuime, B., Hawkesworth, C., Cawood, P., 2011. When continents formed. Science 331, 154-155.

Dickin, A.P., 2000. Crustal formation in the Grenville Province: Nd-isotope evidence. Canadian Journal of Earth Sciences 37, 165-181.

Dickin, A.P., Higgins, M.D., 1992. Sm/Nd evidence for a major 1.5 Ga crust-forming event in the Central Grenville Province. Geology 20, 137-140.

Dickin, A.P., McNutt, R.H., 2007. The Central Metasedimentary Belt (Grenville Province) as a failed backarc rift zone: Nd isotope evidence. Earth and Planetary Science Letters 259, 97-106.

Dickin, A.P., McNutt, R.H., Martin, C., Guo, A., 2010. The extent of juvenile crust in the Grenville Province: Nd isotope evidence. Geological Society of America Bulletin 122, 870-883.

Dons, J.A., 1960. The stratigraphy of supracrustal rocks, granitization and tectonics in the Precambrian Telemark area, southern Norway. Norges geologiske undersøkelse 212h, 1-30.

Dons, J.A., Jorde, K., 1978. Geologisk kart over Norge, berggrunnskart Skien, 1:250000. Norges geologiske undersøkelse.

Drüppel, K., Elsässer, L., Brandt, S., Gerdes, A., 2013. Sveconorwegian mid-crustal ultrahigh-temperature metamorphism in Rogaland, Norway: U-Pb LA-ICP-MS

geochronology and pseudosections of sapphirine granulites and associated paragneisses. Journal of Petrology 54, 305-350.

Duchesne, J.C., 1972. Iron-titanium oxide minerals in the Bjerkrem-Sogndal massif, south-western Norway. Journal of Petrology 13, 57-81.

Duchesne, J.C., Berza, T., Liégeois, J.P., Vander Auwera, J., 1998. Shoshonitic liquid line of descent from diorite to granite: the Late Precambrian post-collisional Tismana pluton (South Carpathians, Romania). Lithos 45, 281-303.

Duchesne, J.C., Charlier, B., 2005. Geochemistry of cumulates from the Bjerkreim-Sokndal layered intrusion (S. Norway). Part I: Constraints from major elements on the mechanism of cumulate formation and on the jotunite liquid line of descent. Lithos 83, 229-254.

Duchesne, J.C., Liégeois, J.P., Vander Auwera, J., Longhi, J., 1999. The crustal tongue melting model and the origin of massive anorthosites. Terra Nova 11, 100-105.

Duchesne, J.C., Maquil, R., Demaiffe, D., 1985. The Rogaland anorthosites: facts and speculations, in: Tobi, A.C., Touret, J.L. (Eds.), The deep Proterozoic crust in the north Atlantic provinces. Reidel, Dordrecht, pp. 449-476.

Duchesne, J.C., Wilmart, E., 1997. Igneous charnockites and related rocks from the Bjerkreim-Sokndal layered intrusion (SW Norway): a jotunite (hypersthene monzodiorite)-derived A-type granitoid suite. Journal of Petrology 38, 337-369.

Duchesne, J.C., Wilmart, E., Demaiffe, D., Hertogen, J., 1989. Monzonorites from Rogaland (southwest Norway): a series of rocks coeval but not comagmatic with massif-type anorthosites. Precambrian Research 45, 111-128.

Eliasson, T., Ahlin, S., Petersson, J., 2003. Emplacement mechanism and thermobarometry of the Sveconorwegian Bohus granite, SW Sweden. GFF 125, 113-130.

Eliasson, T., Schöberg, H., 1991. U-Pb dating of the post-kinematic Sveconorwegian (Grenvillian) Bohus granite, SW Sweden: evidence of restitic zircon. Precambrian Research 51, 337-350.

Elminen, T., Zwingmann, H., Kaakinen, A., 2018. Constraining the timing of brittle deformation and sedimentation in southern Finland: Implications for Neoproterozoic evolution of the eastern Fennoscandian shield. Precambrian Research 304, 110-124.

Emslie, R.F., 1985. Proterozoic anorthosite massifs, in: Tobi, A.C., Touret, J.L. (Eds.), The deep Proterozoic crust in the north Atlantic provinces. Reidel, Dordrecht, pp. 39-60.

Engvik, A.K., Bingen, B., Solli, A., 2016. Localized occurrences of granulite: P-T modeling, U-Pb geochronology and distribution of early-Sveconorwegian high-grade metamorphism in Bamble, South Norway. Lithos 240-243, 84-103.

Engvik, A.K., Corfu, F., Solli, A., Austrheim, H., 2017. Sequence and timing of mineral replacement reactions during albitisation in the high-grade Bamble lithotectonic domain, S-Norway. Precambrian Research 291, 1-16.

Engvik, A.K., Ihlen, P.M., Austrheim, H., 2014. Characterisation of Na-metasomatism in the Sveconorwegian Bamble Sector of South Norway. Geoscience Frontiers 5, 659-672.

Engvik, A.K., Mezger, K., Wortelkamp, S., Bast, R., Corfu, F., Korneliussen, A., Ihlen, P.M., Bingen, B., Austrheim, H., 2011. Metasomatism of gabbro - mineral replacement and element mobilization during the Sveconorwegian metamorphic event. Journal of Metamorphic Geology 29, 399-423.

Erlström, M., 2020. Chapter 24 - Carboniferous–Neogene tectonic evolution of the Fennoscandian transition zone, southern Sweden. Geological Society, London, Memoirs 50, 603-620.

EUGENO-S-working-group, 1988. Crustal structure and tectonic evolution of the transition between the Baltic Shield and the North German Caledonides (the EUGENO-S Project). Tectonophysics 150, 253-348.

Evans, D.A.D., Mitchell, R.N., 2011. Assembly and breakup of the core of Paleoproterozoic-Mesoproterozoic supercontinent Nuna. Geology 39, 443-446.

Falkum, T., 1985. Geotectonic evolution of southern Scandinavia in light of a late-Proterozoic plate-collision, in: Tobi, A.C., Touret, J.L. (Eds.), The deep Proterozoic crust in the north Atlantic provinces. Reidel, Dordrecht, pp. 309-322.

Falkum, T., Petersen, J.S., 1980. The Sveconorwegian orogenic belt, a case of late-Proterozoic plate collision. Geologische Rundschau 69, 622-647.

Field, D., Drury, S.A., Cooper, D.C., 1980. Rare-earth and LIL element fractionation in high-grade charnockitic gneisses, south Norway. Lithos 13, 281-289.

Field, D., Smalley, P.C., Lamb, R.C., Råheim, A., 1985. Geochemical evolution of the 1.6-1.5 Ga-old amphibolite- granulite facies terrain, Bamble sector, Norway: dispelling the myth of grenvillian high-grade reworking, in: Tobi, A.C., Touret, J.L. (Eds.), The deep Proterozoic crust in the north Atlantic provinces. Reidel, Dordrecht, pp. 567-578.

Fram, M.S., Longhi, J., 1992. Phase equilibria of dikes associated with Proterozoic anorthosite complexes. American Mineralogist 77, 605-616.

Frost, B.R., Barnes, C.G., Collins, W.J., Arculus, R.J., Ellis, W.J., Frost, D.J., 2001. A geochemical classification for granitic rocks. Journal of Petrology 42, 2033-2048.

Gabrielsen, R.H., Nystuen, J.P., Jarsve, E.M., Lundmark, A.M., 2015. The Sub-Cambrian Peneplain in southern Norway: its geological significance and its implications for post-Caledonian faulting, uplift and denudation. Journal of the Geological Society of London 172, 777-791.

Gammon, J.B., 1966. Fahlbands in the Precambrian of southern Norway. Economic Geology 61, 174-188.

Gee, D.G., Andréasson, P.G., Lorenz, H., Frei, D., Majka, J., 2015. Detrital zircon signatures of the Baltoscandian margin along the Arctic Circle Caledonides in Sweden: The Sveconorwegian connection. Precambrian Research 265, 40-56.

Geraldes, M.C., Van Schmus, W.R., Condie, K.C., Bell, S., Teixeira, W., Babinski, M., 2001. Proterozoic geologic evolution of the SW part of the Amazonian Craton in Mato Grosso state, Brazil. Precambrian Research 111, 91-128.

Gerya, T., 2014. Precambrian geodynamics: Concepts and models. Gondwana Research 25, 442-463.

Ghani, A.A., Atherton, M.P., 2006. The chemical character of the Late Caledonian Donegal granites, Ireland, with comments on their genesis. Transactions of the Royal Society of Edinburgh-Earth Sciences 97, 437-454.

Godin, L., Grujic, D., Law, R.D., Searle, M.P., 2006. Channel flow, ductile extrusion and exhumation in continental collision zones: an introduction. Geological Society, London, Special Publications 268, 1-23.

Gong, Z., Evans, D.A.D., Elming, S.Å., Söderlund, U., Salminen, J.M., 2018. Paleomagnetism, magnetic anisotropy and U-Pb baddeleyite geochronology of the early Neoproterozoic Blekinge-Dalarna dolerite dykes, Sweden. Precambrian Research 317, 14-32.

Gorbatschev, R., Bogdanova, S., 2006. Report: Aspects of the Proterozoic boundary between SE and SW Sweden. Department of Geology, Lund University, Sweden, pp. 1-50.

Gower, C.F., 1985. Correlations between the Grenville Province and Sveconorwegian orogenic belt - implications for Proterozoic evolution of the southern margins of the Canadian and Baltic Shields, in: Tobi, A.C., Touret, J.L. (Eds.), The deep Proterozoic crust in the north Atlantic provinces. Reidel, Dordrecht, pp. 247-258.

Gower, C.F., Kamo, S., Krogh, T.E., 2008. Indentor tectonism in the eastern Grenville Province. Precambrian Research 167, 201-212.

Granseth, A., Slagstad, T., Coint, N., Roberts, N.M.W., Røhr, T.S., Sørensen, B.E., 2020. Tectonomagmatic evolution of the Sveconorwegian orogen recorded in the chemical and isotopic compositions of 1070–920 Ma granitoids. Precambrian Research 340, 105527.

Graversen, O., Pedersen, S., 1999. Timing of Gothian structural evolution in SE Norway: a Rb-Sr whole-rock age study. Norsk Geologisk Tidsskrift 79, 47-56.

Griffin, W.L., O'Reilly, S.Y., Afonso, J.C., Begg, G.C., 2009. The composition and evolution of lithospheric mantle: a re-evaluation and its tectonic implications. Journal of Petrology 50, 1185-1204.

Griffin, W.L., Pearson, N.J., Belousova, E.A., Jackson, S.E., van Achterbergh, E., O'Reilly, S.Y., Shee, S.R., 2000. The Hf isotope composition of cratonic mantle: LAM-MC-ICPMS analysis of zircon megacrysts in kimberlites. Geochimica et Cosmochimica Acta 64, 133-147.

Groulier, P.A., Indares, A., Dunning, G., Moukhsil, A., Jenner, G., 2018a. Syn-orogenic magmatism over 100 m.y. in high crustal levels of the central Grenville Province: Characteristics, age and tectonic significance. Lithos 312-313, 128-152.

Groulier, P.A., Indares, A., Dunning, G., Moukhsil, A., Wälle, M., 2018b. Peri-Laurentian, Pinwarian-age oceanic arc crust preserved in the Grenville Province: Insights from the Escoumins supracrustal belt. Precambrian Research 311, 37-64.

Grove, T.L., Chatterjee, N., Parman, S.W., Médard, E., 2006. The influence of H2O on mantle wedge melting. Earth and Planetary Science Letters 249, 74-89.

Guenthner, W.R., Reiners, P.W., Drake, H., Tillberg, M., 2017. Zircon, titanite, and apatite (U-Th)/He ages and age-eU correlations from the Fennoscandian Shield, southern Sweden. Tectonics 36, 1254-1274.

Hanmer, S., Corrigan, D., Pehrsson, S., Nadeau, L., 2000. SW Grenville Province, Canada: the case against post-1.4 Ga accretionary tectonics. Tectonophysics 319, 33-51.

Hansen, E., Johansson, L., Andersson, J., LaBarge, L., Harlov, D., Möller, C., Vincent, S., 2015. Partial melting in amphibolites in a deep section of the Sveconorwegian Orogen, SW Sweden. Lithos 236–237, 27-45.

Harley, S., Kelly, N.M., Möller, A., 2007. Zircon behaviour and the thermal histories of mountain chains. Elements 3, 25-30.

Harley, S.L., 2008. Refining the P–T records of UHT crustal metamorphism. Journal of Metamorphic Geology 26, 125-154.

Harlov, D.E., 2000. Pressure-temperature estimation in orthopyroxene-garnet bearing granulite facies rocks, Bamble Sector, Norway. Mineralogy and Petrology 69, 11-33.

Harlov, D.E., Van Den Kerkhof, A., Johansson, L., 2013. The Varberg-Torpa charnockite-granite association, SW Sweden: Mineralogy, petrology, and fluid inclusion chemistry. Journal of Petrology 54, 3-40.

Hartz, E.H., Torsvik, T.H., 2002. Baltica upside down: a new plate tectonic model for Rodinia and the Iapetus Ocean. Geology 30, 255-258.

Haschke, M.R., Scheuber, E., Günther, A., Reutter, K.J., 2002. Evolutionary cycles during the Andean orogeny: repeated slab breakoff and flat subduction. Terra Nova 14, 49-55.

Hawkesworth, C., Cawood, P., Kemp, T., Storey, C., Dhuime, B., 2009. A Matter of preservation. Science 232, 49-50.

He, Z.Y., Klemd, R., Yan, L.L., Zhang, Z.M., 2018. The origin and crustal evolution of microcontinents in the Beishan orogen of the southern Central Asian Orogenic Belt. Earth-Science Reviews 185, 1-14.

Heaman, L.M., Smalley, P.C., 1994. A U–Pb study of the Morkheia Complex and associated gneisses, south Norway: implications for disturbed Rb–Sr systems and for the

temporal evolution of Mesoproterozoic magmatism in Laurentia. Geochimica et Cosmochimica Acta 58, 1899-1911.

Hellström, F.A., Johansson, Å., Larson, S.Å., 2004. Age emplacement of late Sveconorwegian monzogabbroic dykes, SW Sweden. Precambrian Research 128, 39-55.

Henderson, I.H.C., Ihlen, P.M., 2004. Emplacement of polygeneration pegmatites in relation to Sveconorwegian contractional tectonics: examples from southern Norway. Precambrian Research 133, 207-222.

Hervé, F., Pankhurst, R.J., Fanning, C.M., Calderon, M., Yaxley, G.M., 2007. The South Patagonian batholith: 150 my of granite magmatism on a plate margin. Lithos 97, 373-394.

Herzberg, C., Condie, K., Korenaga, J., 2010. Thermal history of the Earth and its petrological expression. Earth and Planetary Science Letters 292, 79-88.

Hetherington, C.J., Harlov, D.E., 2008. Metasomatic thorite and uraninite inclusions in xenotime and monazite from granitic pegmatites, Hidra anorthosite massif, southwestern Norway: Mechanics and fluid chemistry. American Mineralogist 93, 806-820.

Hoffman, P.F., 1991. Did the breakout of Laurentia turn Gondwanaland inside-out? Science 252, 1409-1412.

Högdahl, K., Andersson, U.B., Eklund, O., 2004. The Transcandinavian Igneous Belt (TIB) in Sweden: a review of its character and evolution. Geological Survey of Finland, Special Paper 37.

Holland, T.J., Babu, E.V., Waters, D.J., 1996. Phase relations of osumilite and dehydration melting in pelitic rocks: a simple thermodynamic model for the KFMASH system. Contributions to Mineralogy and Petrology 124, 383-394.

Hynes, A., Rivers, T., 2010. Protracted continental collision - evidence from the Grenville Orogen. Canadian Journal of Earth Sciences 47, 591-620.

Ibanez-Mejia, M., Pullen, A., Arenstein, J., Gehrels, G.E., Valley, J., Ducea, M.N., Mora, A.R., Pecha, M., Ruiz, J., 2015. Unraveling crustal growth and reworking processes in complex zircons from orogenic lower-crust: The Proterozoic Putumayo Orogen of Amazonia. Precambrian Research 267, 285-310.

Ibanez-Mejia, M., Ruiz, J., Valencia, V.A., Cardona, A., Gehrels, G.E., Mora, A.R., 2011. The Putumayo Orogen of Amazonia and its implications for Rodinia reconstructions: new U-Pb geochronological insights into the Proterozoic tectonic evolution of northwestern South America. Precambrian Research 191, 58-77.

Indares, A., 2020. Deciphering the metamorphic architecture and magmatic patterns of large hot orogens: Insights from the central Grenville Province. Gondwana Research 80, 385-409.

INSPIRE_Directive, 2007. INSPIRE Knowledge Base, Infrastructure for spatial information in Europe, registry. European Commission; http://inspire.ec.europa.eu/registry.

Jagoutz, O., Schmidt, M.W., 2013. The composition of the foundered complement to the continental crust and a re-evaluation of fluxes in arcs. Earth and Planetary Science Letters 371-372, 177-190.

Jamieson, R.A., Beaumont, C., 2013. On the origin of orogens. Geological Society of America Bulletin 125, 1671-1702.

Janoušek, V., Konopásek, J., Ulrich, S., Erban, V., Tajčmanová, L., Jeřábek, P., 2010. Geochemical character and petrogenesis of Pan-African Amspoort suite of the Boundary Igneous Complex in the Kaoko Belt (NW Namibia). Gondwana Research 18, 688-707.

Jensen, E., Corfu, F., 2016. The U–Pb age of the Finse batholith, a composite bimodal Sveconorwegian intrusion. Norwegian Journal of Geology 96, 171-178.

Jiménez-Mejía, D.M., Juliani, C., Cordani, U.G., 2006. P–T–t conditions of high-grade metamorphic rocks of the Garzon Massif, Andean basement, SE Colombia. Journal of South American Earth Sciences 21, 322-336.

Johansson, Å., 2009. Baltica, Amazonia and the SAMBA connection - 1000 million years of neighbourhood during the Proterozoic? Precambrian Research 175, 221-234.

Johansson, Å., Waight, T., Andersen, T., Simonsen, S.L., 2016. Geochemistry and petrogenesis of Mesoproterozoic A-type granitoids from the Danish island of Bornholm, southern Fennoscandia. Lithos 244, 94-108.

Johansson, L., Lindh, A., Möller, C., 1991. Late Sveconorwegian (Grenville) high-pressure granulite facies metamorphism in southwest Sweden. Journal of Metamorphic Geology 9, 283-292.

Johansson, L., Möller, C., Söderlund, U., 2001. Geochronology of eclogite facies metamorphism in the Sveconorwegian Province of SW Sweden. Precambrian Research 106, 261-275.

Johnson, T.E., Brown, M., Kaus, B.J.P., VanTongeren, J.A., 2013. Delamination and recycling of Archaean crust caused by gravitational instabilities. Nature Geoscience 7, 47.

Kalsbeek, F., Thrane, K., Nutman, A.P., Jepsen, H., 2000. Late Mesoproterozoic to early Neoproterozoic history of the East Greenland Caledonides: evidence for Grenvillian orogenesis? Journal of the Geological Society of London 157, 1215-1225.

Kelsey, D.E., Clark, C., Hand, M., 2008. Thermobarometric modelling of zircon and monazite growth in melt-bearing systems: examples using model metapelitic and metapsammitic granulites. Journal of Metamorphic Geology 26, 199-212.

Keppie, J.D., Dostal, J., Cameron, K.L., Solari, L.A., Ortega-Gutiérrez, F., Lopez, R., 2003. Geochronology and geochemistry of Grenvillian igneous suites in the northern Oaxacan Complex, southern Mexico: tectonic implications. Precambrian Research 120, 365-389.

Keppie, J.D., Ortega-Gutiérrez, F., 2010. 1.3-0.9 Ga Oaxaquia (Mexico): Remnant of an arc/backarc on the northern margin of Amazonia. Journal of South American Earth Sciences 29, 21-27.

Kirkland, C.L., Daly, J.S., Whitehouse, M.J., 2006. Granitic magmatism of Grenvillian and late Neoproterozoic age in Finnmark, Arctic Norway – Constraining pre-Scandian deformation in the Kalak Nappe Complex. Precambrian Research 145, 24-52.

Kirkland, C.L., Daly, J.S., Whitehouse, M.J., 2007. Provenance and terrane evolution of the Kalak Nappe Complex, Norwegian Caledonides: Implications for Neoproterozoic paleogeography and tectonics. The Journal of Geology 115, 21-41.

Kirkland, C.L., Daly, J.S., Whitehouse, M.J., 2008a. Basement-cover relationships of the Kalak Nappe Complex, Arctic Norwegian Caledonides and constraints on Neoproterozoic terrane assembly in the North Atlantic region. Precambrian Research 160, 245-276.

Kirkland, C.L., Strachan, R.A., Prave, A.R., 2008b. Detrital zircon signature of the Moine Supergroup, Scotland: contrasts and comparisons with other Neoproterozoic successions within the circum-North Atlantic region. Precambrian Research 163, 332-350.

Knudsen, T.L., 1996. Petrology and geothermobarometry of granulite facies metapelites from the Hisøy-Torungen area, south Norway: new data on the Sveconorwegian P-T-t path of the Bamble sector. Journal of Metamorphic Geology 14, 267-287.

Knudsen, T.L., Andersen, T., 1999. Petrology and geochemistry of the Tromøy gneiss complex, South Norway, an alleged example of Proterozoic depleted lower continental crust. Journal of Petrology 40, 909-933.

Knudsen, T.L., Andersen, T., Whitehouse, M.J., Vestin, J., 1997. Detrital zircon ages from southern Norway - implications for the Proterozoic evolution of the southwestern Baltic Shield. Contributions to Mineralogy and Petrology 130, 47-58.

Koistinen, T., Stephens, M.B., Bogatchev, V., Nordgulen, Ø., Wennerström, M., Korhonen, J., 2001. Geological map of the Fennoscandian shield, Scale 1:2000000. Geological Surveys of Finland, Norway and Sweden and the North-West Department of Natural Resources of Russia.

Korenaga, J., 2008. Urey ratio and the structure and evolution of Earth's mantle. Reviews of Geophysics 46, RG2007.

Korja, A., Lahtinen, R., Nironen, M., 2006. The Svecofennian orogen: a collage of microcontinents and island arcs, in: Gee, D.G., Stephenson, R.A. (Eds.), European lithosphere dynamics. Geological Society, London, Memoirs, pp. 561-578.

Köykkä, J., 2011. The sedimentation and paleohydrology of the Mesoproterozoic stream deposits in a strike-slip basin (Svinsaga Formation), Telemark, southern Norway. Sedimentary Geology 236, 239-255.

Köykkä, J., Laajoki, K., 2009. Mesoproterozoic frost action at the base of the Svinsaga Formation, central Telemark, South Norway. Norwegian Journal of Geology 89, 291-303.

Köykkä, J., Lamminen, J., 2011. Tidally influenced clastic epeiric sea at a Mesoproterozoic continental margin, Rjukan Rift Basin, southern Norway. Precambrian Research 185, 164-182.

Krystopowicz, N.J., Currie, C.A., 2013. Crustal eclogitization and lithosphere delamination in orogens. Earth and Planetary Science Letters 361, 195-207.

Laajoki, K., 2002. The Mesoproterozoic sub-Heddal unconformity, Sauland, central Telemark, Norway. Norwegian Journal of Geology 82, 139-152.

Laajoki, K., Corfu, F., 2007. Lithostratigraphy of the Mesoproterozoic Vemork formation, central Telemark, Norway. Bulletin of the Geological Society of Finland 79, 41-67.

Laajoki, K., Corfu, F., Andersen, T., 2002. Lithostratigraphy and U-Pb geochronology of the Telemark supracrustals in the Bandak-Sauland area, Telemark, South Norway. Norwegian Journal of Geology 82, 119-138.

Lahtinen, R., Korja, A., Nironen, M., Heikkinen, P., 2009. Palaeoproterozoic accretionary processes in Fennoscandia. Geological Society, London, Special Publications 318, 237-256.

Lamminen, J., 2011. Provenance and correlation of sediments in Telemark, South Norway: status of the Lifjell Group and implications for early Sveconorwegian fault tectonics. Norwegian Journal of Geology 91, 57-75.

Lamminen, J., Andersen, T., Nystuen, J.P., 2011. Zircon U-Pb ages and Lu-Hf isotopes from basement rocks associated with Neoproterozoic sedimentary successions in the Sparagmite Region and adjacent areas, South Norway: the crustal architecture of western Baltica. Norwegian Journal of Geology 91, 35-55.

Lamminen, J., Andersen, T., Nystuen, J.P., 2015. Provenance and rift basin architecture of the Neoproterozoic Hedmark Basin, South Norway inferred from U-Pb ages and Lu-Hf isotopes of conglomerate clasts and detrital zircons. Geological Magazine 152, 80-105.

Lamminen, J., Köykkä, J., 2010. The provenance and evolution of the Rjukan Rift Basin, Telemark, south Norway: The shift from a rift basin to an epicontinental sea along a Mesoproterozoic supercontinent. Precambrian Research 181, 129-149.

Larsen, B.T., Olaussen, S., Sundvoll, B., Heeremans, M., 2008. The Permo-Carboniferous Olso Rift through six stages and 65 million years. Episodes 31, 52-58.

Larsson, D., Söderlund, U., 2005. Lu-Hf apatite geochronology of mafic cumulates: an example from a Fe-Ti mineralization at Smålands Taberg, southern Sweden. Chemical Geology 224, 201-211.

Lassen, A., Thybo, H., 2012. Neoproterozoic and Palaeozoic evolution of SW Scandinavia based on integrated seismic interpretation. Precambrian Research 204, 75-104.

Laurent, A., Janoušek, V., Magna, T., Schulmann, K., Míková, J., 2014. Petrogenesis and geochronology of a post-orogenic calc-alkaline magmatic association: the Žulová Pluton, Bohemian Massif. Journal of Geosciences 59, 415-440.

Laurent, A.T., Bingen, B., Duchene, S., Whitehouse, M.J., Seydoux-Guillaume, A.M., Bosse, V., 2018a. Decoding protracted zircon geochronological record in ultra-high temperature granulite, and persistence of partial melting in the crust, Rogaland, Norway. Contributions to Mineralogy and Petrology 173, 29.

Laurent, A.T., Duchene, S., Bingen, B., Bosse, V., Seydoux-Guillaume, A.M., 2018b. Two successive phases of ultrahigh temperature metamorphism in Rogaland, S. Norway: evidence from Y-in-monazite thermometry. Journal of Metamorphic Geology 36, 1009-1037.

Laurent, A.T., Seydoux-Guillaume, A.M., Duchene, S., Bingen, B., Bosse, V., Datas, L., 2016. Sulphate incorporation in monazite lattice and dating the cycle of sulphur in metamorphic belts. Contributions to Mineralogy and Petrology 171, 1-19.

Laurent, O., Couzinié, S., Zeh, A., Vanderhaeghe, O., Moyen, J.F., Villaros, A., Gardien, V., Chelle-Michou, C., 2017. Protracted, coeval crust and mantle melting during Variscan late-orogenic evolution: U–Pb dating in the eastern French Massif Central. International Journal of Earth Sciences on line, 1-31.

Lawlor, P.J., Ortega-Gutiérrez, F., Cameron, K.L., Ochoa-Camarillo, H., Lopez, R., Sampson, D.E., 1999. U-Pb geochronology, geochemistry, and provenance of the Grenvillian Huiznopala Gneiss of Eastern Mexico. Precambrian Research 94, 73-99.

Levander, A., Schmandt, B., Miller, M.S., Liu, K., Karlstrom, K.E., Crow, R.S., Lee, C.T.A., Humphreys, E.D., 2011. Continuing Colorado plateau uplift by delamination-style convective lithospheric downwelling. Nature 472, 461-465.

Li, Z.-H., Liu, M., Gerya, T., 2016. Lithosphere delamination in continental collisional orogens: A systematic numerical study. Journal of Geophysical Research: Solid Earth 121, 5186-5211.

Li, Z.X., Bogdanova, S.V., Collins, A.S., Davidson, A., De Waele, B., Ernst, R.E., Fitzsimons, I.C.W., Fuck, R.A., Gladkochub, D.P., Jacobs, J., Karlstrom, K.E., Lu, S., Natapov, L.M., Pease, V., Pisarevsky, S.A., Thrane, K., Vernikovsky, V., 2008. Assembly, configuration, and break-up history of Rodinia: A synthesis. Precambrian Research 160, 179-210.

Liégeois, J.P., Navez, J., Hertogen, J., Black, R., 1998. Contrasting origin of post-collisional high-K calc-alkaline and shoshonitic versus alkaline and peralkaline granitoids. The use of sliding normalization. Lithos 45, 1-28.

Lindh, A., Gorbatschev, R., Lundegårdh, P.H., 1998. Beskrivning till berggrundskartan över Värmlands Län; Västra Värmlands Berggrund. Sveriges Geologiska Undersökning Ser. Ba, 45:2, 1-405.

Longhi, J., 2005. A mantle or mafic crustal source for Proterozoic anorthosites? Lithos 83, 183-198.

Longhi, J., Vander Auwera, J., Fram, M.S., Duchesne, J.C., 1999. Some phase equilibrium constraints on the origin of Proterozoic (massif) anorthosites and related rocks. Journal of Petrology 40, 339-362.

Lorenz, H., Gee, D.G., Larionov, A.N., Majka, J., 2012. The Grenville-Sveconorwegian orogen in the high Arctic. Geological Magazine 149, 875-891.

Loron, C., Moczydłowska, M., 2018. Tonian (Neoproterozoic) eukaryotic and prokaryotic organic-walled microfossils from the upper Visingsö Group, Sweden. Palynology 42, 220-254.

2802 Lundmark, A.M., Corfu, F., 2008. Late-orogenic Sveconorwegian massif anorthosite in the
2803 Jotun Nappe Complex, SW Norway, and causes of repeated AMCG magmatism along the
2804 Baltoscandian margin. Contributions to Mineralogy and Petrology 155, 147-163.
2805 Lundmark, A.M., Lamminen, J., 2016. The provenance and setting of the Mesoproterozoic
2806 Dala Sandstone, western Sweden, and paleogeographic implications for southwestern
2807 Fennoscandia. Precambrian Research 275, 197-208.
2808 Lundqvist, I., Skiöld, T., 1993. U-Pb zircon dating of volcanic rocks of the Åmål Group,
2809 western Sweden, in: Lundqvist, T. (Ed.), Radiometric dating results. Sveriges Geologiska
2810 Undersökning, Research Papers, Uppsala, pp. 24-30.
2811 Maijer, C., 1987. Day 7 - The metamorphic envelope of the Rogaland intrusive complex,
2812 in: Maijer, C., Padget, P. (Eds.), The geology of southernmost Norway: an excursion guide.
2813 Norges Geologiske Undersøkelse, Special Publication No 1, pp. 68-73.
2814 Maijer, C., Verschure, R.H., 1998. Petrology and isotope geology of the Hunnedalen
2815 monzonoritic dyke swarm, SW Norway: a possible late expression of Egersund anorthosite
2816 magmatism. Norges Geologiske Undersøkelse Bulletin 434, 83-107.
2817 Marcantonio, F., McNutt, R.H., Dickin, A.P., Heaman, L.M., 1990. Isotopic evidence for
2818 the crustal evolution of the Frontenac Arch in the Grenville Province of Ontario, Canada.
2819 Chemical Geology 83, 297-314.
2820 Mattila, J., Viola, G., 2014. New constraints on 1.7 Gyr of brittle tectonic evolution in
2821 southwestern Finland derived from a structural study at the site of a potential nuclear waste
2822 repository (Olkiluoto Island). Journal of Structural Geology 67, Part A, 50-74.
2823 McLelland, J.M., Daly, J.S., Chiarenzelli, J., 1993. Sm–Nd and U–Pb isotopic evidence of
2824 juvenile crust in the Adirondack Lowlands and implications for the evolution of the
2825 Adirondack Mts. The Journal of Geology 101, 97-105.

Menuge, J.F., 1985. Neodymium, isotope evidence for the age and origin of the Proterozoic of Telemark, south Norway, in: Tobi, A.C., Touret, J.L. (Eds.), The deep Proterozoic crust in the north Atlantic provinces. Reidel, Dordrecht, pp. 435-448.

Menuge, J.F., 1988. The petrogenesis of massif anorthosites: a Nd and Sr isotopic investigation of the Proterozoic of Rogaland-Vest Agder, SW Norway. Contributions to Mineralogy and Petrology 98, 363-373.

Merdith, A.S., Collins, A.S., Williams, S.E., Pisarevsky, S., Foden, J.D., Archibald, D.B., Blades, M.L., Alessio, B.L., Armistead, S., Plavsa, D., Clark, C., Müller, R.D., 2017. A full-plate global reconstruction of the Neoproterozoic. Gondwana Research 50, 84-134.

Milne, K.P., Starmer, I.C., 1982. Extreme differentiation in the Proterozoic Gjerstad-Morkeheia complex of South Norway. Contributions to Mineralogy and Petrology 79, 381-393.

Moczydłowska, M., Pease, V., Willman, S., Wickström, L., Agic, H., 2018. A Tonian age for the Visingsö Group in Sweden constrained by detrital zircon dating and biochronology: Implications for evolutionary events. Geological Magazine 155, 1175-1189.

Möller, A., O'Brien, P.J., Kennedy, A., Kröner, A., 2002. Polyphase zircon in ultrahigh-temperature granulites (Rogaland, SW Norway): constraints for Pb diffusion in zircon. Journal of Metamorphic Geology 20, 727-740.

Möller, A., O'Brien, P.J., Kennedy, A., Kröner, A., 2003. Linking growth episodes of zircon and metamorphic textures to zircon chemistry: an example from the ultrahigh-temperature granulites of Rogaland (SW Norway), in: Vance, D., Müller, W., Villa, I.M. (Eds.), Geochronology: linking the isotopic record with petrology and textures. Geological Society, London, Special Publications, pp. 65-81.

Möller, C., 1998. Decompressed eclogites in the Sveconorwegian (-Grenvillian) orogen of SW Sweden: petrology and tectonic implications. Journal of Metamorphic Geology 16, 641-656.

Möller, C., 1999. Sapphirine in SW Sweden: a record of Sveconorwegian (-Grenvillian) late-orogenic tectonic exhumation. Journal of Metamorphic Geology 17, 127-141.

Möller, C., Andersson, J., 2018. Metamorphic zoning and behaviour of an underthrusting continental plate. Journal of Metamorphic Geology 36, 567-589.

Möller, C., Andersson, J., Dyck, B., Antal Lundin, I., 2015. Exhumation of an eclogite terrane as a hot migmatitic nappe, Sveconorwegian orogen. Lithos 226, 147-168.

Möller, C., Andersson, J., Lundqvist, I., Hellström, F.A., 2007. Linking deformation, migmatite formation and zircon U-Pb geochronology in polymetamorphic gneisses, Sveconorwegian province, Sweden. Journal of Metamorphic Geology 25, 727-750.

Möller, C., Söderlund, U., 1997. Age constraints on the regional deformation within the Eastern Segment, S Sweden: Late Sveconorwegian granite dyke intrusion and metamorphic deformational relations. GFF 119, 1-12.

Morton, R.D., 1971. Geological investigations in the Bamble sector of the Fennoscandian Shield, S. Norway. No II. Metasediments and metapyroclastics (?) within the Precambrian metamorphic suite of the S Norwegian Skaergaard. Norsk Geologisk Tidsskrift 51, 63-83.

Moyen, J.F., Laurent, O., Chelle-Michou, C., Couzinié, S., Vanderhaeghe, O., Zeh, A., Villaros, A., Gardien, V., 2017. Collision vs. subduction-related magmatism: Two contrasting ways of granite formation and implications for crustal growth. Lithos 277, 154-177.

Mulch, A., Cosca, M.A., Andresen, A., Fiebig, J., 2005. Time scales of deformation and exhumation in extensional detachment systems determined by high-spatial resolution in situ UV-laser $^{40}Ar/^{39}Ar$ dating. Earth and Planetary Science Letters 233, 375-390.

Müller, A., Ihlen, P.M., Snook, B., Larsen, R., Flem, B., Bingen, B., Williamson, B.J., 2015. The chemistry of quartz in granitic pegmatites of southern Norway: petrogenetic and economic implications. Economic Geology 110, 1737-1757.

Müller, A., Romer, R.L., Pedersen, R.B., 2017. The Sveconorwegian Pegmatite Province – Thousands of pegmatites without parental granite. Canadian Mineralogist 55, 283-315.

Munz, I.A., 1990. Whiteschists and orthoamphibole-cordierite rocks and the P-T-t path of the Modum Complex, South Norway. Lithos 24, 181-200.

Munz, I.A., Morvik, R., 1991. Metagabbros in the Modum Complex, southern Norway: an important heat source for Sveconorwegian metamorphism. Precambrian Research 52, 97-113.

Munz, I.A., Wayne, D., Austrheim, H., 1994. Retrograde fluid infiltration in the high-grade Modum Complex, South Norway - Evidence for age, source and REE mobility. Contributions to Mineralogy and Petrology 116, 32-46.

Neilson, J.C., Kokelaar, B.P., Crowley, Q.G., 2009. Timing, relations and cause of plutonic and volcanic activity of the Siluro-Devonian post-collision magmatic episode in the Grampian Terrane, Scotland. Journal of the Geological Society of London 166, 545-561.

Nielsen, F.M., Campbell, I.H., McCulloch, M., Wilson, J.R., 1996. A strontium isotopic investigation of the Bjerkreim-Sokndal layered intrusion, Southwest Norway. Journal of Petrology 37, 171-193.

Nijland, T.G., deHaas, G.J.L.M., Andersen, T., 2000. Rifting-related (sub)alkaline magmatism in the Bamble sector (Norway) during the ‘Gothian’–Sveconorwegian interlude. GFF 122, 297-305.

Nijland, T.G., Harlov, D.E., Andersen, T., 2014. The Bamble Sector, South Norway: a review. Geoscience Frontiers 5, 635-658.

Nijland, T.G., Maijer, C., 1993. The regional amphibolite to granulite facies transition at Arendal, Norway: evidence for a thermal dome. Neues Jahrbuch für Mineralogie, Abhandlungen 165, 191-221.

Nijland, T.G., Maijer, C., Senior, A., Verschure, R.H., 1993. Primary sedimentary structures and compositions of the high-grade metamorphic Nidelva Quartzite Complex (Bamble, Norway), and the origin of nodular gneisses. Proceedings Koninklijke Nederlandse Akademie van Wetenschappen 96, 217-232.

Nijland, T.G., Touret, J.L.R., Visser, D., 1998. Anomalously low temperature orthopyroxene, spinel, and sapphirine occurrences in metasediments from the Bamble amphibolite-to-granulite facies transition zone (South Norway): possible evidence for localized action of saline fluids. The Journal of Geology 106, 575-590.

Nordgulen, Ø., 1999. Geologisk kart over Norge, berggrunnskart Hamar, 1:250000. Norges geologiske undersøkelse.

Nystuen, J.P., Andresen, A., Kumpulainen, R.A., Siedlecka, A., 2008. Neoproterozoic basin evolution in Fennoscandia, East Greenland and Svalbard. Episodes 31, 35-43.

Olesen, O., Smethurst, M.A., Torsvik, T.H., Bidstrup, T., 2004. Sveconorwegian igneous complexes beneath the Norwegian-Danish Basin. Tectonophysics 387, 105-130.

Olivarius, M., Friis, H., Kokfelt, T.F., Wilson, J.R., 2015. Proterozoic basement and Palaeozoic sediments in the Ringkøbing–Fyn High characterized by zircon U–Pb ages and heavy minerals from Danish onshore wells. Bulletin of the Geological Society of Denmark 63, 29-43.

Page, L.M., Möller, C., Johansson, L., 1996a. $^{40}Ar/^{39}Ar$ geochronology across the Mylonite Zone and the Southwestern Granulite Province in the Sveconorwegian Orogen of S Sweden. Precambrian Research 79, 239-259.

Page, L.M., Stephens, M.B., Wahlgren, C.H., 1996b. $^{40}Ar/^{39}Ar$ geochronological constraints on the tectonothermal evolution of the Eastern Segment of the Sveconorwegian Orogen, south-central Sweden, in: Brewer, T.S. (Ed.), Precambrian crustal evolution in the North Atlantic Region. Geological Society, London, Special Publications, pp. 315-330.

Paludan, J., Hansen, U.B., Olesen, N.O., 1994. Structural evolution of the Precambrian Bjerkreim–Sokndal intrusion, South Norway. Norsk Geologisk Tidsskrift 74, 185-198.

Park, R.G., Åhäll, K.I., Boland, M.P., 1991. The Sveconorwegian shear-zone network of SW Sweden in relation to mid-Proterozoic plate movements. Precambrian Research 49, 245-260.

Pasteels, P., Demaiffe, D., Michot, J., 1979. U-Pb and Rb-Sr geochronology of the eastern part of the south Rogaland igneous complex, southern Norway. Lithos 12, 199-208.

Pearce, J.A., Harris, N.B., Tindle, A.G., 1984. Trace element discrimination diagrams for the tectonic interpretation of granitic rocks. Journal of Petrology 25, 956-983.

Peccerillo, A., Taylor, S.R., 1976. Geochemistry of eocene calc-alkaline volcanic rocks from the Kastamonu area, Northern Turkey. Contributions to Mineralogy and Petrology 58, 63-81.

Pedersen, S., 1981. Rb-Sr age determinations on late Proterozoic granitoids from the Evje area, South Norway. Bulletin of the Geological Society of Denmark 29, 129-143.

Pedersen, S., Andersen, T., Konnerup-Madsen, J., Griffin, W.L., 2009. Recurrent Mesoproterozoic continental magmatism in South-Central Norway. International Journal of Earth Sciences 98, 1151-1171.

Persson-Nilsson, K., Lundqvist, L., 2014. Abstract. The Gillberga synform - and upper-crustal orogenic lid?, 31st Nordic Geological Winter Meeting, Lund, Sweden. Geologiska Föreningen.

Petersson, A., Scherstén, A., Andersson, J., Möller, C., 2015a. Zircon U-Pb and Hf isotopes from the eastern part of the Sveconorwegian Orogen, SW Sweden: implications for the growth of Fennoscandia, in: Roberts, N.M.W., van Kranendonk, M., Parman, S., Shirey, S., Clift, P.D. (Eds.), Continent formation through time. Geological Society, London, Special Publications, pp. 281-303.

Petersson, A., Scherstén, A., Bingen, B., Gerdes, A., Whitehouse, M.J., 2015b. Mesoproterozoic continental growth: U-Pb-Hf-O zircon record in the Idefjorden Terrane, Sveconorwegian Orogen. Precambrian Research 261, 75-95.

Pettersson, C.H., Pease, V., Frei, D., 2009. U-Pb zircon provenance of metasedimentary basement of the Northwestern Terrane, Svalbard: Implications for the Grenvillian-Sveconorwegian orogeny and development of Rodinia. Precambrian Research 175, 206-220.

Piñán-Llamas, A., Andersson, J., Möller, C., Johansson, L., Hansen, E., 2015. Polyphasal foreland-vergent deformation in a deep section of the 1 Ga Sveconorwegian orogen. Precambrian Research 265, 121-149.

Pisarevsky, S.A., Elming, S.Å., Pesonen, L.J., Li, Z.X., 2014. Mesoproterozoic paleogeography: Supercontinent and beyond. Precambrian Research 244, 207-225.

Plank, T., Kelley, K.A., Zimmer, M.M., Hauri, E.H., Wallace, P.J., 2013. Why do mafic arc magmas contain c. 4 wt% water on average? Earth and Planetary Science Letters 364, 168-179.

Poudjom Djomani, Y.H., O'Reilly, S.Y., Griffin, W.L., Morgan, P., 2001. The density structure of subcontinental lithosphere through time. Earth and Planetary Science Letters 184, 605-621.

Pulsipher, M.A., Dehler, C.M., 2019. U-Pb detrital zircon geochronology, petrography, and synthesis of the middle Neoproterozoic Visingsö Group, Southern Sweden. Precambrian Research 320, 323-333.

Rämö, O.T., 1991. Petrogenesis of the Proterozoic rapakivi granites and related basic rocks of southeastern Fennoscandia: Nd and Pb isotopic and general geochemic constraints. Geological Survey of Finland Bulletin 355, 1-161.

Rey, P., Vanderhaeghe, O., Teyssier, C., 2001. Gravitational collapse of the continental crust: definition, regimes and modes. Tectonophysics 342, 435-449.

Rey, P.F., Houseman, G., 2006. Lithospheric scale gravitational flow: the impact of body forces on orogenic processes from Archaean to Phanerozoic. Geological Society, London, Special Publications 253, 153-167.

Ripa, M., Stephens, M.B., 2020a. Chapter 9 - Continental magmatic arc and siliciclastic sedimentation in the far-field part of a 1.7 Ga accretionary orogen. Geological Society, London, Memoirs 50, 253-268.

Ripa, M., Stephens, M.B., 2020b. Chapter 10 - Magmatism (1.6–1.4 Ga) and Mesoproterozoic sedimentation related to intracratonic rifting coeval with distal accretionary orogenesis. Geological Society, London, Memoirs 50, 269-288.

Ripa, M., Stephens, M.B., 2020c. Chapter 12 - Dolerites (1.27–1.25 Ga) and alkaline ultrabasic dykes (c. 1.14 Ga) related to intracratonic rifting. Geological Society, London, Memoirs 50, 315-323.

Ripa, M., Stephens, M.B., 2020d. Chapter 13 - Siliciclastic sedimentation in a foreland basin to the Sveconorwegian orogen and dolerites (0.98–0.95 Ga) related to intracratonic rifting. Geological Society, London, Memoirs 50, 325-333.

Rivers, T., 2008. Assembly and preservation of lower, mid, and upper orogenic crust in the Grenville Province-Implications for the evolution of large hot long-duration orogens. Precambrian Research 167, 237-259.

Rivers, T., 2012. Upper-crustal orogenic lid and mid-crustal core complexes: signature of a collapsed orogenic plateau in the hinterland of the Grenville Province. Canadian Journal of Earth Sciences 49, 1-42.

Roberts, N.M.W., 2013. The boring billion? – Lid tectonics, continental growth and environmental change associated with the Columbia supercontinent. Geoscience Frontiers 4, 681-691.

Roberts, N.M.W., Slagstad, T., 2015. Continental growth and reworking on the edge of the Columbia and Rodinia supercontinents; 1.86–0.9 Ga accretionary orogeny in southwest Fennoscandia. International Geology Review 57, 1582-1606.

Roberts, N.M.W., Slagstad, T., Parrish, R.R., Norry, M.J., Marker, M., Horstwood, M.S.A., 2013. Sedimentary recycling in arc magmas: geochemical and U-Pb-Hf-O constraints on the Mesoproterozoic Suldal Arc, SW Norway. Contributions to Mineralogy and Petrology 165, 507-523.

Robins, B., Tumyr, O., Tysseland, M., Garmann, L.B., 1997. The Bjerkreim-Sokndal layered intrusion, Rogaland, SW Norway: Evidence from marginal rocks for a jotunite parent magma. Lithos 39, 121-133.

Rodhe, A., 1987. Depositional environments and lithostratigraphy of the Middle Proterozoic Almesåkra group, southern Sweden. Sveriges Geologiska Undersökning Ca 69, 1-80.

Roffeis, C., Corfu, F., 2014. Caledonian nappes of southern Norway and their correlation with Sveconorwegian basement domains, in: Corfu, F., Gasser, D., Chew, D.M. (Eds.), New perspectives on the Caledonides of Scandinavia and related areas. Geological Society, London, Special Publications, pp. 193-221.

Rogers, J.J.W., Santosh, M., 2002. Configuration of Columbia, a Mesoproterozoic Supercontinent. Gondwana Research 5, 5-22.

Røhr, T.S., Bingen, B., Robinson, P., Reddy, S.M., 2013. Geochronology of Paleoproterozoic augen gneisses in the Western Gneiss Region, Norway: evidence for Sveconorwegian zircon neocrystallization and Caledonian zircon deformation. The Journal of Geology 121, 105-128.

Romer, R.L., Smeds, S.A., 1996. U-Pb columbite ages of pegmatites from Sveconorwegian terranes in southwestern Sweden. Precambrian Research 76, 15-30.

Royden, L.H., Burchfiel, B.C., van der Hilst, R.D., 2008. The geological evolution of the Tibetan Plateau. Science 321, 1054-1058.

Rubatto, D., Hermann, J., Berger, J., Engi, M., 2009. Protracted fluid-induced melting during Barrovian metamorphism in the Central Alps. Contributions to Mineralogy and Petrology 158, 703-722.

Ruiz, J., Patchett, P.J., Ortega-Gutierrez, F., 1988. Proterozoic and Phanerozoicbasement terranes of Mexico from Nd isotopic studies. Geological Society of America Bulletin 100, 274-281.

Saintot, A., Stephens, M.B., Viola, G., Nordgulen, Ø., 2011. Brittle tectonic evolution and paleostress field reconstruction in the southwestern part of the Fennoscandian Shield, Forsmark, Sweden. Tectonics 30.

Schärer, U., Wilmart, E., Duchesne, J.C., 1996. The short duration and anorogenic character of anorthosite magmatism: U-Pb dating of the Rogaland complex, Norway. Earth and Planetary Science Letters 139, 335-350.

Scheiber, T., Viola, G., Bingen, B., Peters, M., Solli, A., 2015. Multiple reactivation and strain localization along a Proterozoic orogen-scale deformation zone: the Kongsberg-Telemark boundary in southern Norway revisited. Precambrian Research 265, 78-103.

Scherer, E., Munker, C., Mezger, K., 2001. Calibration of the lutetium-hafnium clock. Science 293, 683-687.

Scherstén, A., Årebäck, H., Cornell, D., Hoskin, P., Åberg, A., Armstrong, R., 2000. Dating mafic-ultramafic intrusions by ion-microprobing contact-melt zircon: examples from SW Sweden. Contributions to Mineralogy and Petrology 139, 115-125.

Schiellerup, H., Lambert, D.D., Prestvik, T., Robins, B., McBride, J.S., Larsen, R.B., 2000. Re–Os isotopic evidence for a lower crustal origin of massif-type anorthosites. Nature 405, 781-784.

Seydoux-Guillaume, A.M., Montel, J.M., Bingen, B., Bosse, V., de Parseval, P., Paquette, J.L., Janots, E., Wirth, R., 2012. Low-temperature alteration of monazite: Fluid mediated coupled dissolution-precipitation, irradiation damage, and disturbance of the U-Pb and Th-Pb chronometers. Chemical Geology 330-331, 140-158.

Sigmond, E.M.O., 1975. Geologisk kart over Norge, berggrunnskart Sauda, 1:250000. Norges geologiske undersøkelse, Trondheim.

Sigmond, E.M.O., 1978. Beskrivelse til det berggrunnsgeologiske kartbladet Sauda 1:250000. Norges geologiske undersøkelse Bulletin 341, 1-94.

Sigmond, E.M.O., 1985. The Mandal–Ustaoset line, a newly discovered major fault zone in south Norway, in: Tobi, A.C., Touret, J.L. (Eds.), The deep Proterozoic crust in the north Atlantic provinces. Reidel, Dordrecht, pp. 323-331.

Sigmond, E.M.O., 1998. Geologisk kart over Norge, berggrunnskart Odda, 1:250000. Norges geologiske undersøkelse, Trondheim.

Sigmond, E.M.O., Ragnhildstveit, J., 2004. Berggrunnskart Kalhovd 1515 II, 1:50000. Norges geologiske undersøkelse, Trondheim.

Sizova, E., Gerya, T., Brown, M., 2014. Contrasting styles of Phanerozoic and Precambrian continental collision. Gondwana Research 25, 522-545.

Slagstad, T., Kulakov, E., Kirkland, C.L., Roberts, N.M.W., Ganerød, M., 2019. Breaking the Grenville–Sveconorwegian link in Rodinia reconstructions. Terra Nova 31, 430-437.

Slagstad, T., Marker, M., Roberts, N.M.W., Saalmann, K., Kirkland, C.L., Kulakov, E., Ganerød, M., Røhr, T.S., Møkkelgjerd, S.H.H., Granseth, A., Sørensen, B.E., 2020. The Sveconorwegian orogeny – Reamalgamation of the fragmented southwestern margin of Fennoscandia. Precambrian Research 350, 105877.

Slagstad, T., Roberts, N.M.W., Coint, N., Høy, I., Sauer, S., Kirkland, K.L., Marker, M., Røhr, T.S., Henderson, I.H.C., Stormoen, M.A., Skår, Ø., Sørensen, B.E., Bybee, G.M., 2018. Magma-driven, high-grade metamorphism in the Sveconorwegian Province, southwest Norway, during the terminal stages of Fennoscandian Shield evolution. Geosphere 14, 861-882.

Slagstad, T., Roberts, N.M.W., Kulakov, E., 2017. Linking orogenesis across a supercontinent; the Grenvillian and Sveconorwegian margins on Rodinia. Gondwana Research 44, 109-115.

Slagstad, T., Roberts, N.M.W., Marker, M., Røhr, T.S., Schiellerup, H., 2013. A non-collisional, accretionary Sveconorwegian orogen. Terra Nova 25, 30-37.

Sláma, J., Walderhaug, O., Fonneland, H., Košler, J., Pedersen, R.B., 2011. Provenance of Neoproterozoic to Upper Cretaceous sedimentary rocks, eastern Greenland: Implications for recognizing the sources of sediments in the Norwegian Sea. Sedimentary Geology 238, 254-267.

Sobolev, A.V., Chaussidon, M., 1996. H_2O concentrations in primary melts from supra-subduction zones and mid-ocean ridges: Implications for H_2O storage and recycling in the mantle. Earth and Planetary Science Letters 137, 45-55.

Söderlund, P., Söderlund, U., Möller, C., Gorbatschev, R., Rodhe, A., 2004. Petrology and ion microprobe U-Pb chronology applied to a metabasic intrusion in southern Sweden: a study on zircon formation during metamorphism and deformation. Tectonics 23, TC5005, doi:5010.1029 /2003TC001498.

Söderlund, U., Ask, R., 2006. Evidence for two pulses (1215-1224 and ca. 1205 Ma) of bimodal magmatism along the Protogine Zone, S Sweden. GFF 128, 303-310.

Söderlund, U., Elming, S.Å., Ernst, R.E., Schissel, D., 2006. The Central Scandinavian Dolerite Group - Protracted hotspot activity or back-arc magmatism? Constraints from U-Pb baddeleyite geochronology and Hf isotopic data. Precambrian Research 150, 136-152.

Söderlund, U., Hellström, F.A., Kamo, S.L., 2008a. Geochronology of high-pressure mafic granulite dykes in SW Sweden; tracking the P-T-t path of metamorphism using Hf isotopes in zircon and baddeleyite. Journal of Metamorphic Geology 26, 539-560.

Söderlund, U., Isachsen, C.E., Bylund, G., Heaman, L.M., Patchett, P.J., Vervoort, J.D., Andersson, U.B., 2005. U-Pb baddeleyite ages, and Hf, Nd isotope chemistry constraining repeated mafic magmatism in the Fennoscandian Shield from 1.6 to 0.9 Ga. Contributions to Mineralogy and Petrology 150, 174-194.

Söderlund, U., Jarl, L.G., Persson, P.O., Stephens, M.B., Wahlgren, C.H., 1999. Protolith ages and timing of deformation in the eastern, marginal part of the Sveconorwegian orogen, southwestern Sweden. Precambrian Research 94, 29-48.

Söderlund, U., Karlsson, C., Johansson, L., Larsson, K., 2008b. The Kullaberg peninsula - a glimpse of the Proterozoic evolution of SW Fennoscandia. GFF 130, 1-10.

Söderlund, U., Möller, C., Andersson, J., Johansson, L., Whitehouse, M.J., 2002. Zircon geochronology in polymetamorphic gneisses in the Sveconorwgian orogen, SW Sweden: ion microprobe evidence for 1.46-1.42 Ga and 0.98-0.96 Ga reworking. Precambrian Research 113, 193-225.

Solari, L.A., Ortega-Gutiérrez, F., Elías-Herrera, M., Ortega-Obregón, C., Macías-Romo, C., Reyes-Salas, M., 2014. Detrital provenance of the Grenvillian Oaxacan Complex, southern Mexico: a zircon perspective. International Journal of Earth Sciences 103, 1301-1315.

Spear, F.S., 1993. Metamorphic phase equilibria and pressure-temperature-time paths. Mineralogical Society of America, Monograph, Washington D.C.

Spencer, C.J., Roberts, N.M.W., Cawood, P.A., Hawkesworth, C.J., Prave, A.R., Antonini, A.S.M., Horstwood, M.S.A., 2014. Intermontane basins and bimodal volcanism at the onset of the Sveconorwegian Orogeny, southern Norway. Precambrian Research 252, 107-118.

Stacey, J.S., Kramers, J.D., 1975. Approximation of terrestrial lead isotope evolution by a two-stage model. Earth and Planetary Science Letters 26, 207-221.

Starmer, I.C., 1985. The evolution of the south Norwegian Proterozoic as revealed by the major and mega-tectonics of the Kongsberg and Bamble sector, in: Tobi, A.C., Touret, J.L. (Eds.), The deep Proterozoic crust in the north Altantic provinces. Reidel, Dordrecht, pp. 259-290.

Starmer, I.C., 1991. The Proterozoic evolution of the Bamble sector shear belt, southern Norway: correlations across southern Scandinavia and the Grenvillian controversy. Precambrian Research 49, 107-139.

Stein, H.J., Bingen, B., 2002. 1.05-1.01 Ga Sveconorwegian metamorphism and deformation of the supracrustal sequence at Sæsvatn, South Norway: Re-Os dating of Cu-Mo mineral occurrences, in: Blundell, D., Neubauer, F., von Quadt, A. (Eds.), The timing and location of major ore deposits in an evolving orogen. Geological Society, London, Special Publications, pp. 319-335.

Stephens, M.B., 2020. Chapter 8 - Outboard-migrating accretionary orogeny at 1.9–1.8 Ga (Svecokarelian) along a margin to the continent Fennoscandia. Geological Society, London, Memoirs 50, 237-250.

Stephens, M.B., Bergström, U., Wahlgren, C.H., 2020. Chapter 14 - Regional context and lithotectonic framework of the 1.1–0.9 Ga Sveconorwegian orogen, southwestern Sweden. Geological Society, London, Memoirs 50, 337-349.

Stephens, M.B., Wahlgren, C.H., 2020a. Chapter 15 - Polyphase (1.9–1.8, 1.5–1.4 and 1.0–0.9 Ga) deformation and metamorphism of Proterozoic (1.9–1.2 Ga) continental crust, Eastern Segment, Sveconorwegian orogen. Geological Society, London, Memoirs 50, 351-396.

Stephens, M.B., Wahlgren, C.H., 2020b. Chapter 17 - Accretionary orogens reworked in an overriding plate setting during protracted continent–continent collision, Sveconorwegian orogen, southwestern Sweden. Geological Society, London, Memoirs 50, 435-448.

Stephens, M.B., Wahlgren, C.H., Weijermars, R., Cruden, A.R., 1996. Left lateral transpressive deformation and its tectonic implications, Sveconorwegian Orogen, Baltic Shield, Southwestern Sweden. Precambrian Research 79, 261-279.

Strachan, R.A., Nutman, A.P., Friderichsen, J.D., 1995. SHRIMP U-Pb geochronology and metamorphic history of the Smallefjord sequence, NE Greenland Caledonides. Journal of the Geological Society of London 152, 779-784.

Strachan, R.A., Prave, A.R., Kirkland, C.L., Storey, C.D., 2013. U–Pb detrital zircon geochronology of the Dalradian Supergroup, Shetland Islands, Scotland: implications for regional correlations and Neoproterozoic–Palaeozoic basin development. Journal of the Geological Society of London 170, 905-916.

Thybo, H., 2001. Crustal structure along the EGT profile across the Tornquist Fan interpreted from seismic, gravity and magnetic data. Tectonophysics 334, 155-190.

Tobi, A.C., Hermans, G.A., Maijer, C., Jansen, J.B.H., 1985. Metamorphic zoning in the high-grade Proterozoic of Rogaland-Vest Agder, SW Norway, in: Tobi, A.C., Touret, J.L. (Eds.), The deep Proterozoic crust in the north Atlantic provinces. Reidel, Dordrecht, pp. 477-497.

Tohver, E., Bettencourt, J.S., Tosdal, R., Mezger, K., Leite, W.B., Payolla, B.L., 2004a. Terrane transfer during the Grenville orogeny: tracing the Amazonian ancestry of southern

Appalachian basement through Pb and Nd isotopes. Earth and Planetary Science Letters 228, 161-176.

Tohver, E., van der Pluijm, B.A., Mezger, K., Essene, E., Scandolara, J.E., Rizzotto, G., 2004b. Significance of the Nova Bresilândia metasedimentary belt in western Brazil: Redefining the Mesoproterozoic boundary of the Amazon craton. Tectonics 23, TC6004, doi: 6010.1029/2003TC001563, 001561-001520.

Tohver, E., van der Pluijm, B.A., Mezger, K., Scandolara, J.E., Essene, E., 2005. Two stage tectonic history of the SW Amazon craton in the late Mesoproterozoic: identifying a cryptic suture zone. Precambrian Research 137, 35-59.

Tomkins, H.S., Williams, I.S., Ellis, D.J., 2005. In situ U-Pb dating of zircon formed from retrograde garnet breakdown during decompression in Rogaland, SW Norway. Journal of Metamorphic Geology 23, 201-215.

Torgersen, E., Henderson, I.H.C., Bingen, B., Svendby, K., Nasuti, A., 2018. Abstract. The Nisser Shear Zone – Discovery of a Sveconorwegian crustal-scale detachment zone in southern Norway 33rd Nordic Geological Winter Meeting. Geological Society of Denmark, Copenhagen, Denmark p. 59.

Torgersen, E., Viola, G., Zwingmann, H., Henderson, I.H.C., 2015. Inclined K-Ar illite age spectra in brittle fault gouges: effects of fault reactivation and wall-rock contamination. Terra Nova 27, 106-113.

Torsvik, T.H., 2003. The Rodinia jigsaw puzzle. Science 300, 1379-1381.

Torsvik, T.H., Smethurst, M.A., Meert, J.G., Van der Voo, R., Mc Kerrow, W.S., Brasier, M.D., Sturt, B.A., Walderhaug, H.J., 1996. Continental break up and collision in the Neoproterozoic and Paleozoic - A tale of Baltica and Laurentia. Earth-Science Reviews 40, 229-258.

Touret, J.L., 1971a. Le facies granulite en Norvège méridionale. 1. Les associations minéralogiques. Lithos 4, 239-249.

Touret, J.L., 1971b. Le facies granulite en Norvège méridionale. 2. Les inclusions fluides. Lithos 4, 423-436.

Touret, J.L., 1987. Day 2 - The high-grade metamorphic Bamble sector, in: Maijer, C., Padget, P. (Eds.), The geology of southernmost Norway: an excursion guide. Norges Geologiske Undersøkelse, Special Publication No 1, pp. 25-30.

Tual, L., Piñán-Llamas, A., Möller, C., 2015. High-temperature deformation in the basal shear zone of an eclogite-bearing fold nappe, Sveconorwegian orogen, Sweden. Precambrian Research 265, 104-120.

Tual, L., Pitra, P., Möller, C., 2017. P–T evolution of Precambrian eclogite in the Sveconorwegian orogen, SW Sweden. Journal of Metamorphic Geology, n/a-n/a.

Tucker, R.D., Krogh, T.E., Råheim, A., 1990. Proterozoic evolution and age - province boundaries in the central part of the Western Gneiss Region, Norway: results of U-Pb dating of accessory minerals from Trondheimsfjord to Geiranger, in: Gower, C.F., Rivers, T., Ryan, B. (Eds.), Mid-Proterozoic Laurentia-Baltica. Geological Association of Canada, Special Paper 38, pp. 149-173.

Ulmius, J., Andersson, J., Möller, C., 2015. Hallandian 1.45 Ga high-temperature metamorphism in Baltica: P-T evolution and SIMS U-Pb zircon ages of aluminous gneisses, SW Sweden. Precambrian Research 265, 10-39.

Ulmius, J., Möller, C., Page, L., Johansson, L., Ganerød, M., 2018. The eastern boundary of Sveconorwegian reworking in the Baltic Shield, defined by 40Ar/39Ar geochronology across the southernmost Sveconorwegian Province. Precambrian Research 307, 201-217.

Vaasjoki, M., 1981. The lead isotopic composition of some Finnish galenas. Geological Survey of Finland Bulletin 316, 25.

Valentino, D.W., Chiarenzelli, J.R., Regan, S.P., 2019. Spatial and temporal links between Shawinigan accretionary orogenesis and massif anorthosite intrusion, southern Grenville province, New York, U.S.A. Journal of Geodynamics 129, 80-97.

Vander Auwera, J., Bogaerts, M., Bolle, O., Longhi, J., 2008. Genesis of intermediate igneous rocks at the end of the Sveconorwegian (Grenvillian) orogeny (S Norway) and their contribution to intracrustal differentiation. Contributions to Mineralogy and Petrology 156, 721-743.

Vander Auwera, J., Bogaerts, M., Liégeois, J.P., Demaiffe, D., Wilmart, E., Bolle, O., Duchesne, J.C., 2003. Derivation of the 1.0-0.9 Ga ferro-potassic A-type granitoids of southern Norway by extreme differentiation from basic magmas. Precambrian Research 124, 107-148.

Vander Auwera, J., Bolle, O., Bingen, B., Liégeois, J.P., Bogaerts, M., Duchesne, J.C., DeWaele, B., Longhi, J., 2011. Sveconorwegian massif-type anorthosites and related granitoids result from post-collisional melting of a continental root. Earth-Science Reviews 107, 375-397.

Vander Auwera, J., Bolle, O., Dupont, A., Pin, C., Paquette, J.L., Charlier, B., Duchesne, J.C., Mattielli, N., Bogaerts, M., 2014a. Source-derived heterogeneities in the composite (charnockite-granite) ferroan Farsund intrusion (SW Norway). Precambrian Research 251, 141-163.

Vander Auwera, J., Charlier, B., Duchesne, J.C., Bingen, B., Longhi, J., Bolle, O., 2014b. Comment on Bybee et al. (2014): Pyroxene megacrysts in Proterozoic anorthosites: Implications for tectonic setting, magma source and magmatic processes at the Moho. Earth and Planetary Science Letters 401, 378-380.

Vander Auwera, J., Longhi, J., 1994. Experimental study of a jotunite (hypersthene monzodiorite): constraints on the parent magma composition and crystallization conditions

(P, T, fO_2) of the Bjerkreim-Sokndal layered intrusion (Norway). Contributions to Mineralogy and Petrology 118, 60-78.

Vander Auwera, J., Longhi, J., Duchesne, J.C., 1998. A liquid line of descent of the Jotunite (Hypersthene Monzodiorite) suite. Journal of Petrology 39, 439-468.

Vanderhaeghe, O., 2012. The thermal–mechanical evolution of crustal orogenic belts at convergent plate boundaries: A reappraisal of the orogenic cycle. Journal of Geodynamics 56-57, 124-145.

Vermeesch, P., 2012. On the visualisation of detrital age distributions. Chemical Geology 312, 190-194.

Verschure, R.H., Andriessen, P.A.M., Boelrijk, N.A.M., Hebeda, E.H., Maijer, C., Priem, H.N.A., Verdurmen, E.A.T., 1980. On the thermal stability of Rb-Sr and K-Ar biotite systems: evidence from coexisting Sveconorwegian (ca. 870 Ma) and (ca. 400 Ma) biotites in SW Norway. Contributions to Mineralogy and Petrology 74, 245-252.

Villaseca, C., Barbero, L., Herreros, V., 1998. A re-examination of the typology of peraluminous granite types in intracontinental orogenic belts. Transactions of the Royal Society of Edinburgh: Earth Sciences 89, 113-119.

Viola, G., Bingen, B., Solli, A., 2016. Berggrunnskart Kongsberg lithotectoniske enhet, Kongsberg-Modum-Hønefoss, M 1:100000 - Bedrock geology map of the Kongsberg lithotectonic unit, Kongsberg-Modum-Hønefoss, scale 1:100000, 1 sheet. Norges Geologiske Undersøkelse - Geological Survey of Norway, pp. Scale 1:100000, 100001 sheet.

Viola, G., Henderson, I.H.C., 2010. Inclined transpression at the toe of an arcuate thrust: an example from the Precambrian "Mylonite Zone" of the Sveconorwegian orogen, in: Law, R., Butler, R., Holdsworth, R.E., Krabbendam, M., Strachan, R.A. (Eds.), Continental Tectonics and Mountain Building - The Legacy of Peach and Horne. Geological Society, London, Special Publications, pp. 715-737.

Viola, G., Henderson, I.H.C., Bingen, B., Hendriks, B.W.H., 2011. The Grenvillian-Sveconorwegian orogeny in Fennoscandia: Back-thrusting and extensional shearing along the "Mylonite Zone". Precambrian Research 189, 368-388.

Viola, G., Venvik Ganerød, G., Wahlgren, C.H., 2009. Unraveling 1.5 Ga of brittle deformation history in the Laxemar-Simpevarp area, southeast Sweden: A contribution to the Swedish site investigation study for the disposal of highly radioactive nuclear waste. Tectonics 28, TC5007.

Viola, G., Zwingmann, H., Mattila, J., Käpyaho, A., 2013. K-Ar illite age constraints on the Proterozoic formation and reactivation history of a brittle fault in Fennoscandia. Terra Nova 25, 236-244.

Wahlgren, C.H., Cruden, A.R., Stephens, M.B., 1994. Kinematics of a major fan-like structure in the eastern part of the Sveconorwegian orogen, Baltic Shield, south-central Sweden. Precambrian Research 70, 67-91.

Wahlgren, C.H., Page, L., Kübler, L., Delin, H., 2015. ^{40}Ar-^{39}Ar biotite age of a lamprophyre dyke and constraints on the timing of ductile deformation inside the Idefjorden terrane and along the Mylonite Zone, Sveconorwegian orogen, south-west Sweden. GFF first view, 1-9.

Wahlgren, C.H., Stephens, M.B., 2020. Chapter 11 - Reworking of older (1.8 Ga) continental crust by Mesoproterozoic (1.5–1.4 Ga) orogeny, Blekinge–Bornholm orogen, southeastern Sweden. Geological Society, London, Memoirs 50, 291-312.

Wallace, P.J., 2005. Volatiles in subduction zone magmas: concentrations and fluxes based on melt inclusion and volcanic gas data. Journal of Volcanology and Geothermal Research 140, 217-240.

Wang, X.D., Söderlund, U., Lindh, A., Johansson, L., 1998. U-Pb and Sm-Nd dating of high-pressure granulite- and upper amphibolite facies rocks from SW Sweden. Precambrian Research 92, 319-339.

Weber, B., Köhler, H., 1999. Sm–Nd, Rb–Sr and U–Pb geochronology of a Grenville Terrane in Southern Mexico: origin and geologic history of the Guichicovi Complex. Precambrian Research 96, 245-262.

Weber, B., Scherer, E.E., Schulze, C., Valencia, V.A., Montecinos, P., Mezger, K., Ruiz, J., 2010. U-Pb and Lu-Hf isotope systematics of lower crust from central-southern Mexico - Geodynamic significance of Oaxaquia in a Rodinia Realm. Precambrian Research 182, 149-162.

Weis, D., 1986. Genetic implications of Pb isotopic geochemistry in the Rogaland anorthositic complex (Southwest Norway). Chemical Geology 57, 181-199.

Wickström, L.M., Stephens, M.B., 2020. Chapter 18 - Tonian–Cryogenian rifting and Cambrian–Early Devonian platformal to foreland basin development outside the Caledonide orogen. Geological Society, London, Memoirs 50, 451-477.

Wiest, J.D., Jacobs, J., Ksienzyk, A.K., Fossen, H., 2018. Sveconorwegian vs. Caledonian orogenesis in the eastern Øygarden Complex, SW Norway – Geochronology, structural constraints and tectonic implications. Precambrian Research 305, 1-18.

Wilmart, E., Demaiffe, D., Duchesne, J.C., 1989. Geochemical constraints on the genesis of the Tellnes ilmenite deposit, southwest Norway. Economic Geology 84, 1047-1056.

Zhang, S., Li, Z.-X., Evans, D.A.D., Wu, H., Li, H., Dong, J., 2012. Pre-Rodinia supercontinent Nuna shaping up: A global synthesis with new paleomagnetic results from North China. Earth and Planetary Science Letters 353-354, 145-155.

Zhang, W., Roberts, D., Pease, V., 2015. Provenance characteristics and regional implications of Neoproterozoic, Timanian-margin successions and a basal Caledonian nappe in northern Norway. Precambrian Research 268, 153-167.

Zhang, W., Roberts, D., Pease, V., 2016. Provenance of sandstones from Caledonian nappes in Finnmark, Norway: Implications for Neoproterozoic–Cambrian palaeogeography. Tectonophysics 691, 198-205.

11 Figure captions

Inserted into the document

12 Table captions and Inline Supplementary Material captions

Table 1. Chart of geological events in the Sveconorwegian orogen. (Austin Hegardt, 2010; Bingen et al., 2003; Bybee et al., 2014; Charlier et al., 2010; Coint et al., 2015; Eliasson et al., 2003; Engvik et al., 2016; Hansen et al., 2015, Lamminen, 2011 #5583; Laurent et al., 2018b; Moczydłowska et al., 2018; Müller et al., 2017; Ripa and Stephens, 2020d; Söderlund et al., 2008a; Söderlund et al., 2005; Spencer et al., 2014; Vander Auwera et al., 2014a; Vander Auwera and Longhi, 1994)

Table 2. Summary of sampling and zircon U-Pb data for migmatitic gneisses, Eidsvoll-Auli area, Idefjorden lithotectonic unit.

Inline Supplementary Material 1. Text document. New zircon U–Pb geochronological data in the Idefjorden lithotectonic unit.

Table S2. Inline Supplementary Material 2. SIMS (SHRIMP) U–Pb analyses of zircon from leucosome samples from the Eidsvoll-Auli area, Idefjorden lithotectonic unit.

Table S3. Inline Supplementary Material 2. Compilation of samples of metasediments for which detrital zircon U-Pb data are published and compilation of geochronological data recording magmatic-migmatitic events in the Sveconorwegian orogen.